Watershed Climate Change Vulnerability Assessment
Lolo National Forest

Supplementary Materials
Appendix 2
Figures

Accompanying Publication Number R1-16-05 is available on-line at:
http://www.fs.usda.gov/main/lolo/workingtogether.

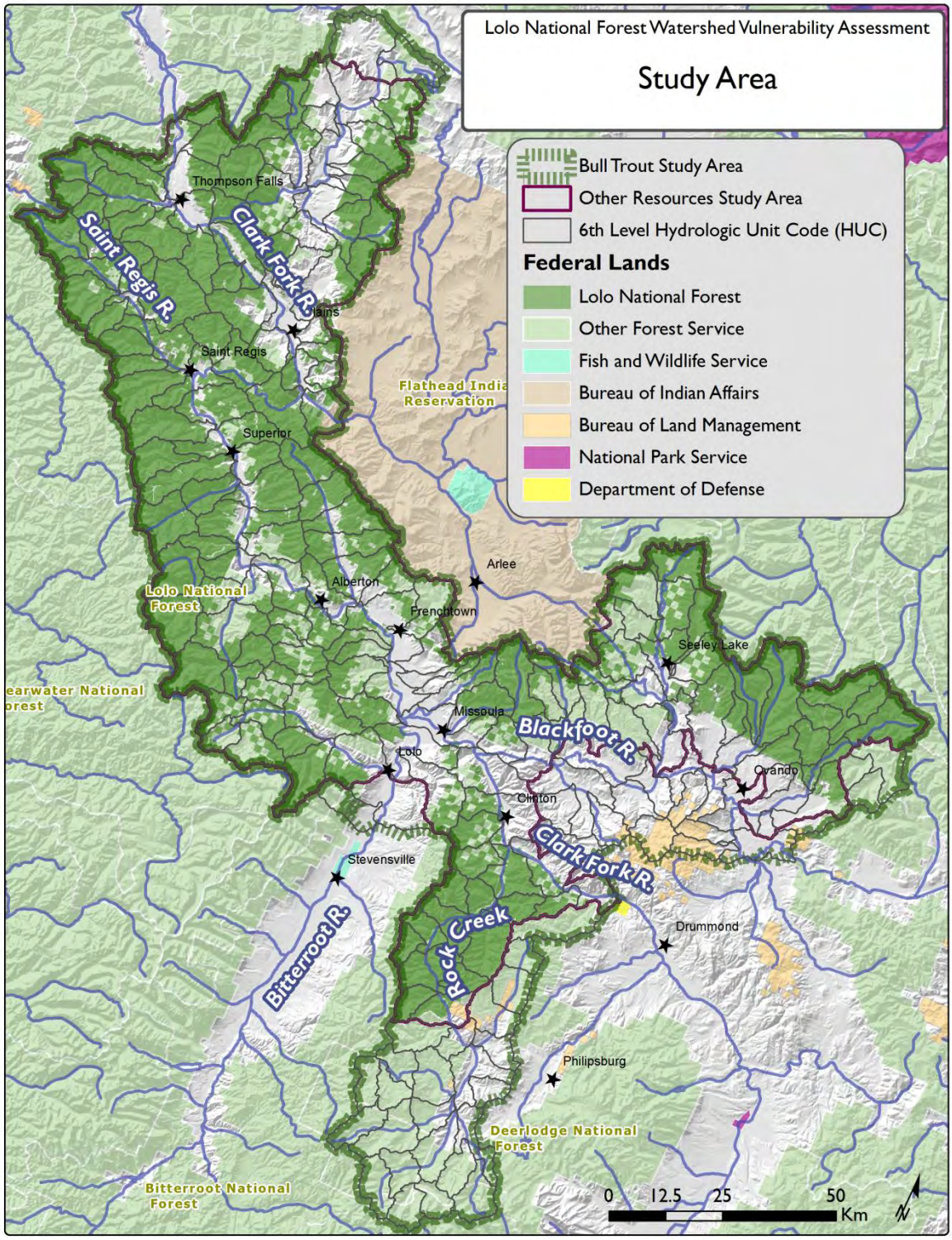

Figure 1. Study area for the Lolo National Forest (LNF) Watershed Vulnerability Assessment. For the bull trout analysis, the study area incorporated all of the LNF lands and neighboring watersheds of particular interest for bull trout. For other resource areas and values, we only considered watersheds covering LNF and intervening private lands.

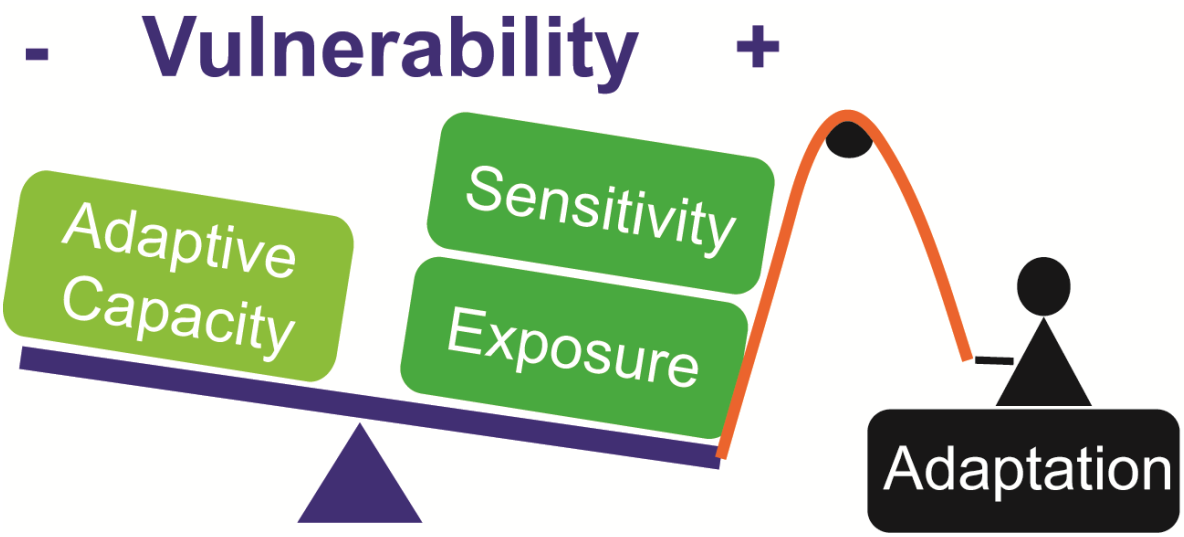

Figure 2. (and Figure V.1). Vulnerability is a function of climate exposure and sensitivity. Adaptive capacity (a system's intrinsic ability to reduce its sensitivity) can reduce vulnerability. We do not address the adaptive capacity of each resource value in this report, but managers should consider this in planning. The goal of the vulnerability assessment is to plan for climate change adaptation management actions, which may reduce vulnerability, primarily through reducing climate sensitivity.

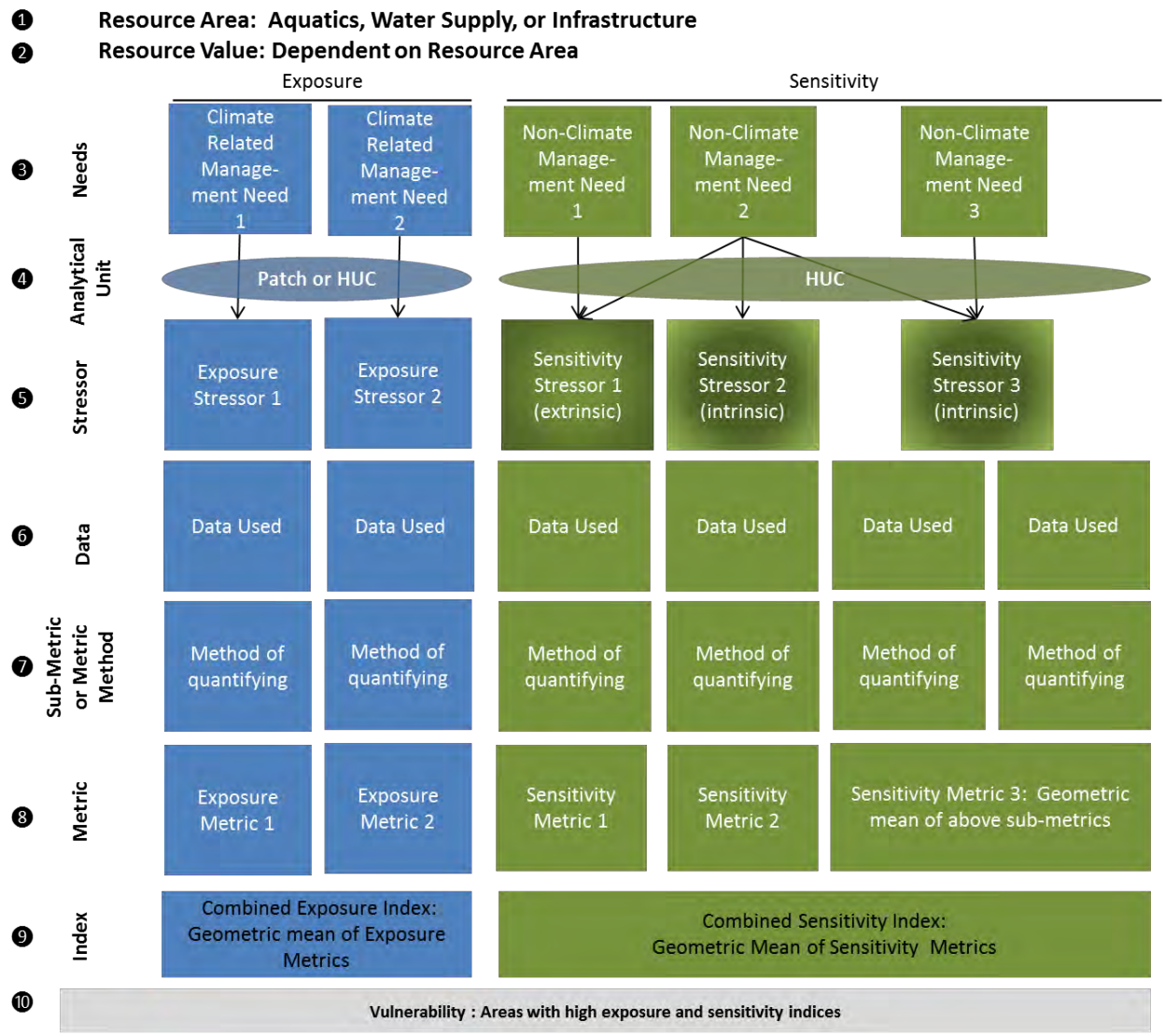

Figure 3. Schematic of conceptual models used to link resource needs to each metric calculated in this analysis for each resource value analyzed.

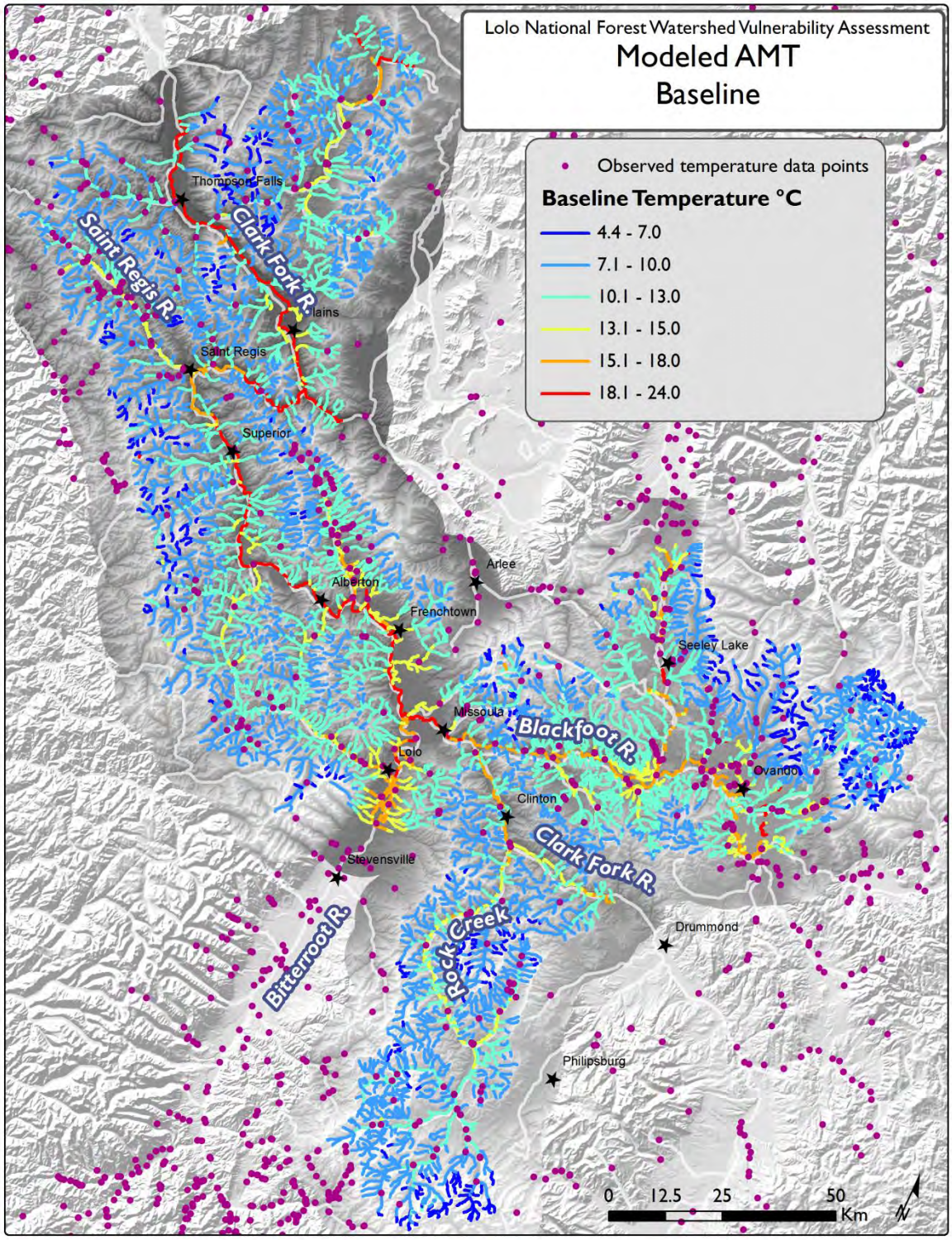

Figure 4. NorWeST modeled August mean stream temperature (AMT) data for baseline (1993-2011) time period. Purple points denote locations of empirical stream temperature measurements upon which the modeled temperatures were based.

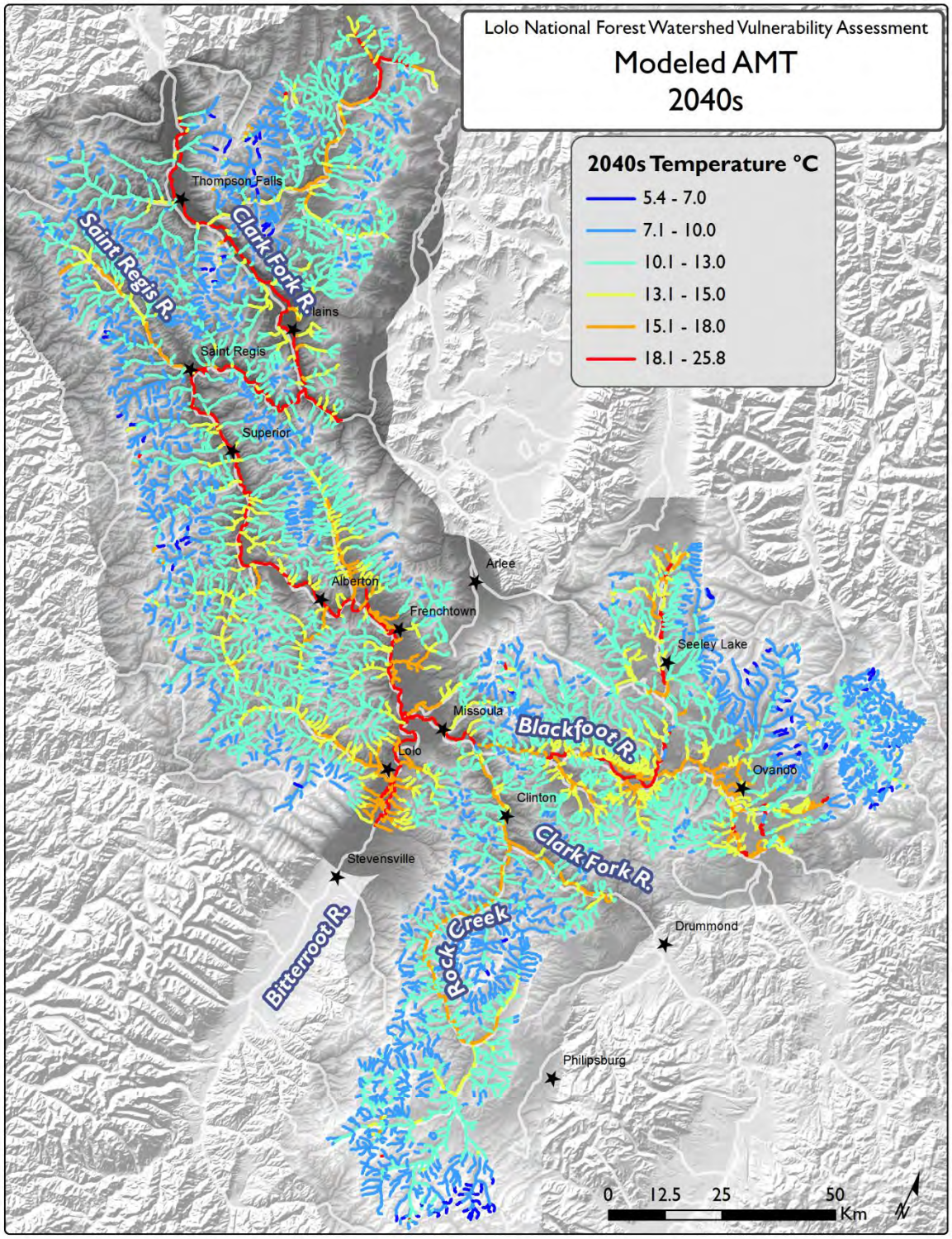

Figure 5. NorWeST modeled August mean stream temperature (AMT) data the 2040s (2030-2059).

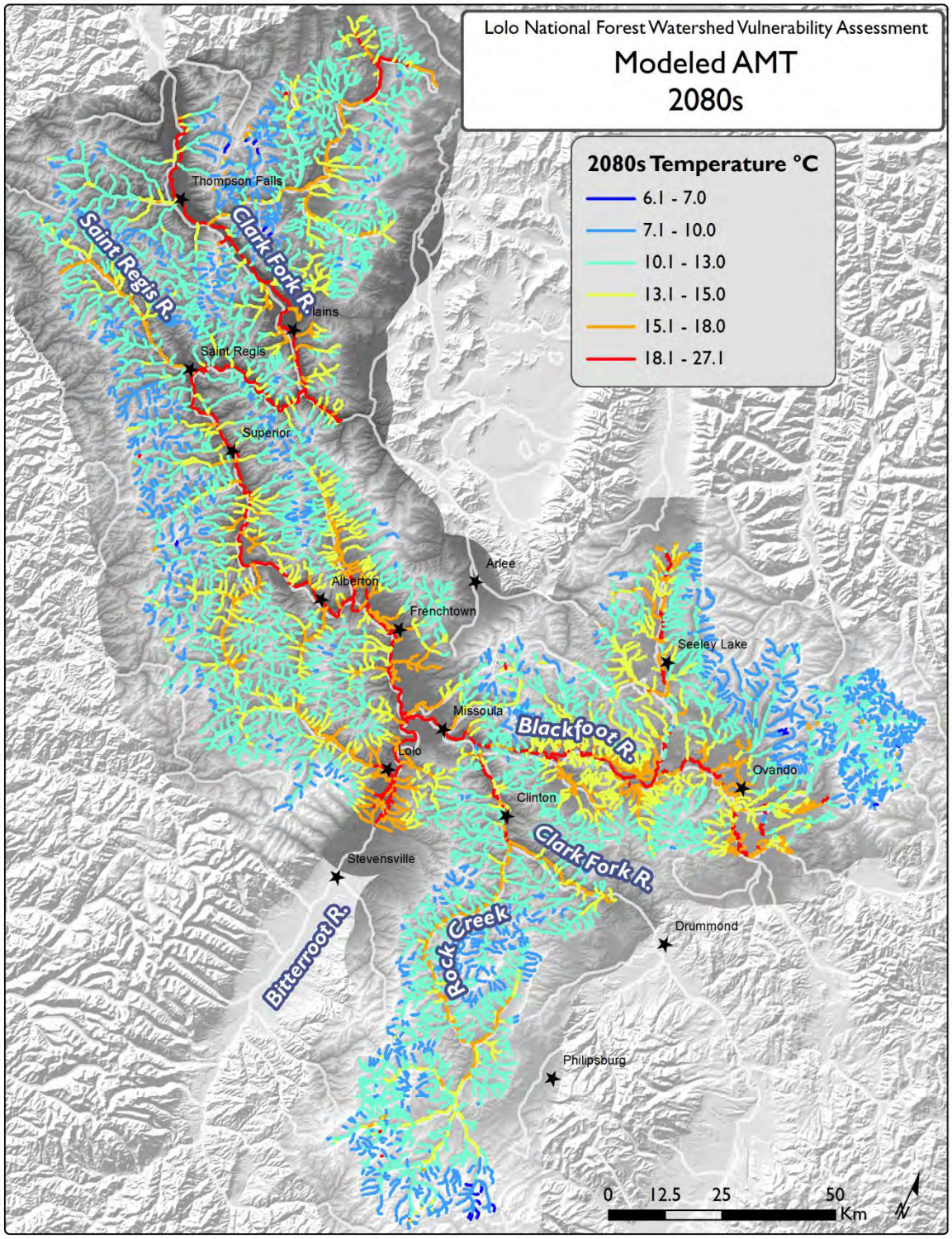

Figure 6. NorWeST modeled August mean stream temperature (AMT) data for the 2080s (2070-2099).

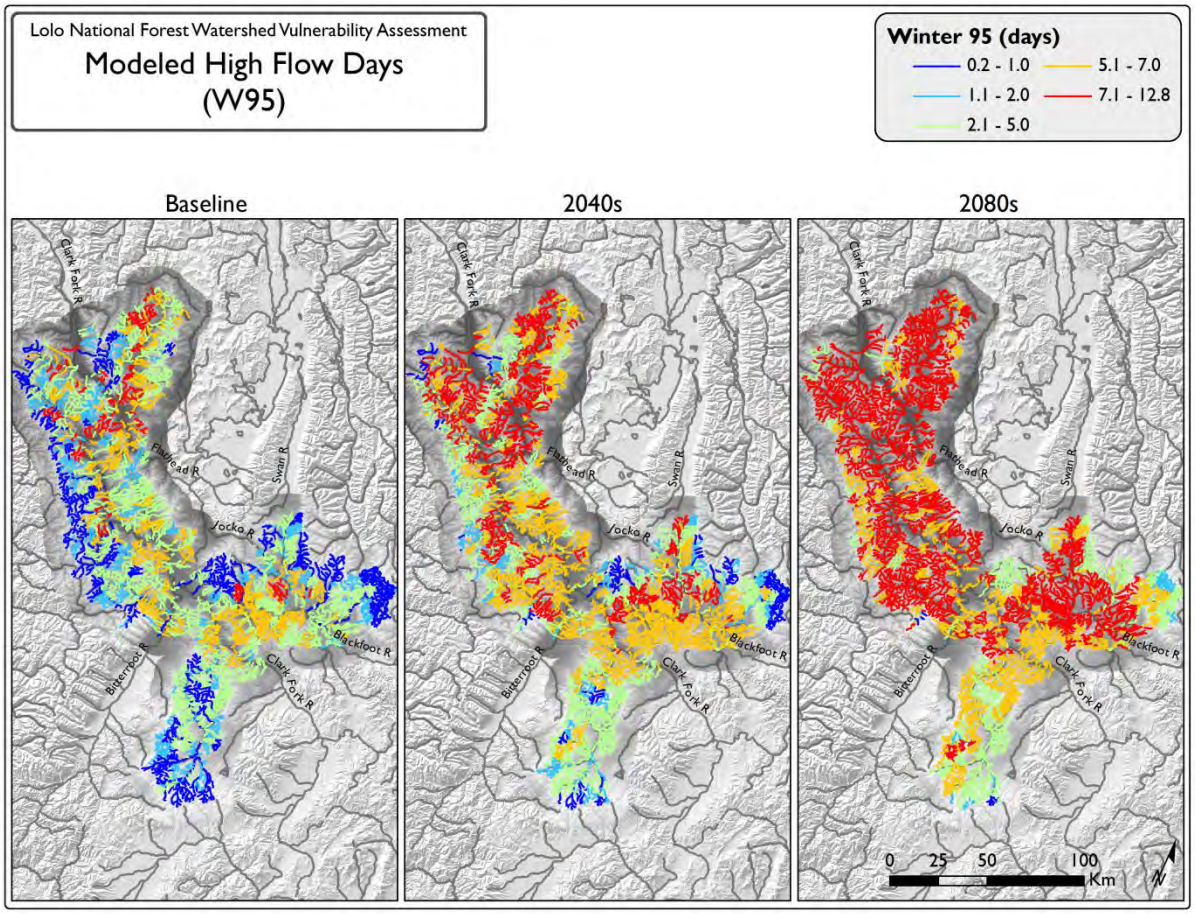

Figure 7. Modeled winter high flow days (W95) for baseline and for the 2040s and 2080s using an ensemble of GCMs. See Figure 8 for a larger map of the baseline modeled W95 and see Figure 9 for a comparison of model outputs for the 2040s using different GCMs.

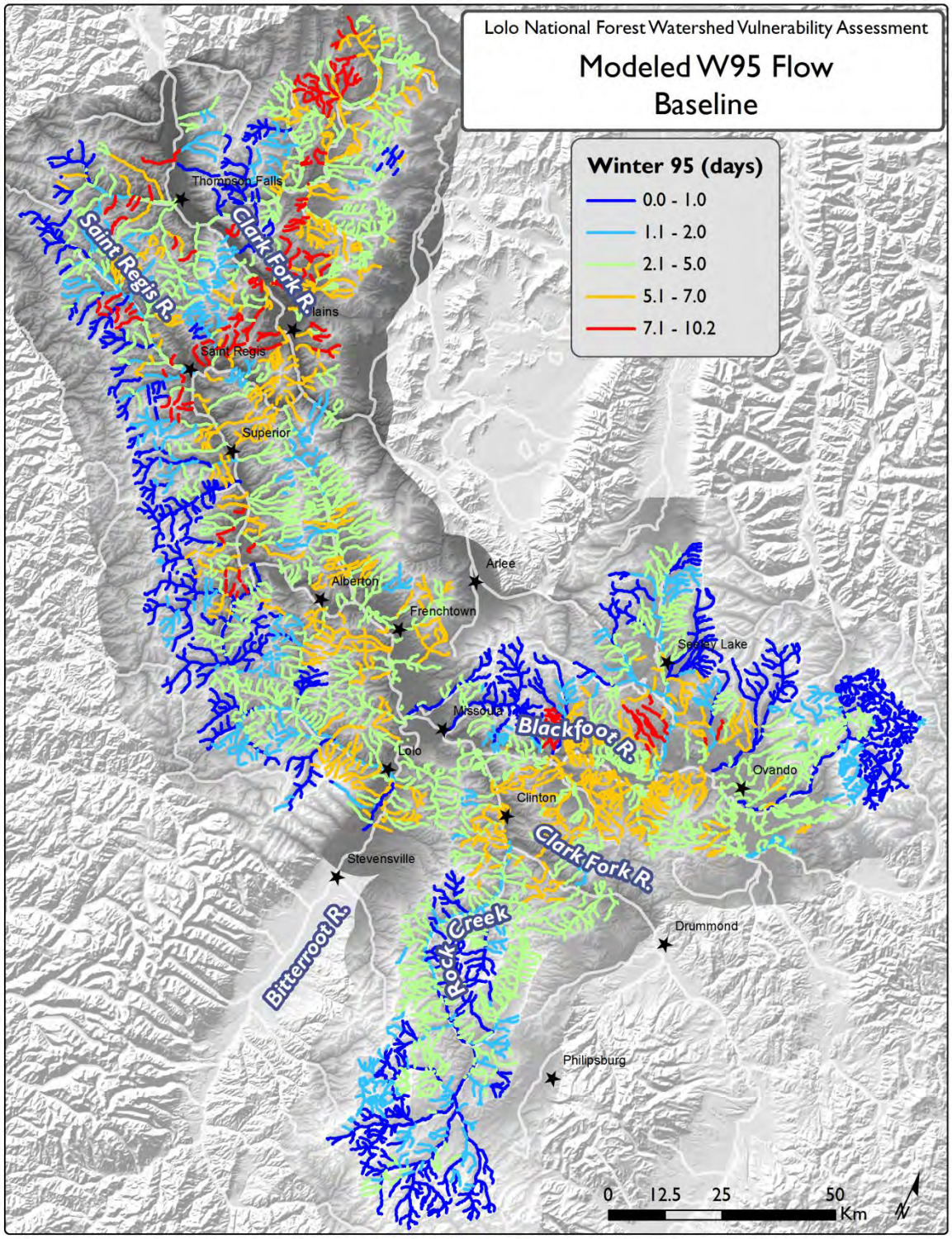

Figure 8. Modeled high winter flow days (W95) for baseline time period.

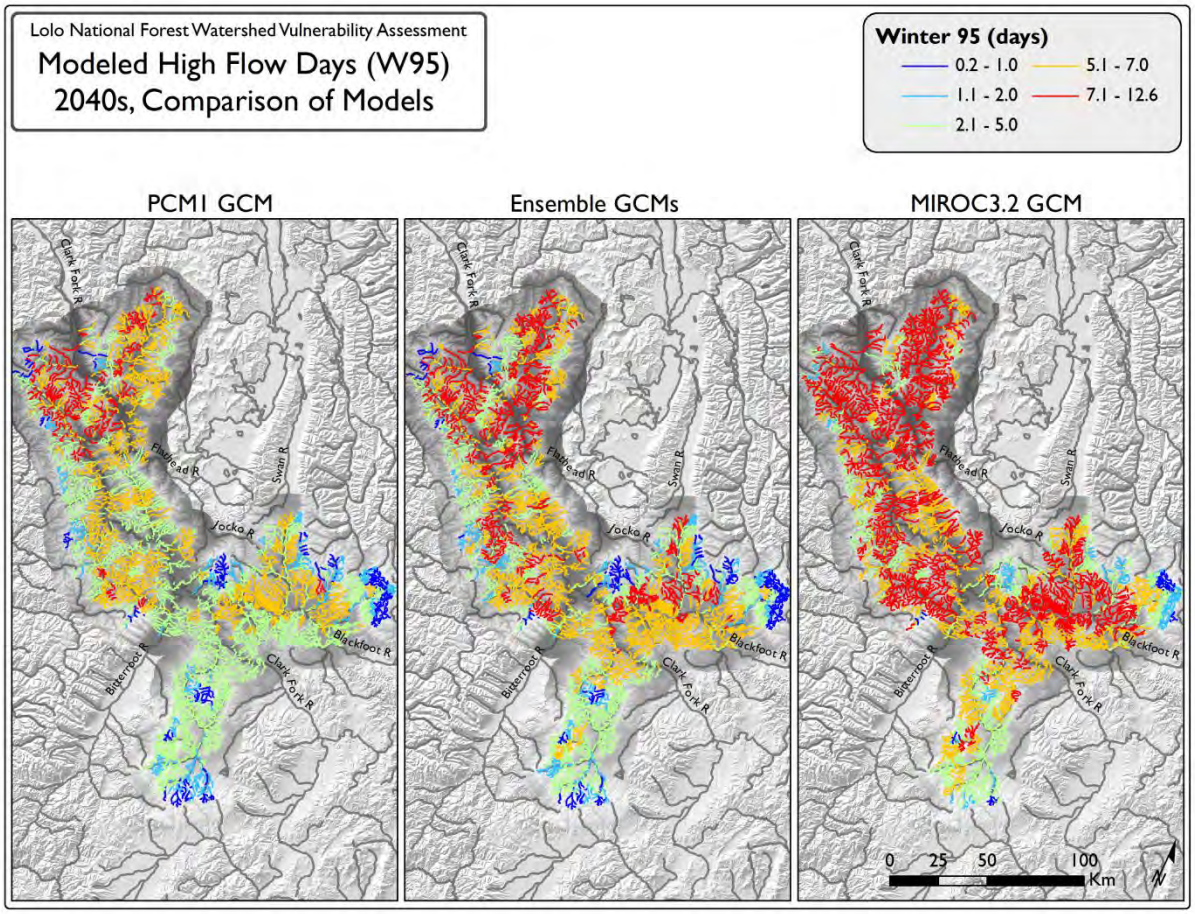

Figure 9. Comparison of modeled high winter flows (W95) using different GCM input for the 2040s. MIROC 3.2 GCM tends to project higher warming and less summer precipitation; PCM1 tends to project the opposite. In the middle panel is the output using an ensemble of GCMs; the data used for the analyses in this report.

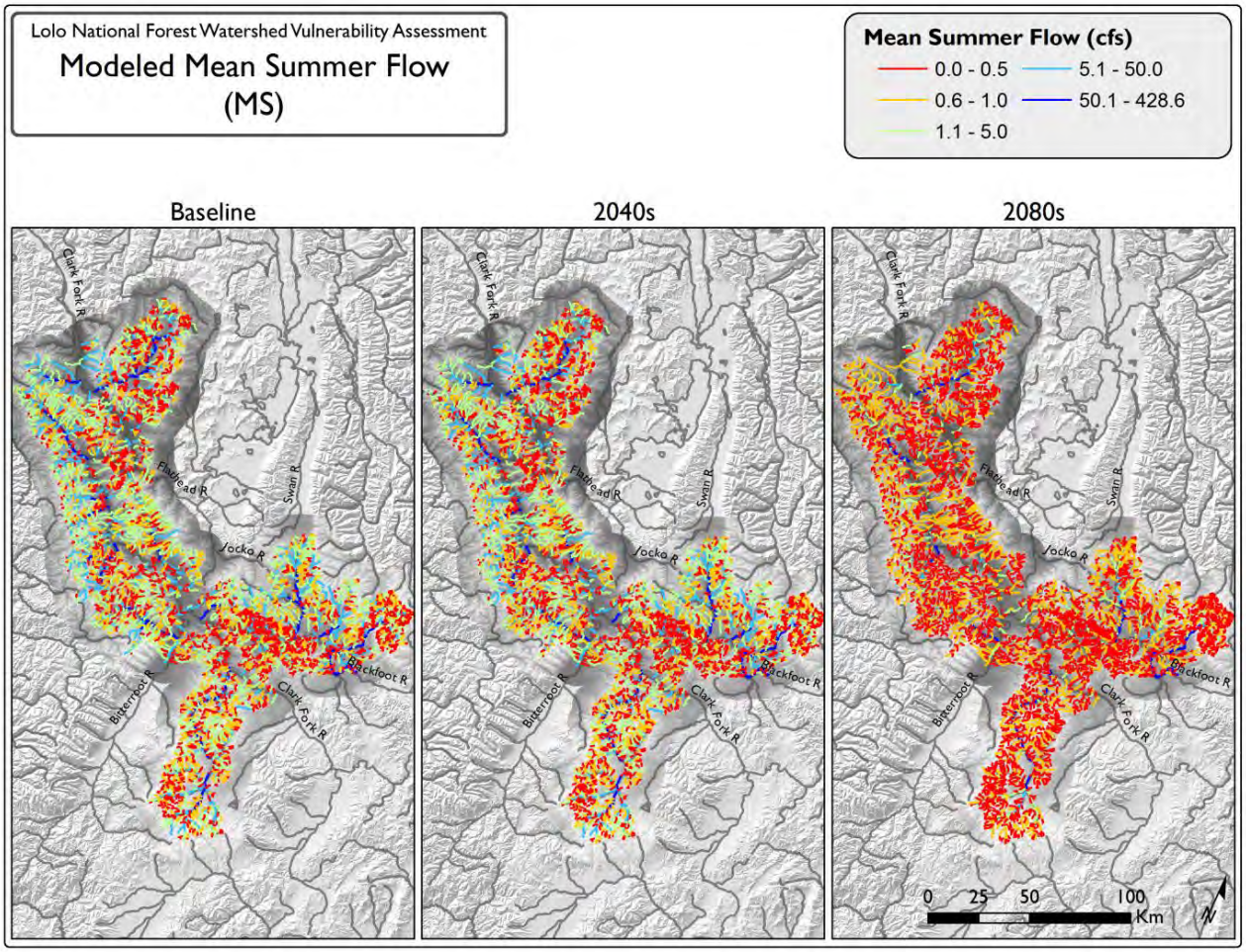

Figure 10. Modeled mean summer flow (MS) for baseline and for the 2040s and 2080s using an ensemble of GCMs. See Figure 11 for a larger map of the baseline modeled MS and see Figure 12 for a comparison of model outputs for the 2040s using different GCMs.

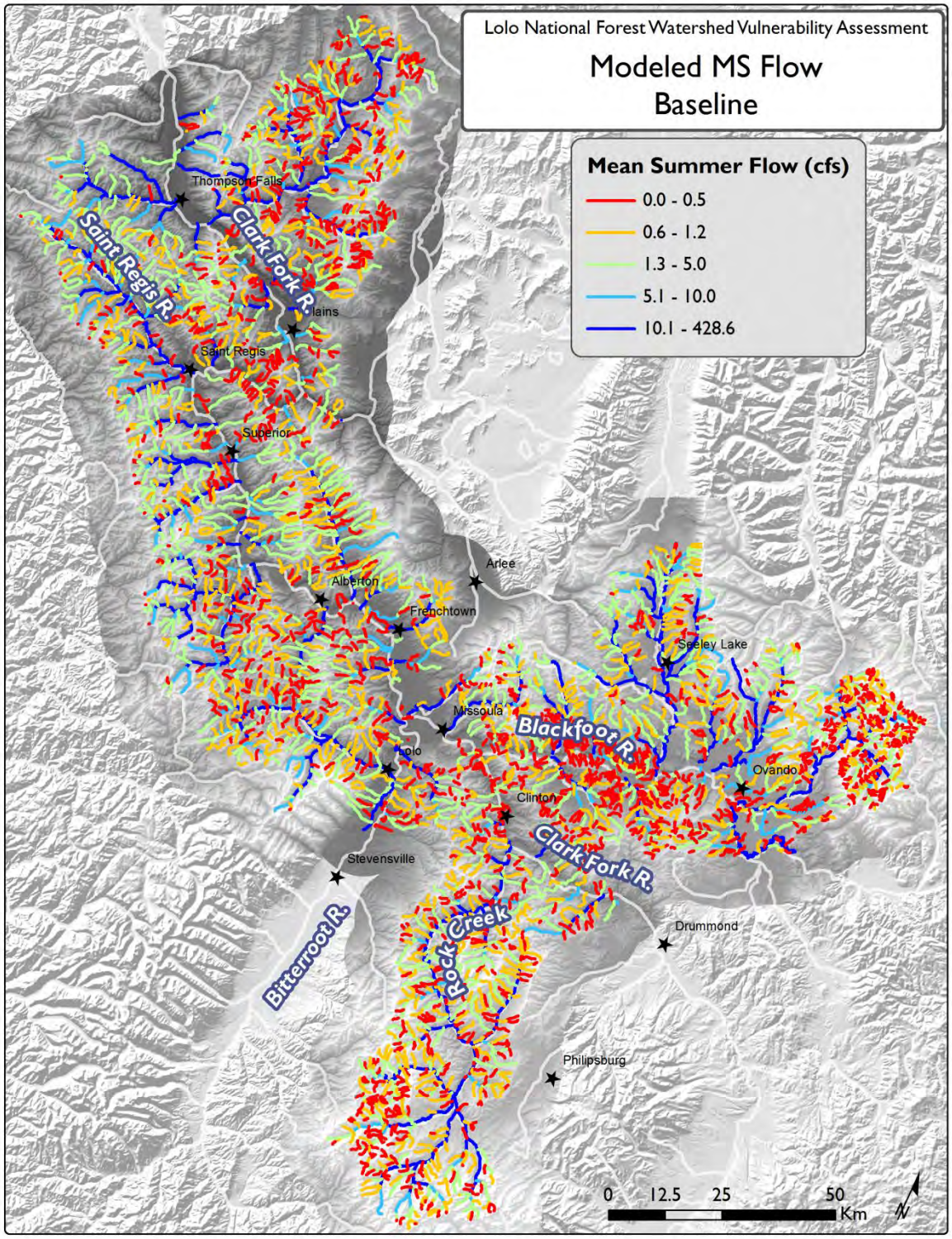

Figure 11. Modeled mean summer flow (MS) for baseline time period.

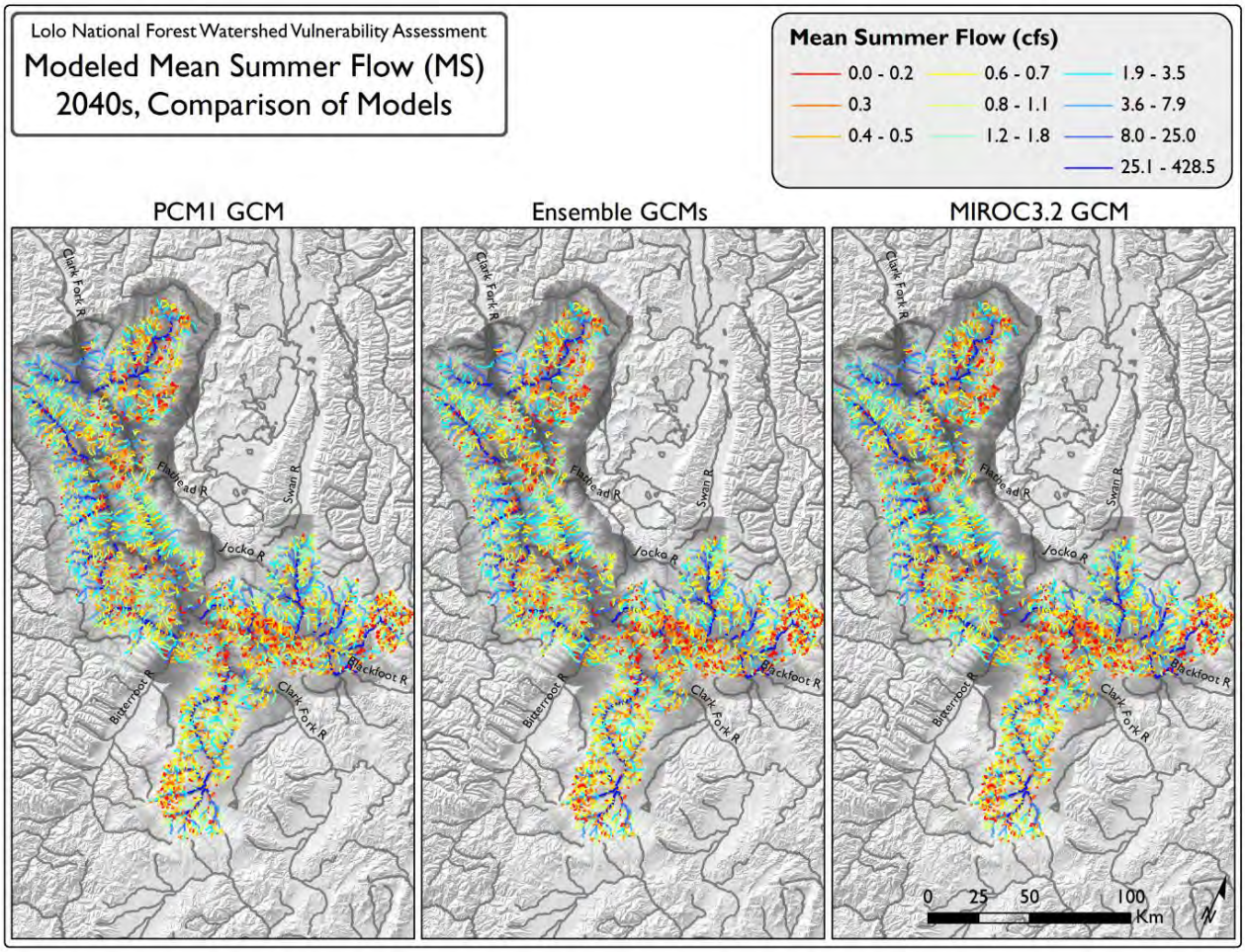

Figure 12. Comparison of modeled mean summer flow (MS) using different GCM input for the 2040s. MIROC 3.2 GCM tends to project higher warming and less summer precipitation; PCM1 tends to project the opposite. In the middle panel is the output using an ensemble of GCMs; the data used for the analyses in this report.

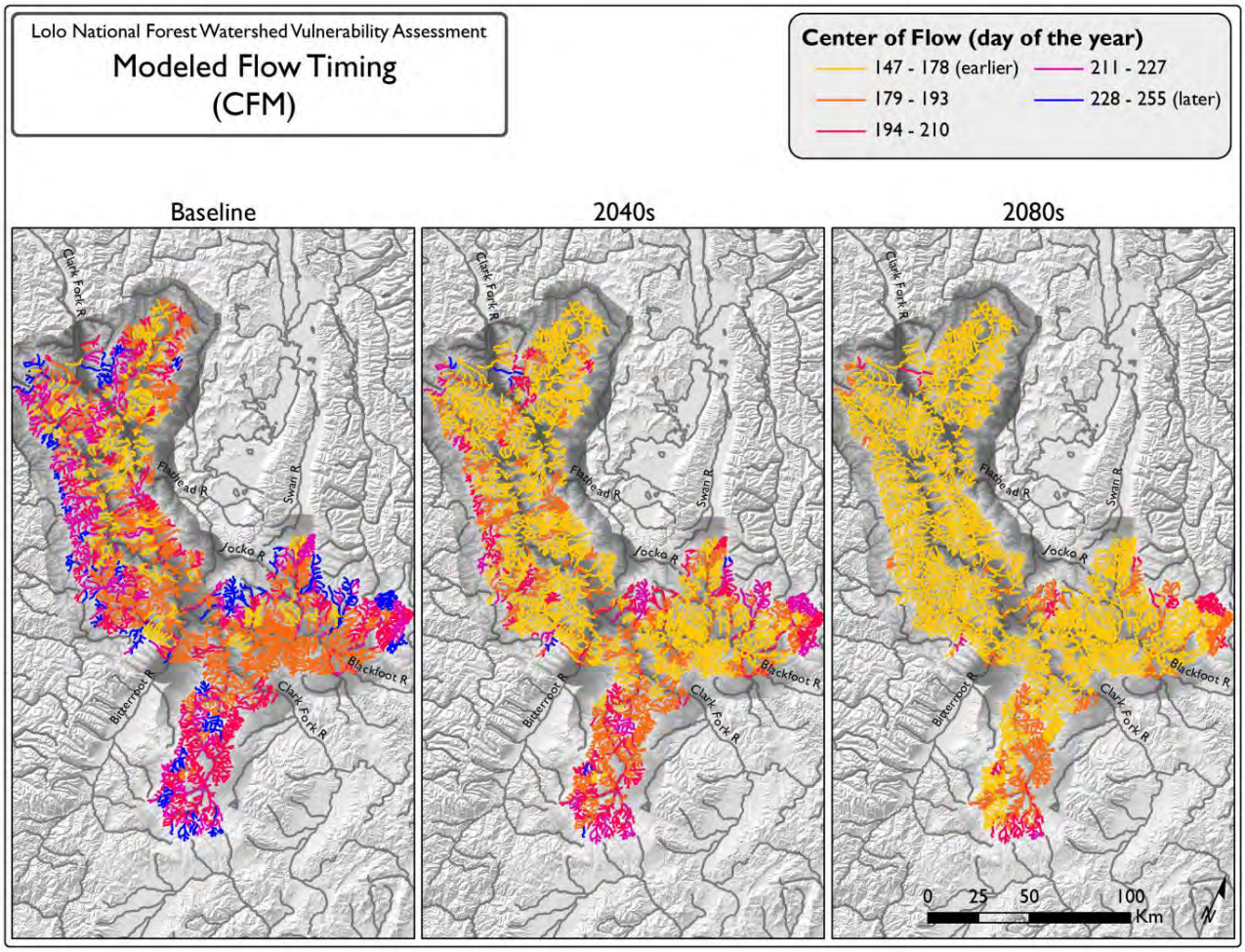

Figure 13. Modeled flow timing (CFM) for baseline and for the 2040s and 2080s using an ensemble of GCMs. See Figure 14 for a larger map of the baseline modeled MS and see Figure 15 for a comparison of model outputs for the 2040s using different GCMs

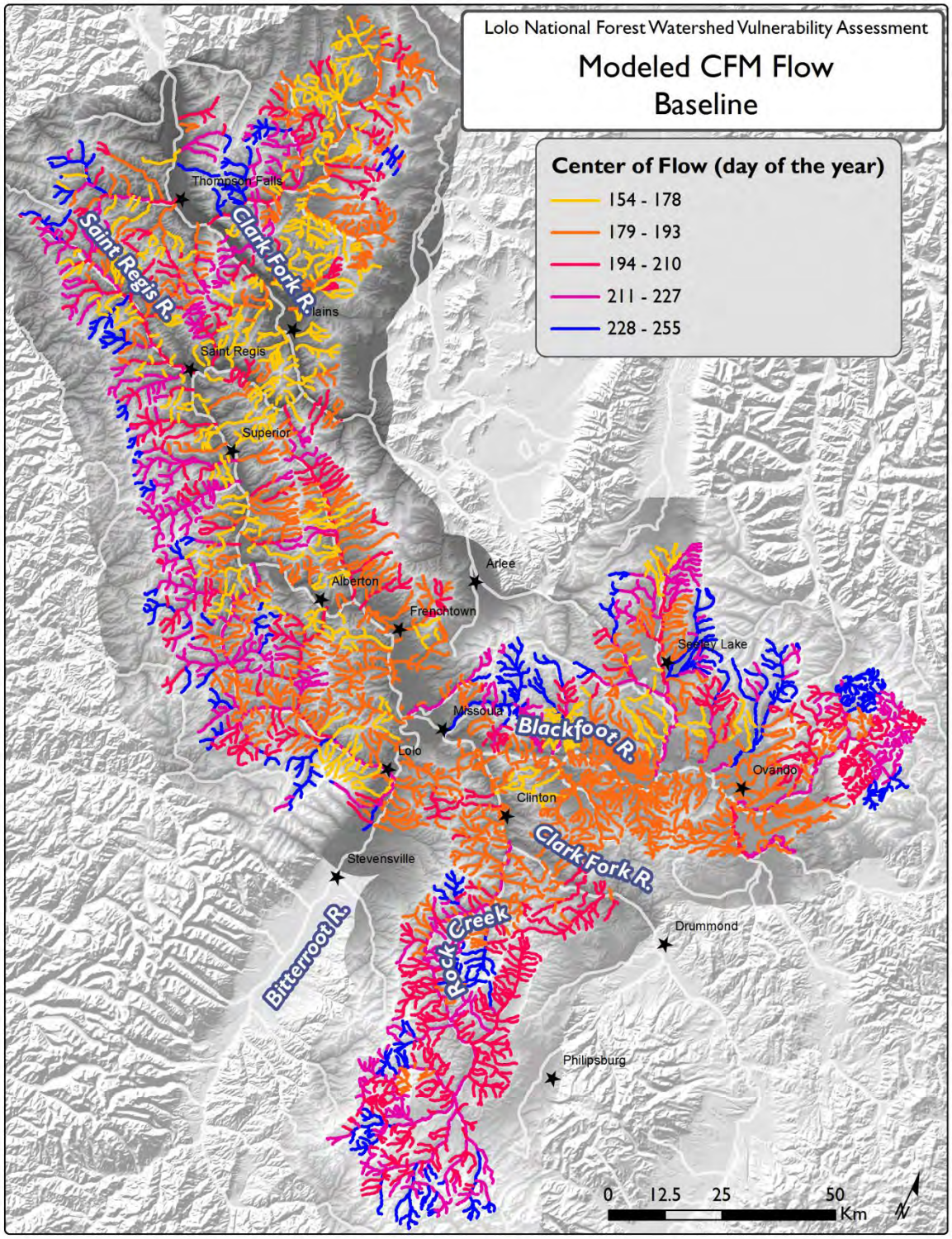

Figure 14. Modeled shift in timing of flows (CFM) for baseline time period.

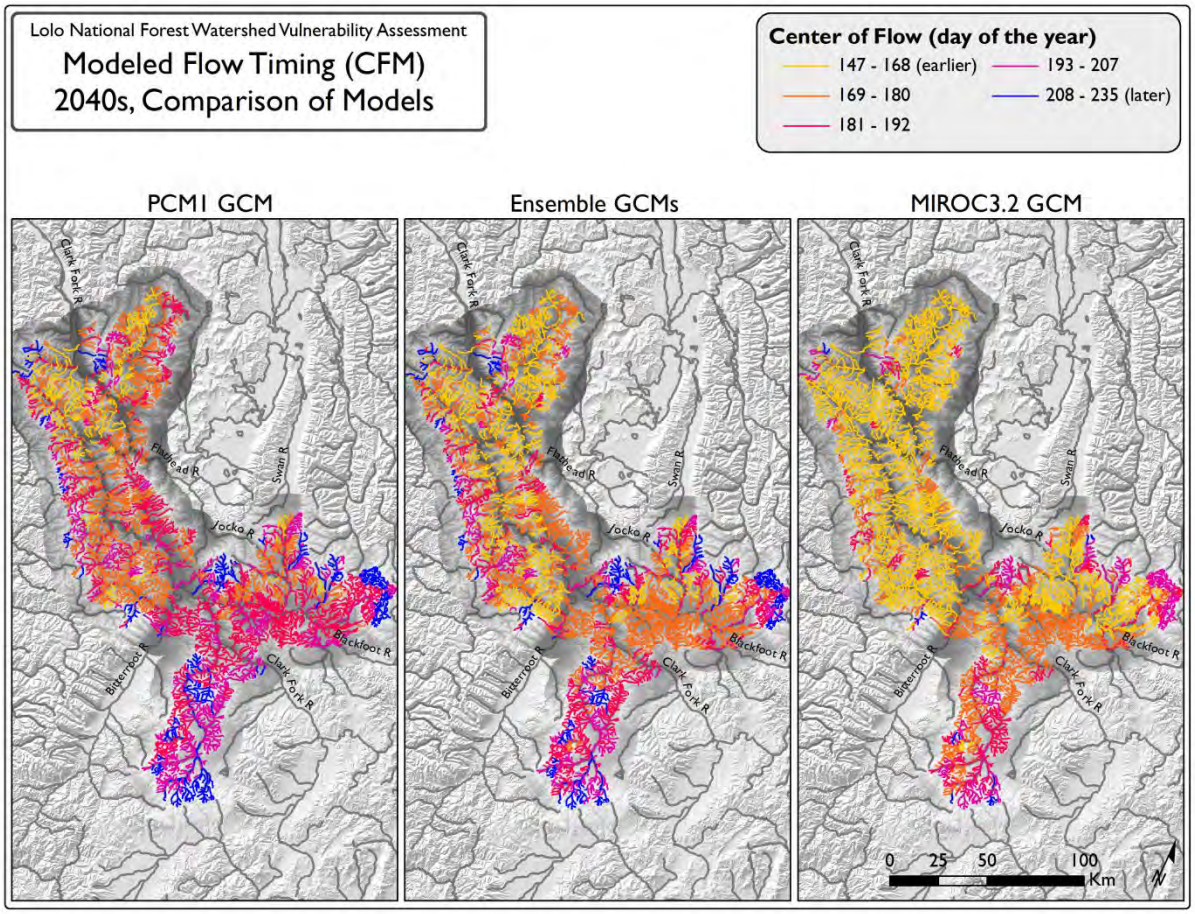

Figure 15. Comparison of modeled shift in timing of flows (CFM) using different GCM input for the 2040s. MIROC 3.2 GCM tends to project higher warming and less summer precipitation; PCM1 tends to project the opposite. In the middle panel is the output using an ensemble of GCMs; the data used for the analyses in this report.

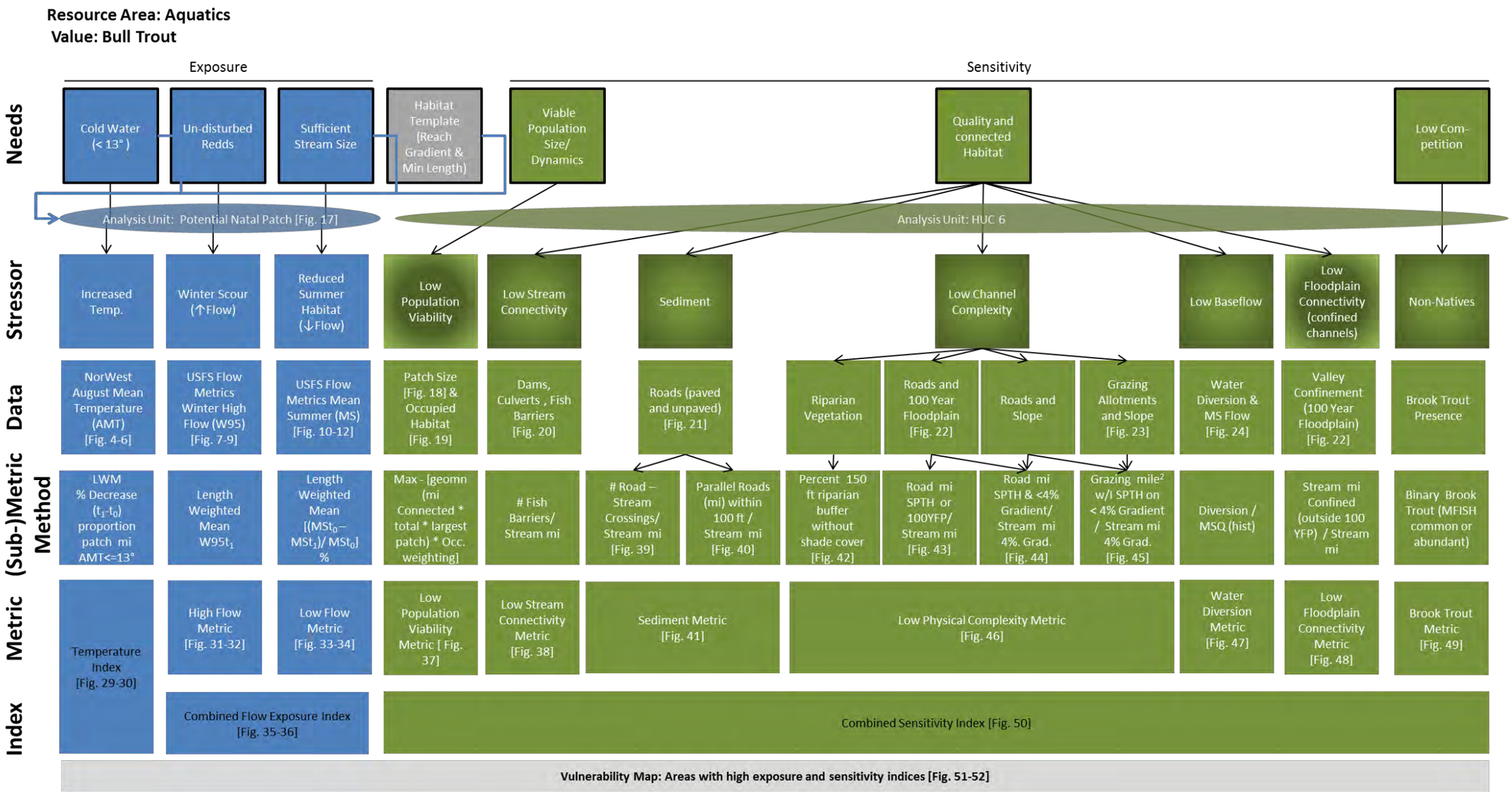

Figure 16. Conceptual model for bull trout resource needs and resource stressors used in determining exposure and sensitivity indices.

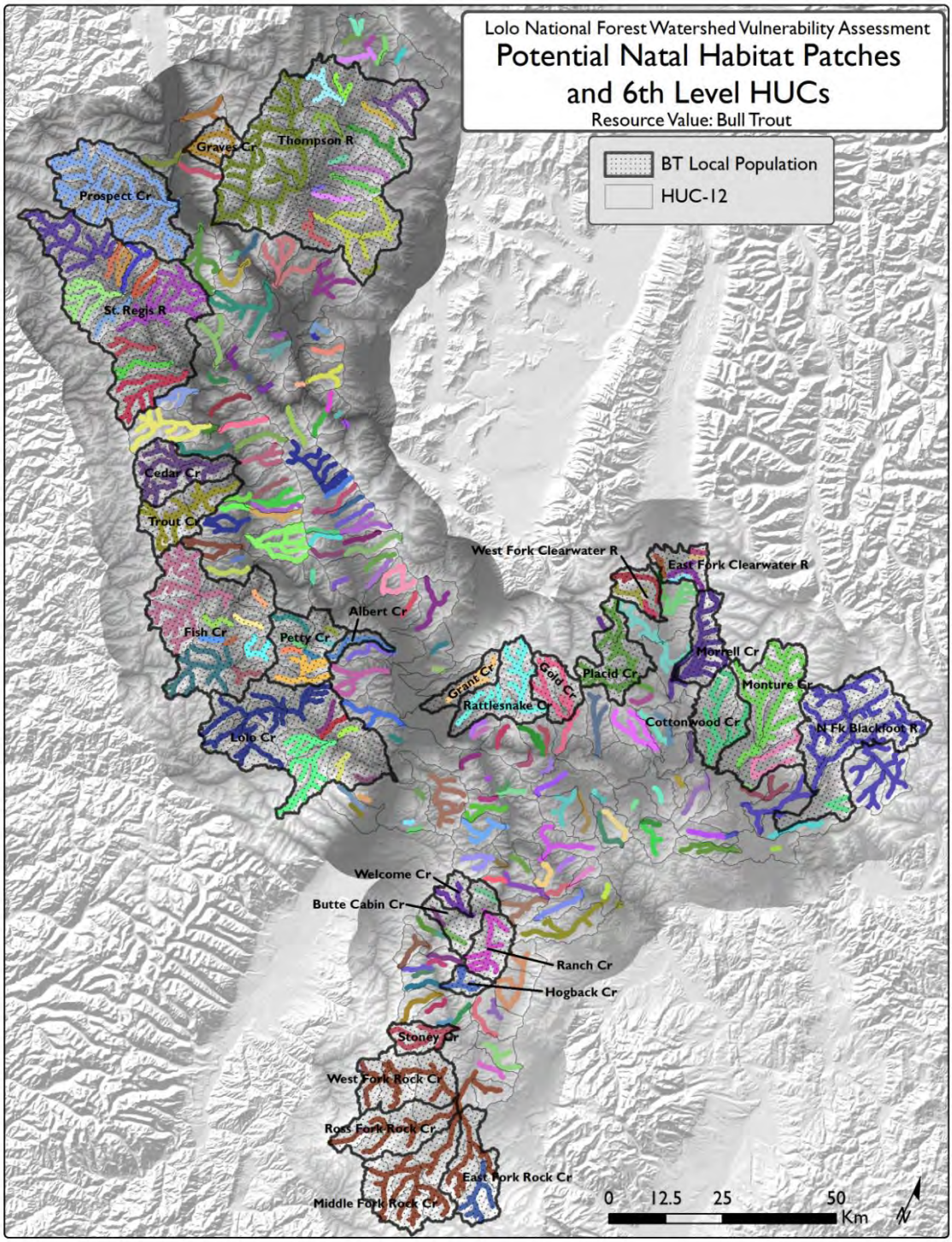

Figure 17. For the bull trout analysis, we used potential natal habitat patches as the unit of analysis for exposure metrics. Each unique color represents a unique patch. Exposure metrics were summarized by 6th level hydrological unit code (HUC-12). We summarize results by local populations. We show bull trout core areas (USFS & USFWS 2013), into which local populations are nested, for reference. Overall, in western Montana, there are 13 complex core areas containing 108 local populations and 6 simple core areas (with one local population each). Our study area includes portions of 6 core areas.

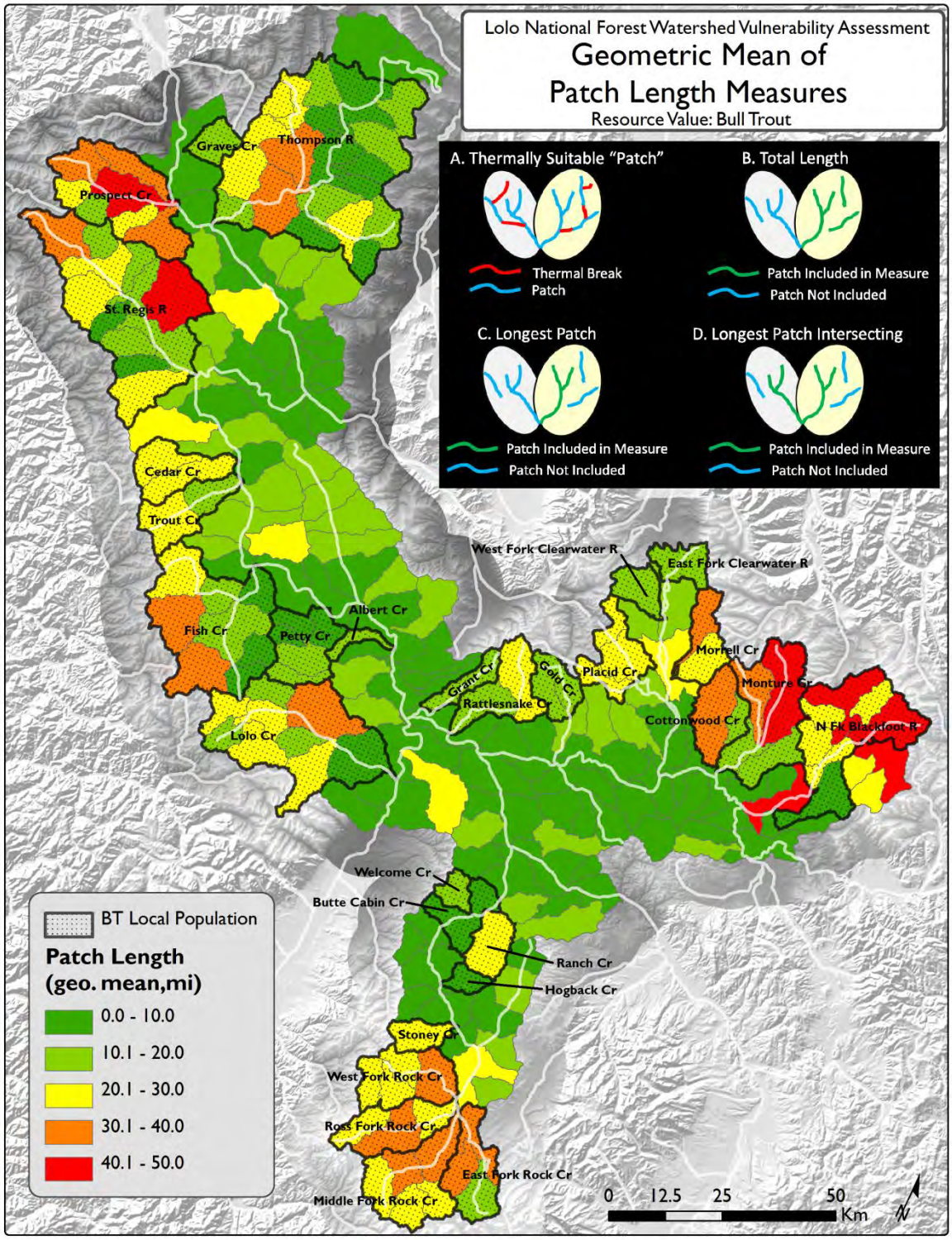

Figure 18. To calculate the low population viability metric (Figure 37), we first calculated the amount of patch in each HUC-12 (see insert of schematic of our methods: the patch area shown as green) We calculated the geometric mean of 3 patch length measures: 1) the total length (mi) of all patch contained within a given HUC-12 boundary (schematic panel B) (, 2) the longest (mi) patch contained within the HUC-12 boundary (schematic panel C), and 3) the longest patch (mi) that intersected the HUC-12 boundary (but may have extended beyond the given HUC-12 boundary; schematic panel D).

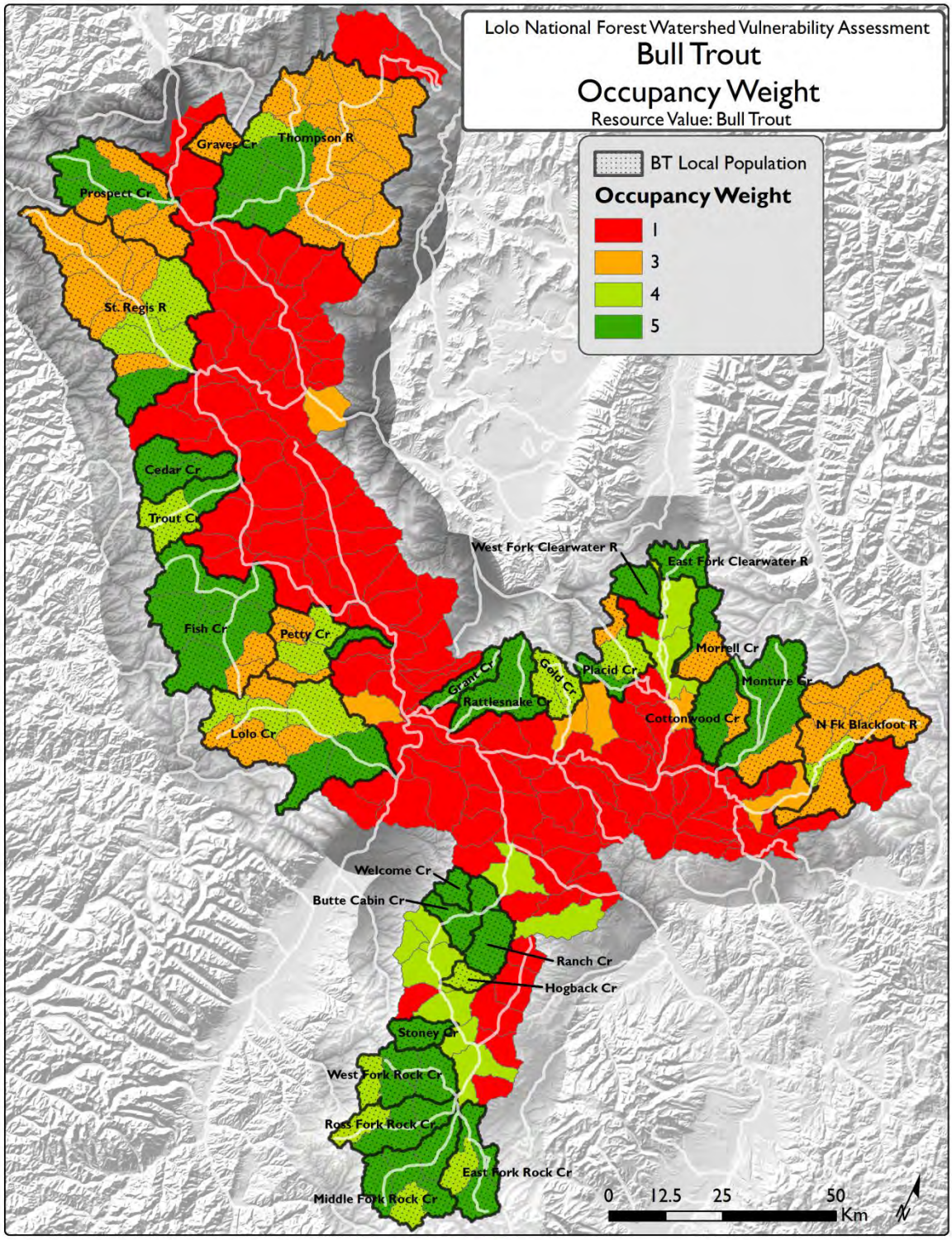

Figure 19. We weighted the amount of patch in a HUC-12 (Figure 18) by an "occupancy weight" to create the final population viability metric (Figure 37). The occupancy weight compared three datasets that depicted known presence of bull trout or exceptional bull trout habitat. The occupancy weight was 1 (lowest occupancy) if the HUC-12 had no datasets depicting presence, otherwise it was the number of datasets depicting presence + 2.

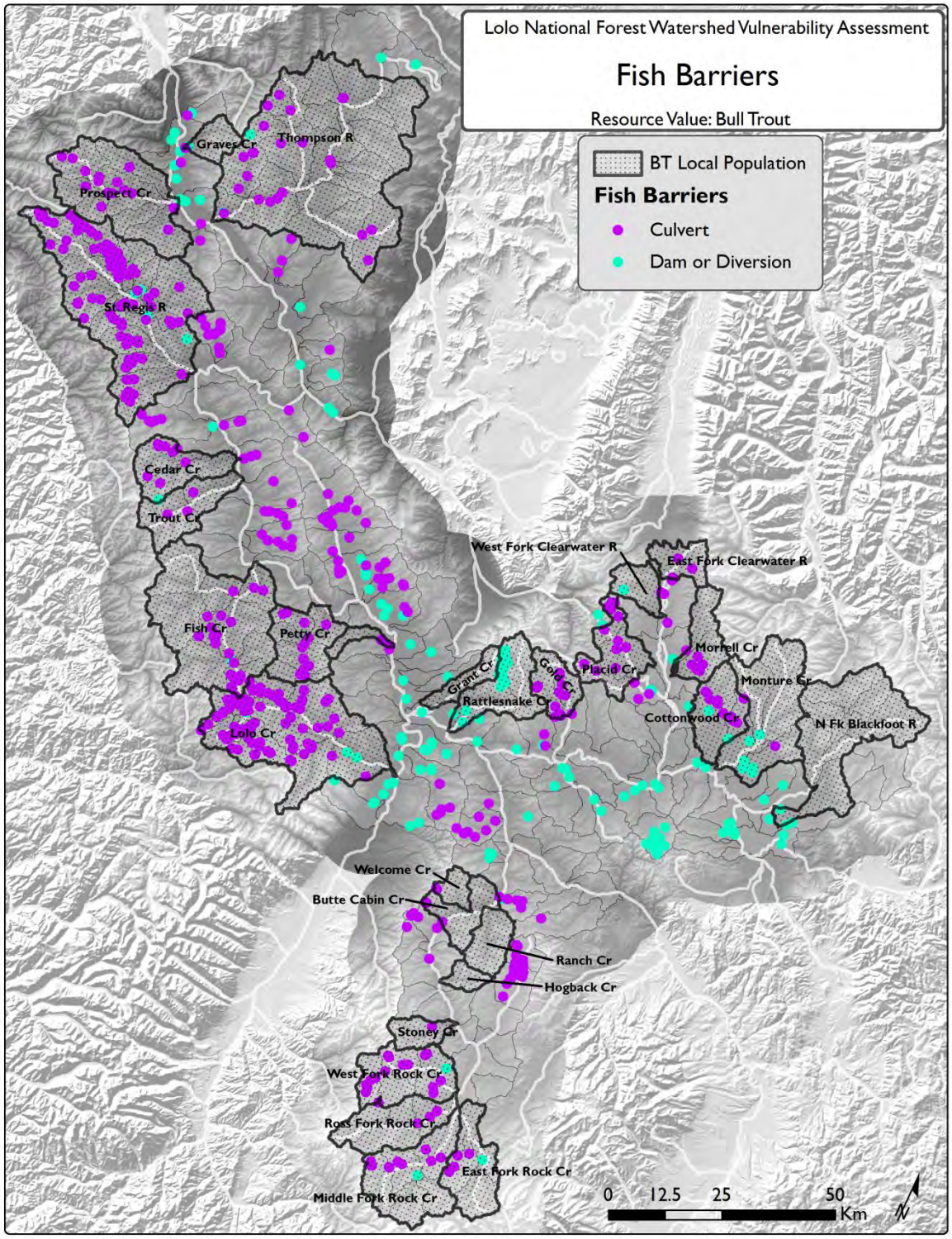

Figure 20. Fish barriers, colored by type (culvert vs. dam or diversion) used in calculating low stream connectivity metric (Figure 38).

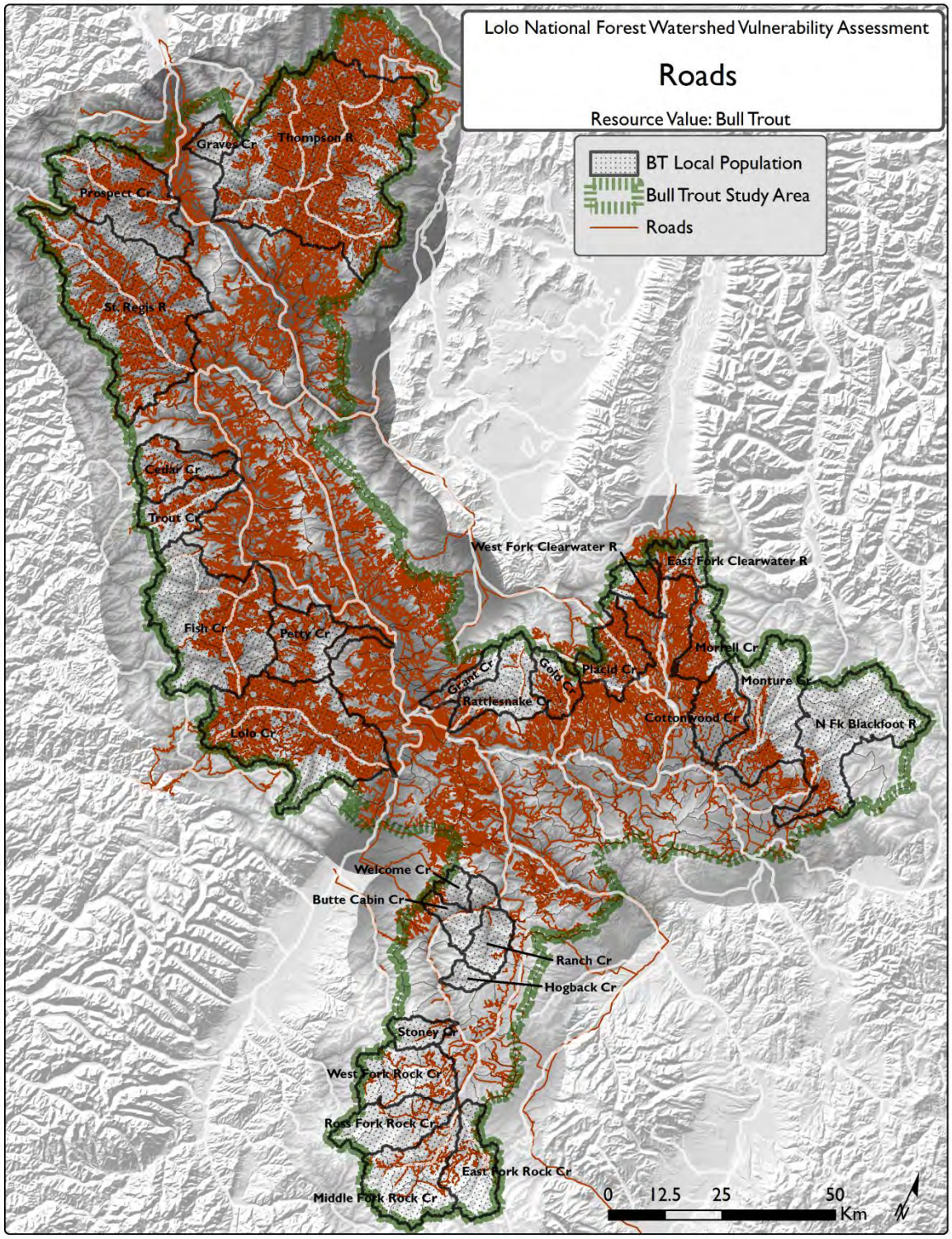

Figure 21. Roads used in bull trout analysis.

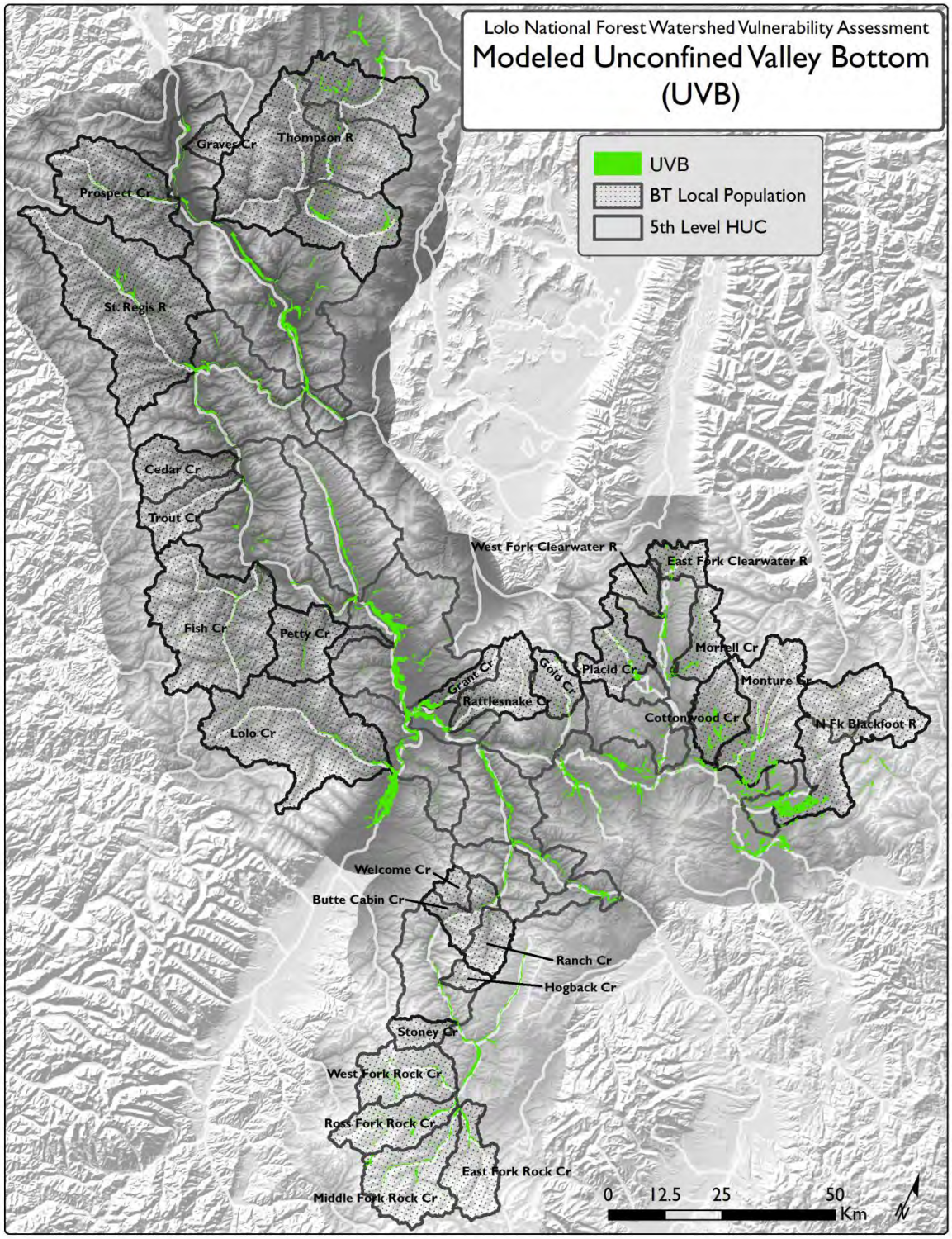

Figure 22. Modeled unconfined valley bottom (UVB) using algorithm from Nagel et al. (2014), used in calculating floodplain related metrics (Figure 43, Figure 63, Figure 64, and Figure 65) and low floodplain connectivity metric (Figure 48).

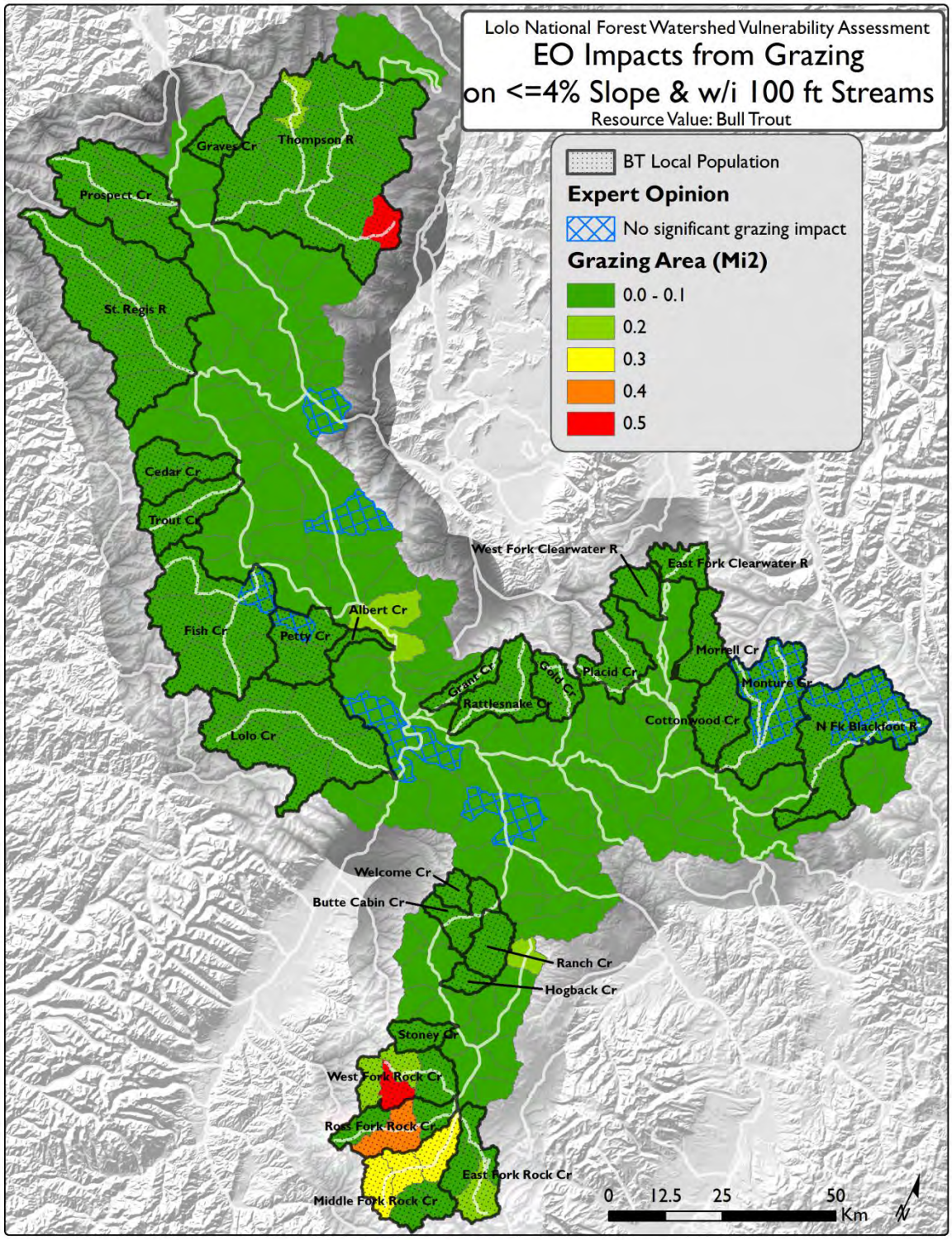

Figure 23. HUC-12s with grazing allotments within 100 feet of streams and on <=4% slopes and those HUC-12s identified as having no grazing related impacts by expert opinion (blue cross hatching).

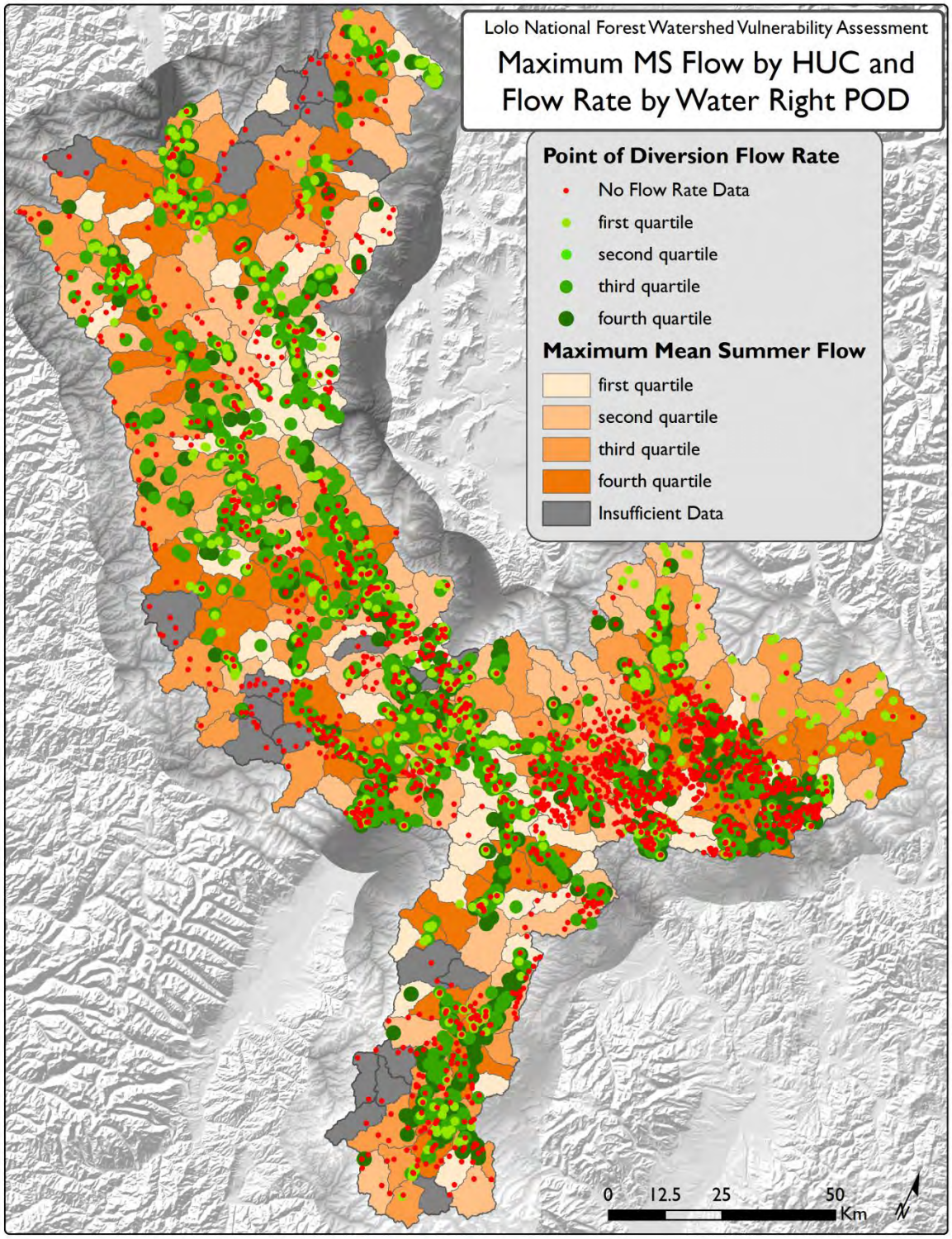

Figure 24. The water diversion metric (Figure 47, Figure 59) required data on the maximum mean summer (MS) flow in each HUC-12 and the flow rate associated with all water right points of diversion (POD) in each HUC-12. There were no flow rate data for 35% of the POD; the majority of which were located in the vicinity of the Blackfoot River.

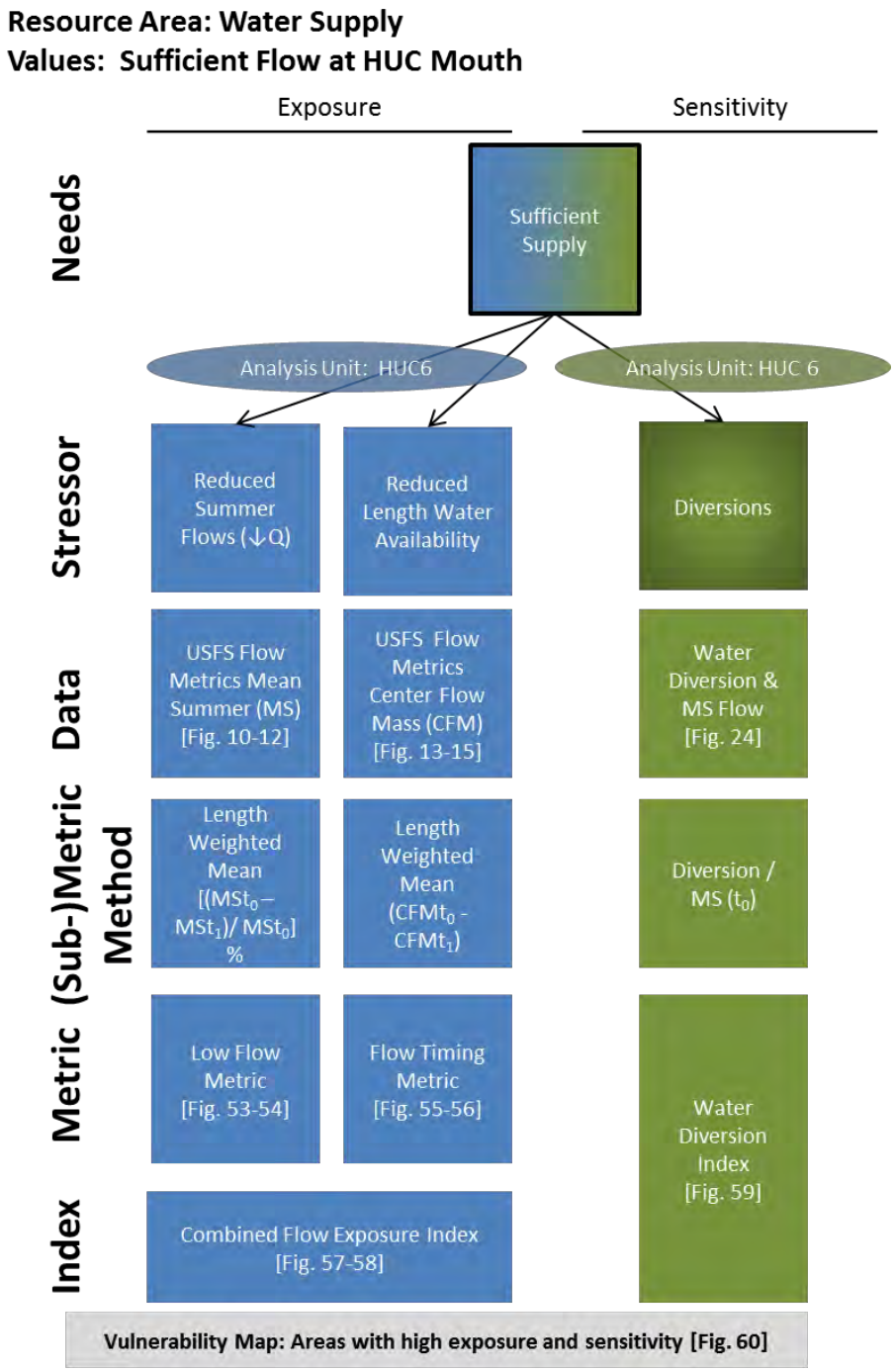

Figure 25. Conceptual model for water supply resource needs and resource stressors used in determining exposure and sensitivity indices.

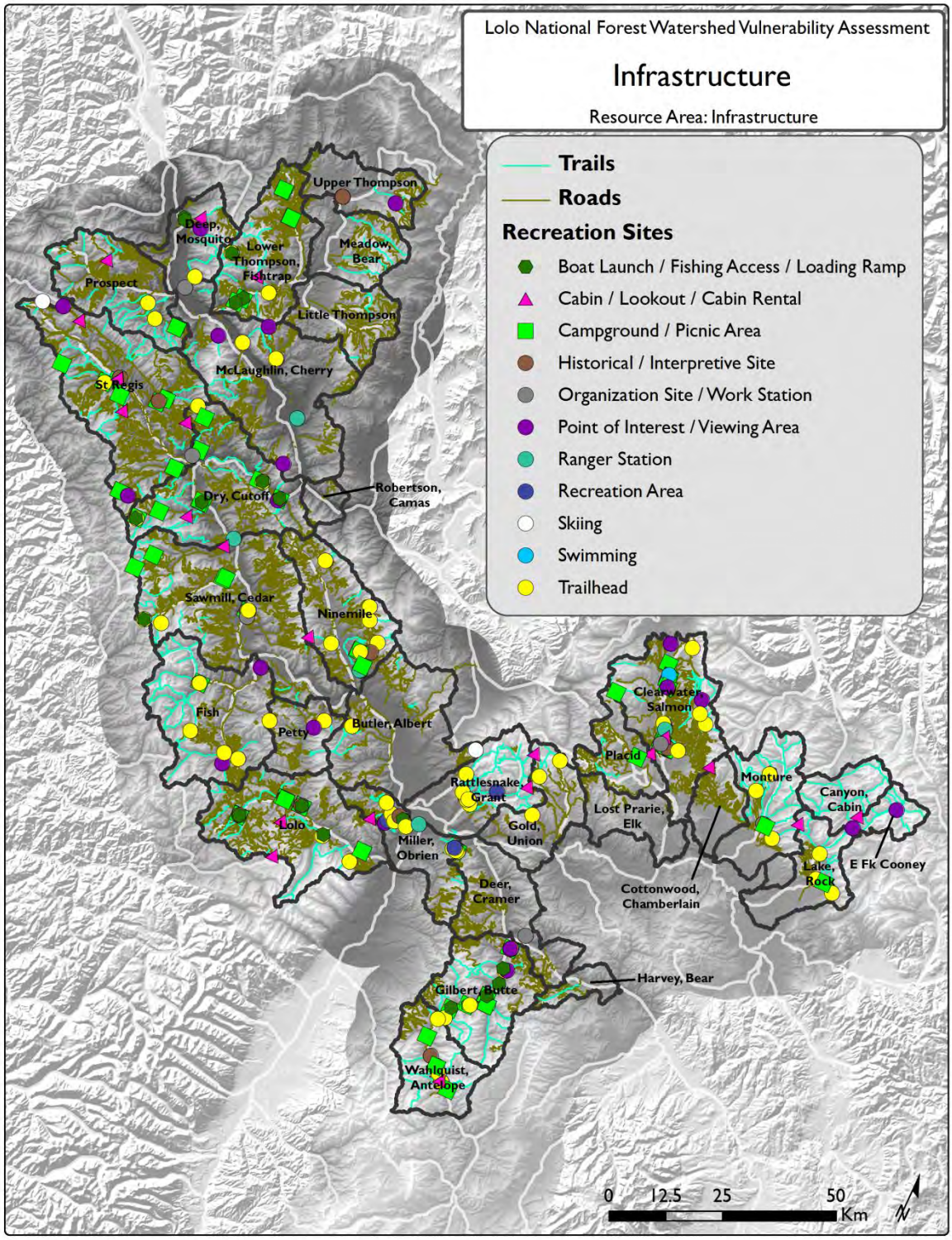

Figure 26. Map of infrastructure assessed for vulnerability: trails, roads, and recreation sites.

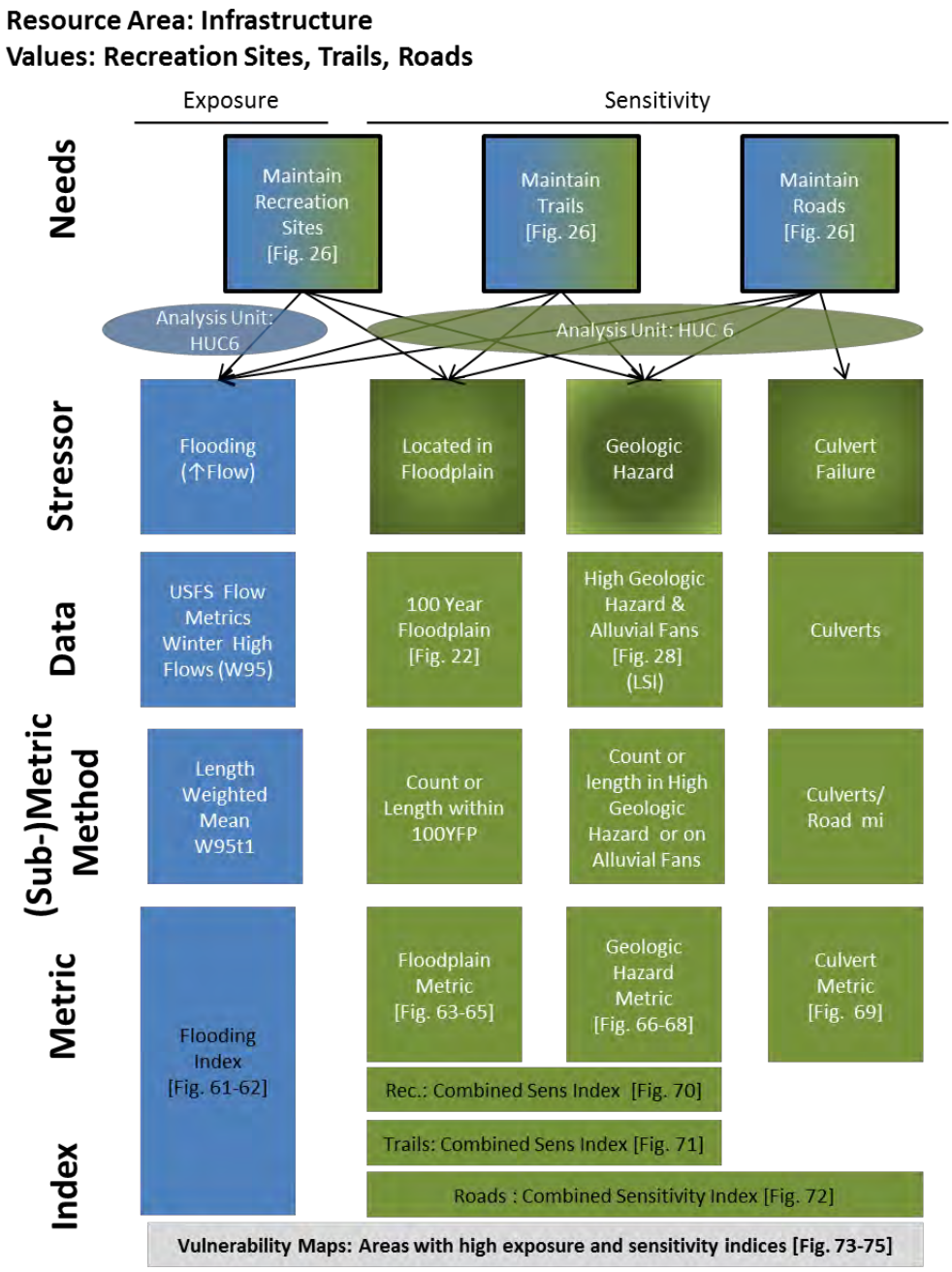

Figure 27. Conceptual model for infrastructure resource needs and resource stressors used in determining exposure and sensitivity indices.

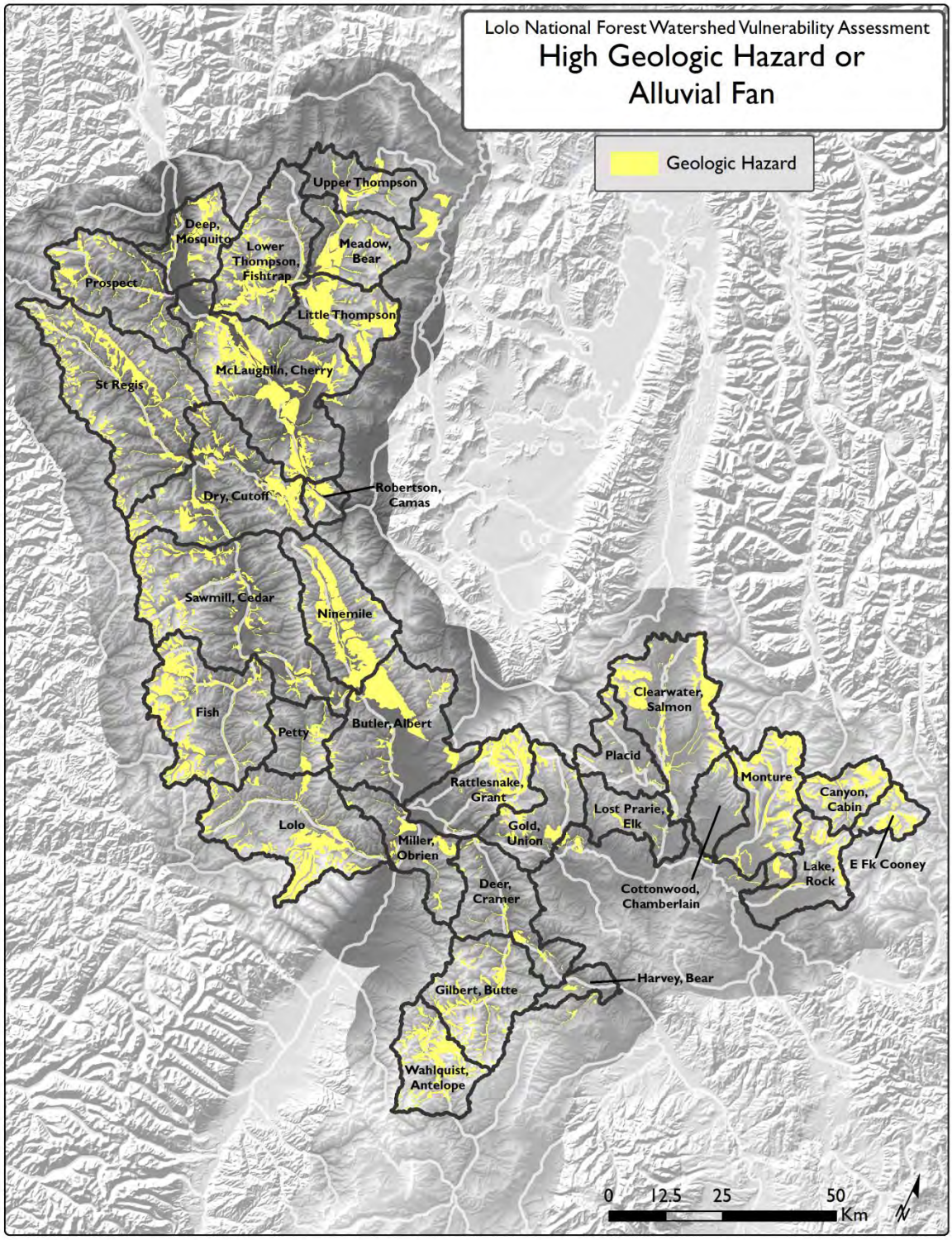

Figure 28. Areas with high geologic hazard or alluvial fan used in calculating the geologic hazard metrics (Figures 66, 67 and 68).

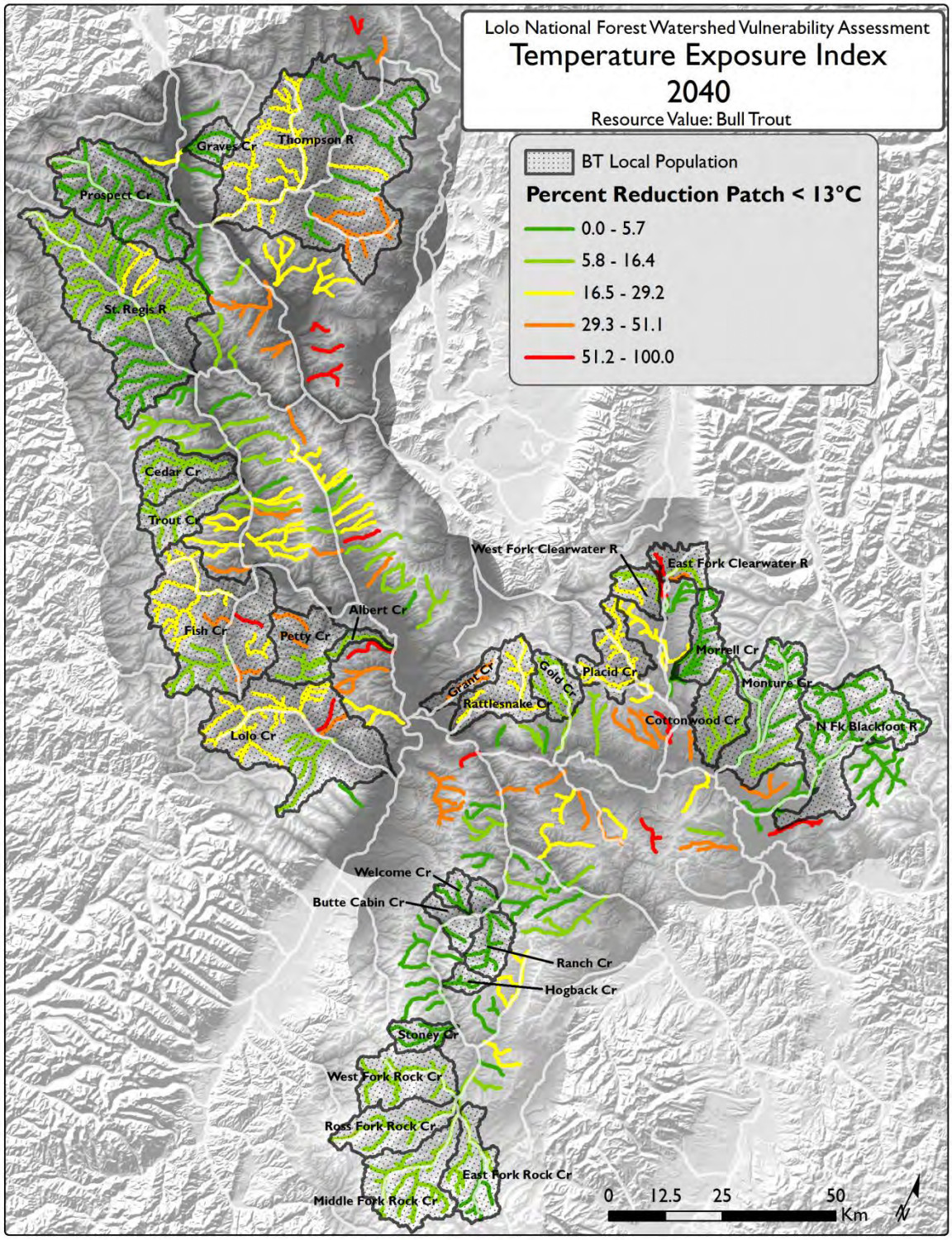

Figure 29. Temperature exposure index (here, only one metric used for this index) for bull trout by the 2040s. We calculated the percent decrease in the proportion of the patch length with AMT <=13°C between baseline modeled conditions and the 2040s. Local bull trout populations, designated in the *Conservation Strategy for Bull Trout* are shown overlain in stipling (here and in all following bull trout maps).

Confidence in metric: **moderate-high**

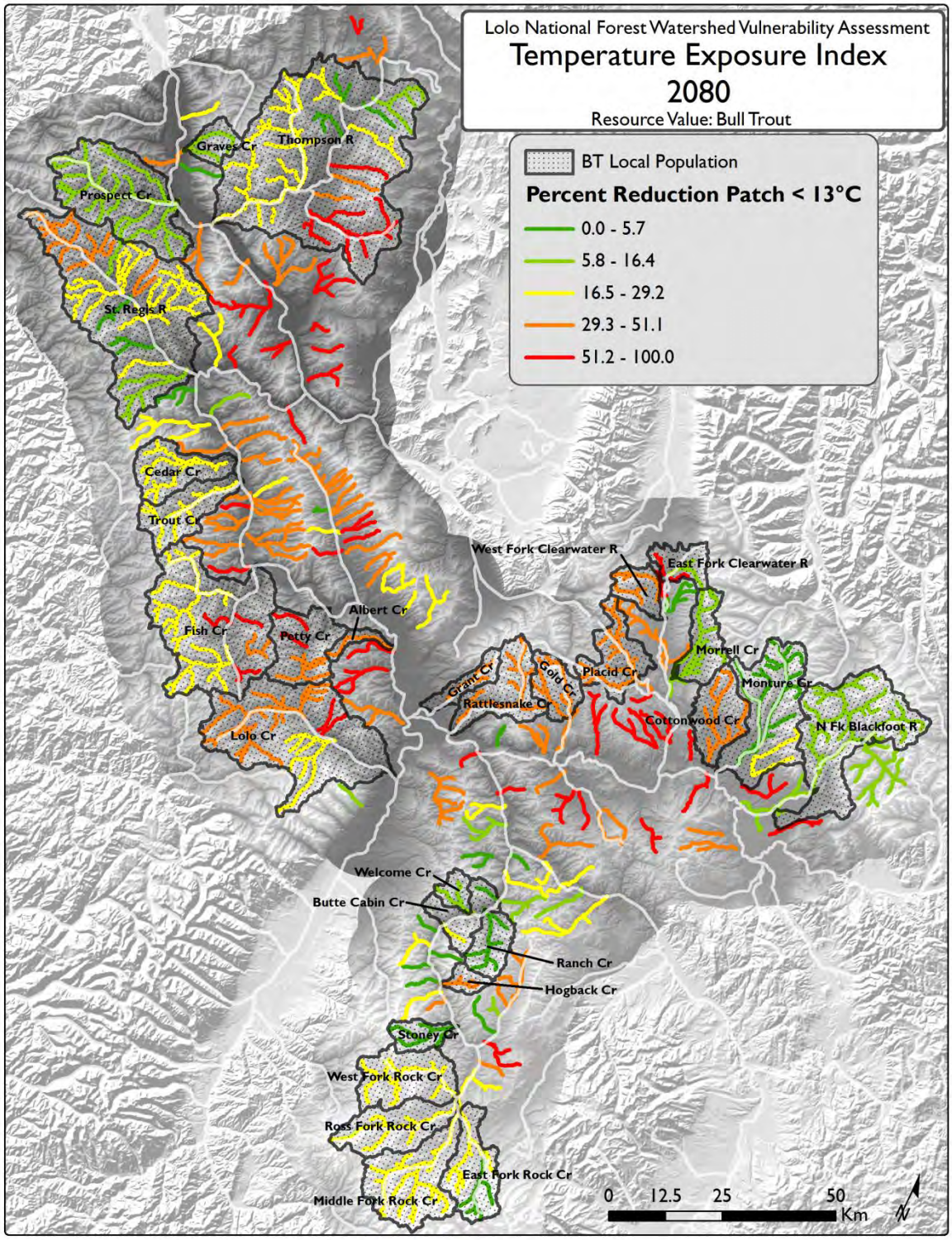

Figure 30. Temperature exposure index (and metric) for bull trout by the 2080s.
Confidence in metric: moderate

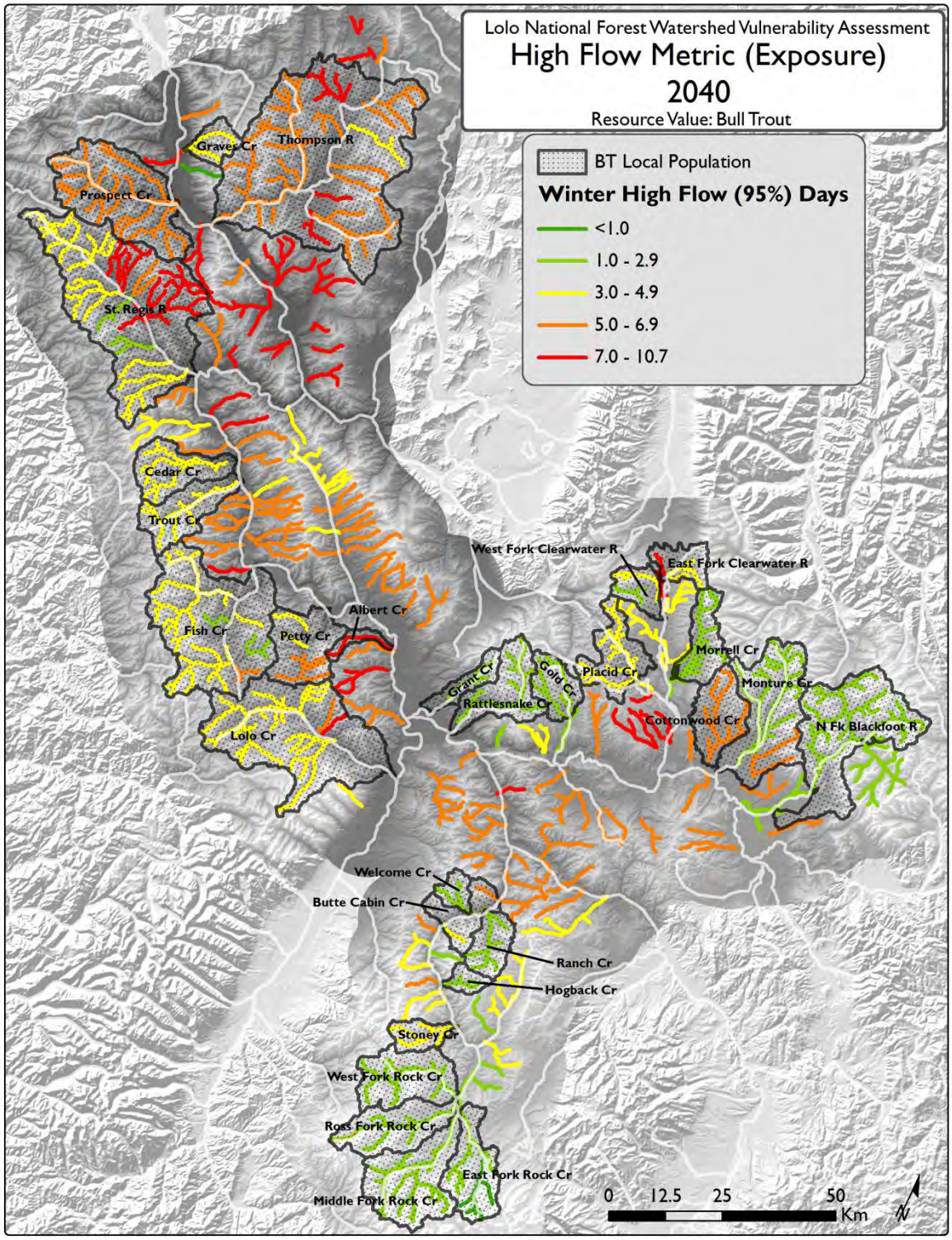

Figure 31. High flow exposure metric for bull trout by the 2040s. We used the number of projected future days with high (95%) winter flows.

Confidence in metric: **low-moderate**

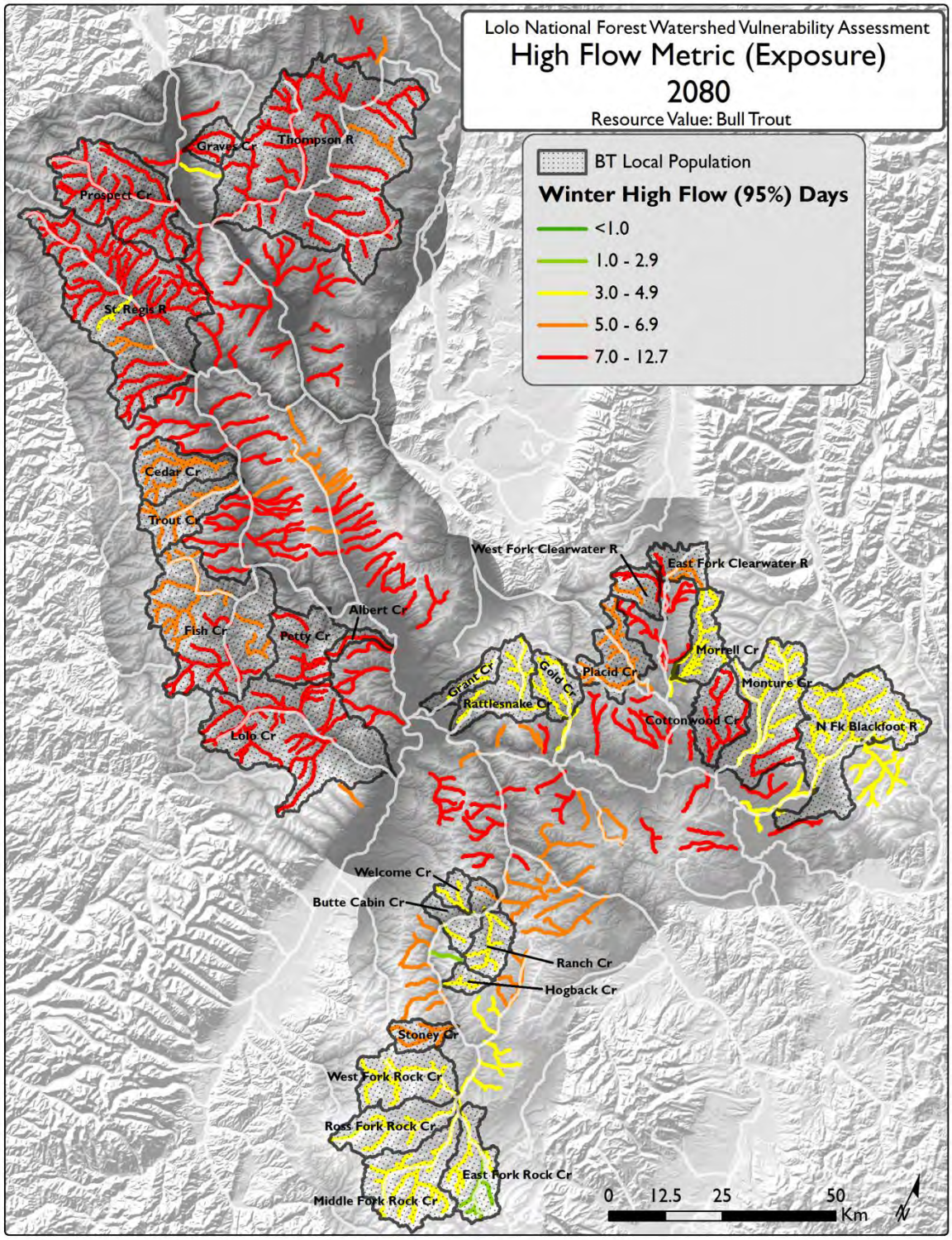

Figure 32. High flow exposure metric for bull trout by the 2080s.
Confidence in metric: **low**

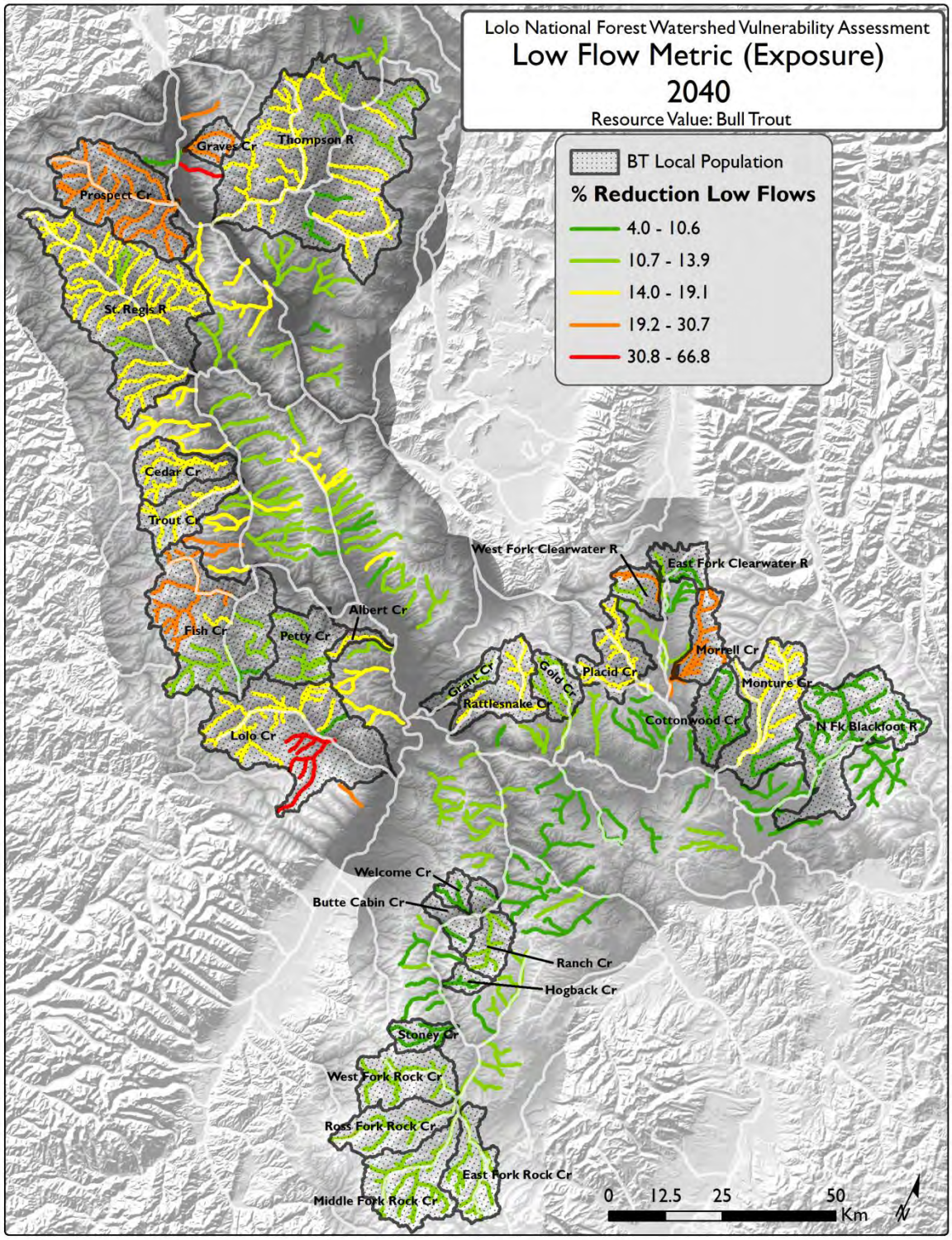

Figure 33. Low flow exposure metric for bull trout by the 2040s. We calculated the percent decrease in mean summer flows between baseline modeled conditions and the 2040s.

Confidence in metric: **low-moderate**

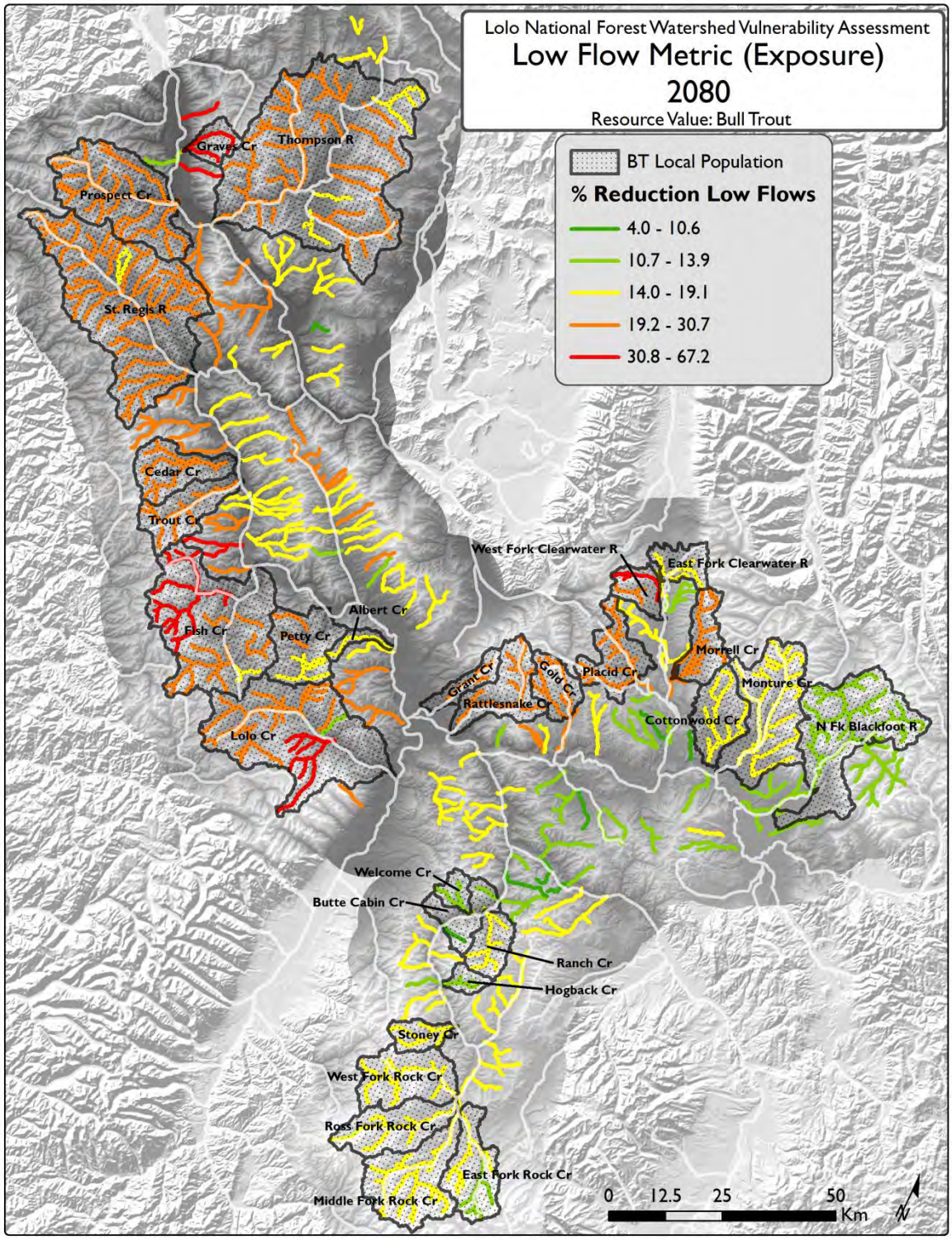

Figure 34. Low flow exposure metric for bull trout by the 2080s.
Confidence in metric: **low**

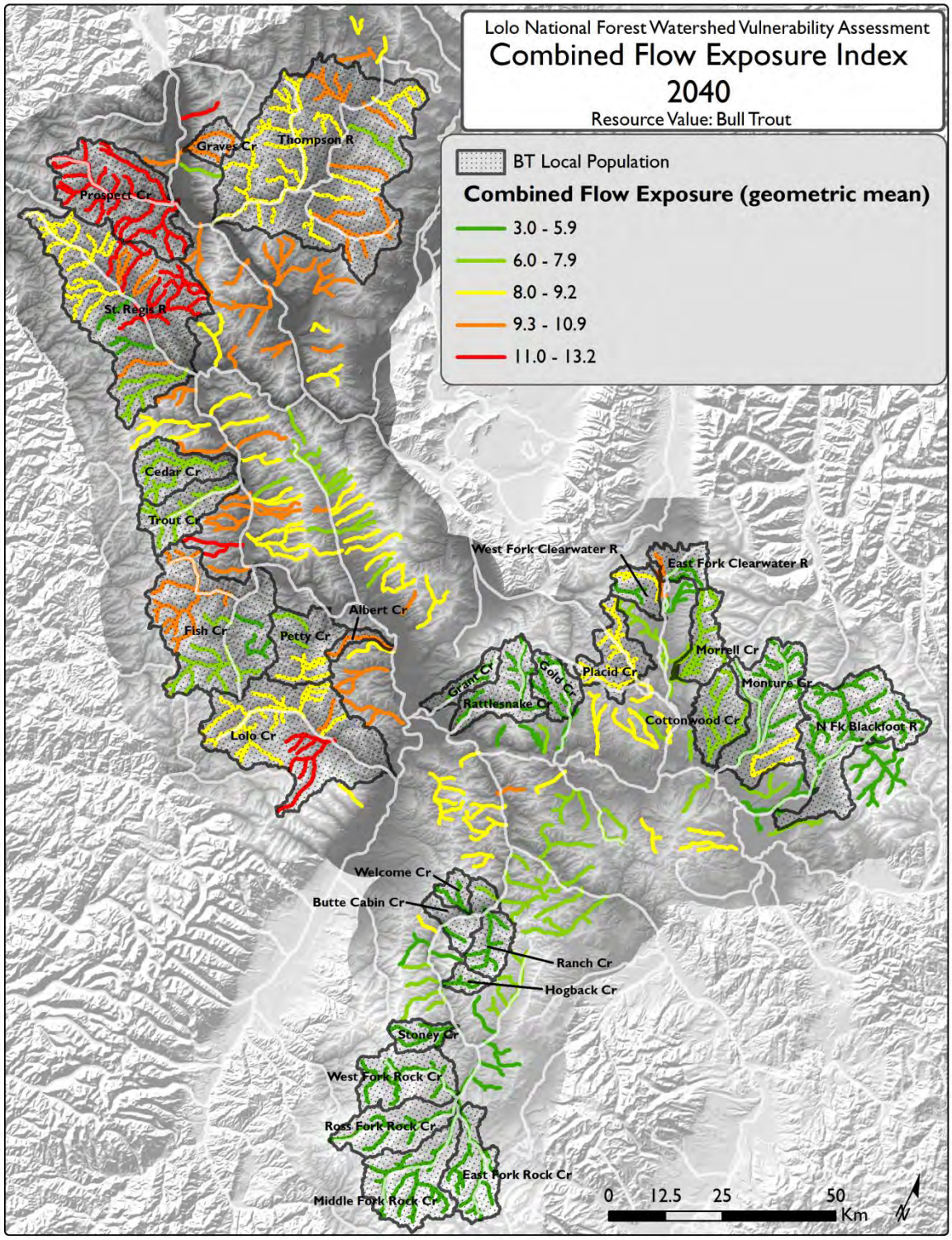

Figure 35. Combined flow exposure index for bull trout by the 2040s. We calculated the geometric mean of the high (Figure 31) and low (Figure 33) flow exposure metrics.

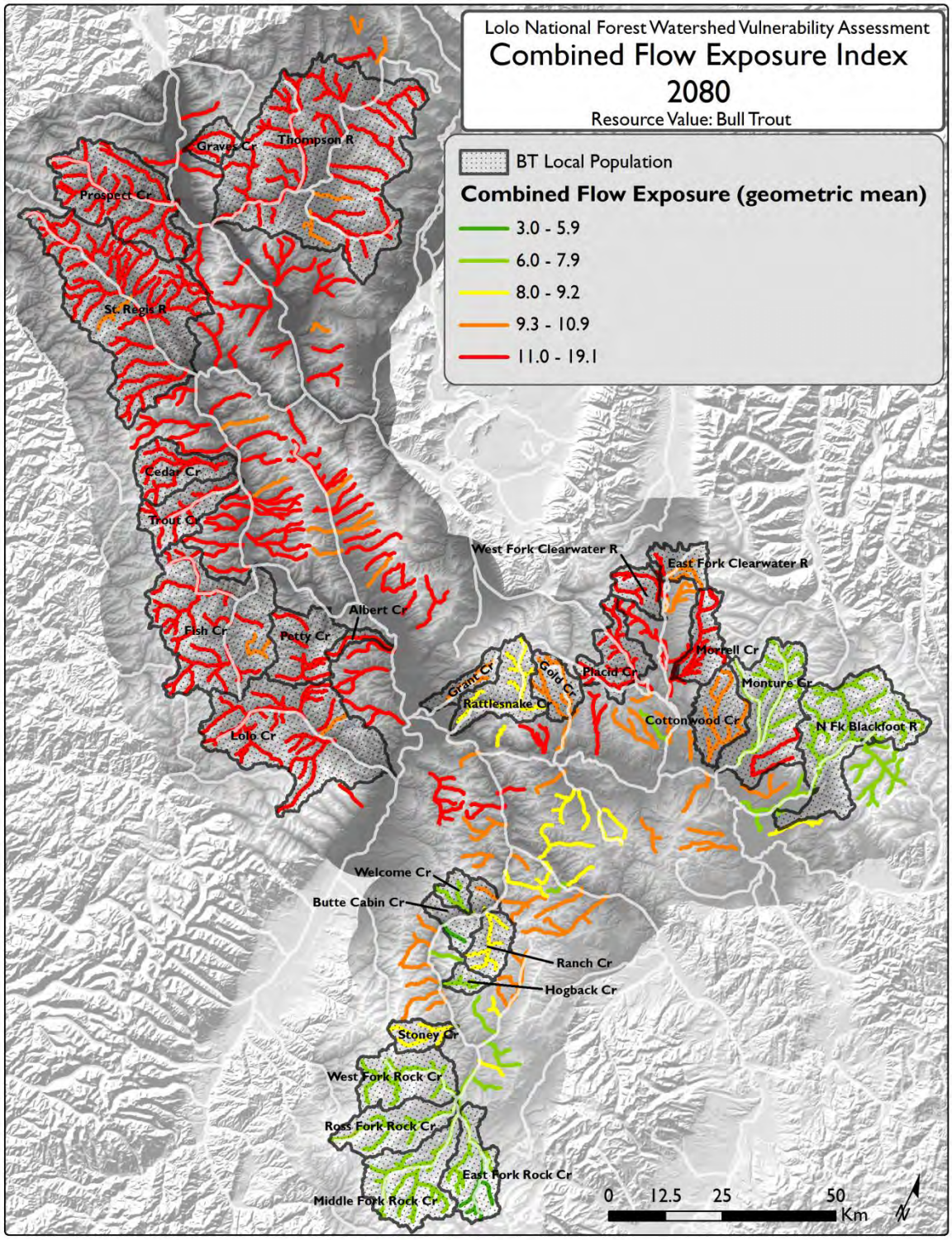

Figure 36. Combined flow exposure index for bull trout by the 2080s.

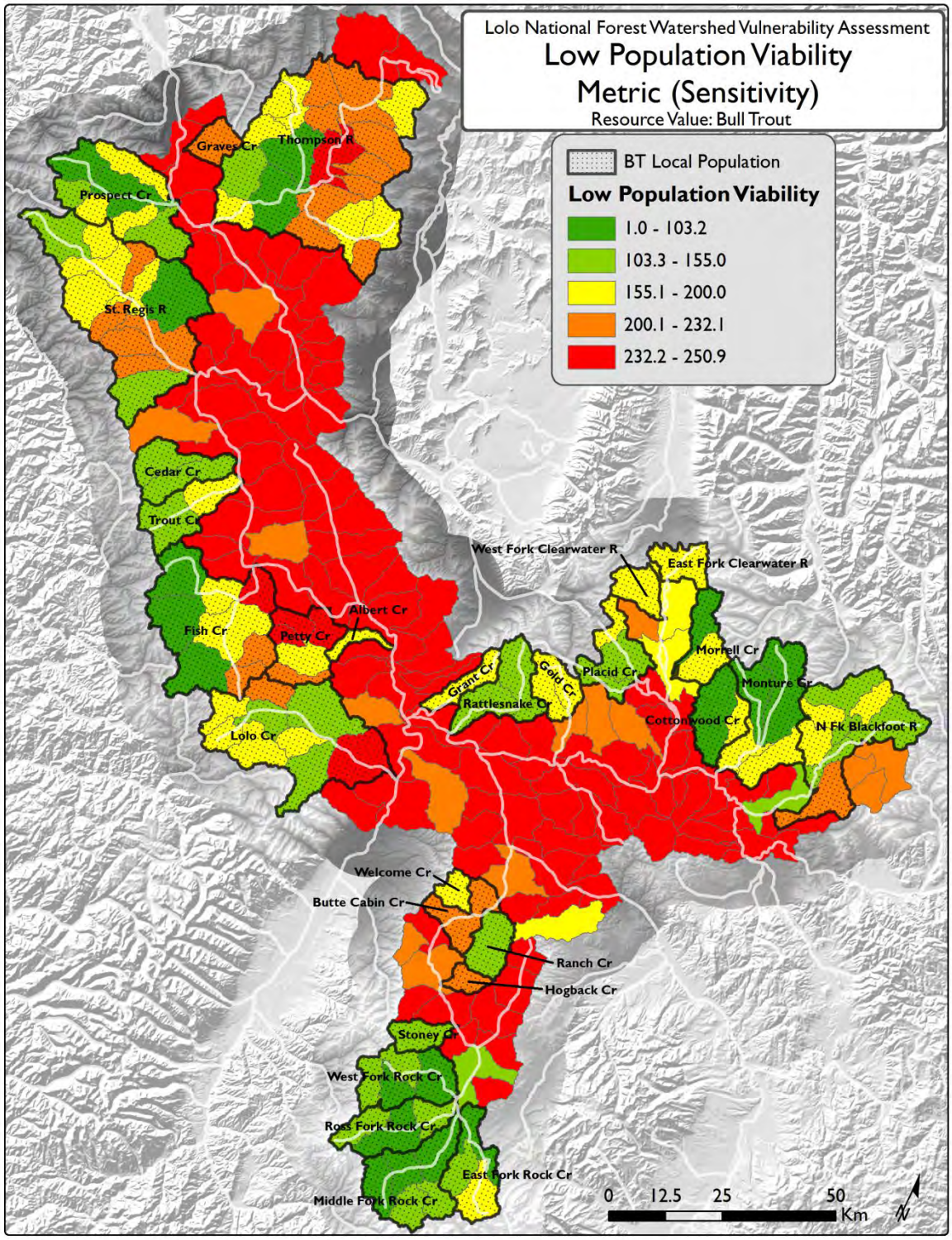

Figure 37. Low population viability metric (sensitivity), calculated from combining two measures, representing the amount of patch in a HUC-12 (Figure 18) and the presence of bull trout or exceptional bull trout habitat (Figure 19). We subtracted the product of these two measures from the maximum resulting product (so that high values represented high stress, as is the case in all sensitivity metrics). Local bull trout populations, designated in the bull trout conservation strategy (BTCS), are shown overlain in stippling (here and in all following bull trout maps). Confidence in metric: **moderate-high**

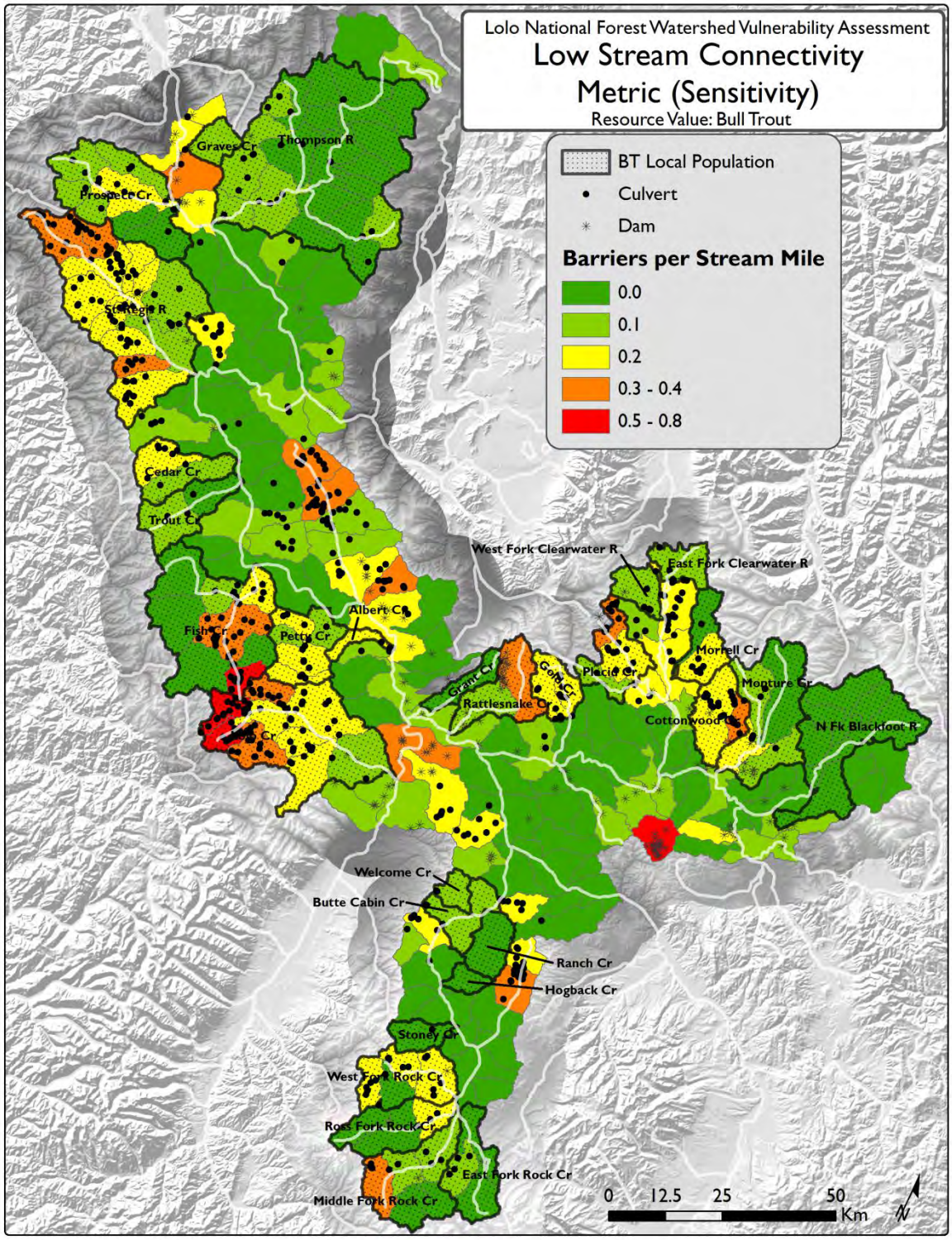

Figure 38. Low stream connectivity metric (sensitivity), calculated as the number of fish barriers (Figure 20).

Confidence in metric: **moderate-high**

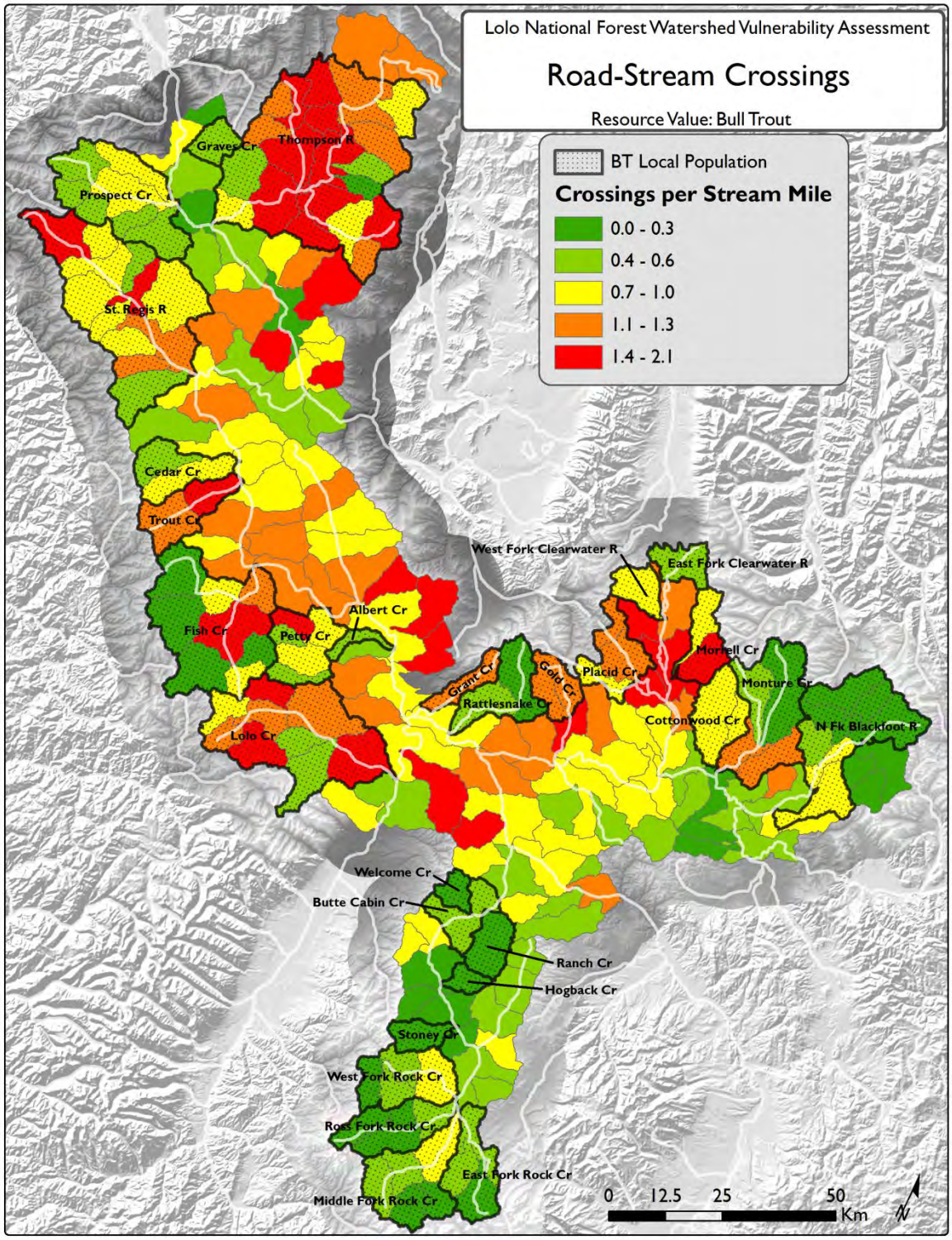

Figure 39. Total number of road-stream crossings by HUC-12. This sub-metric is used in calculating the sediment metric (Figure 41).

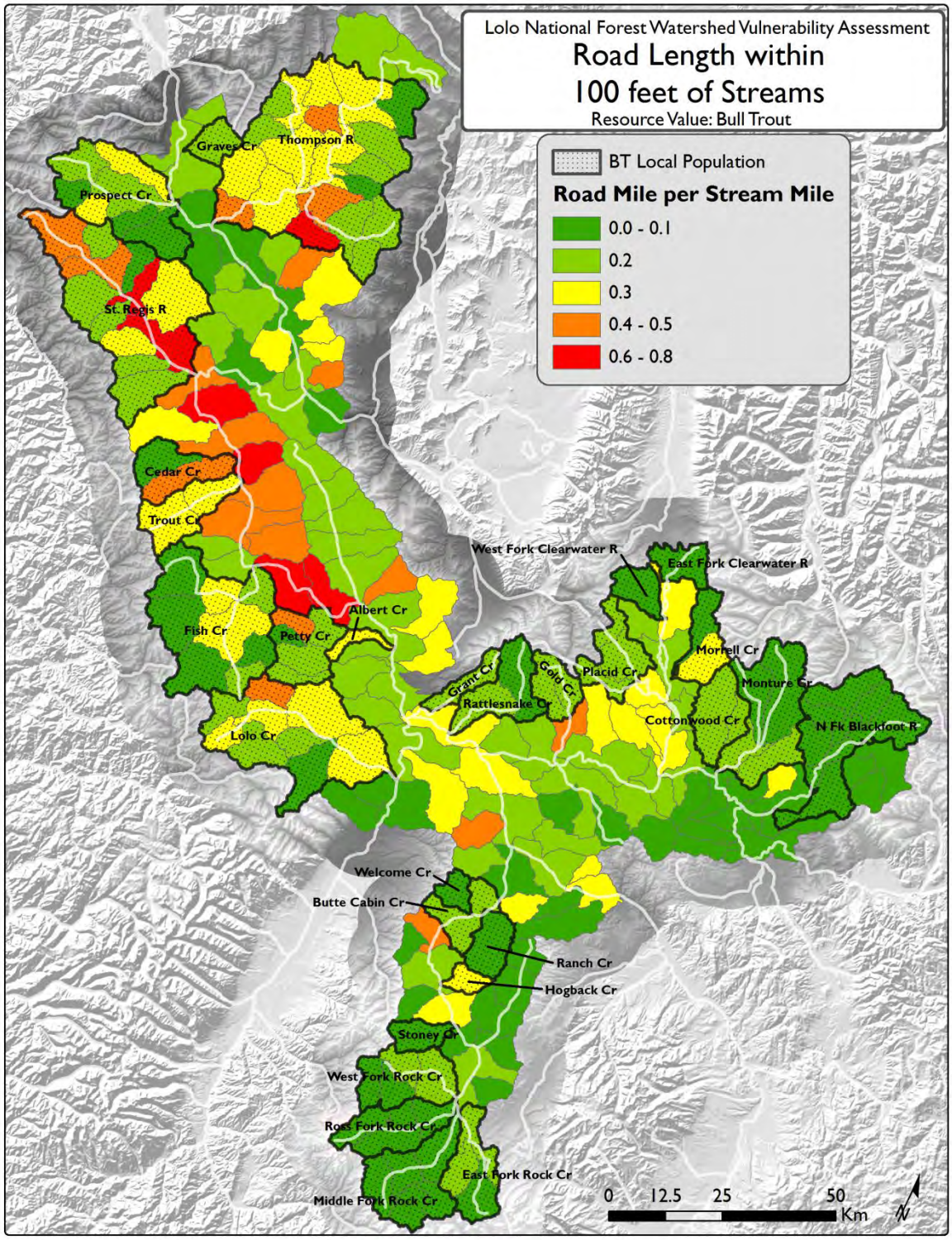

Figure 40. Length of roads within 100 feet of streams as a proportion of stream length in each HUC-12. This sub-metric is used in calculating the sediment metric (Figure 41).

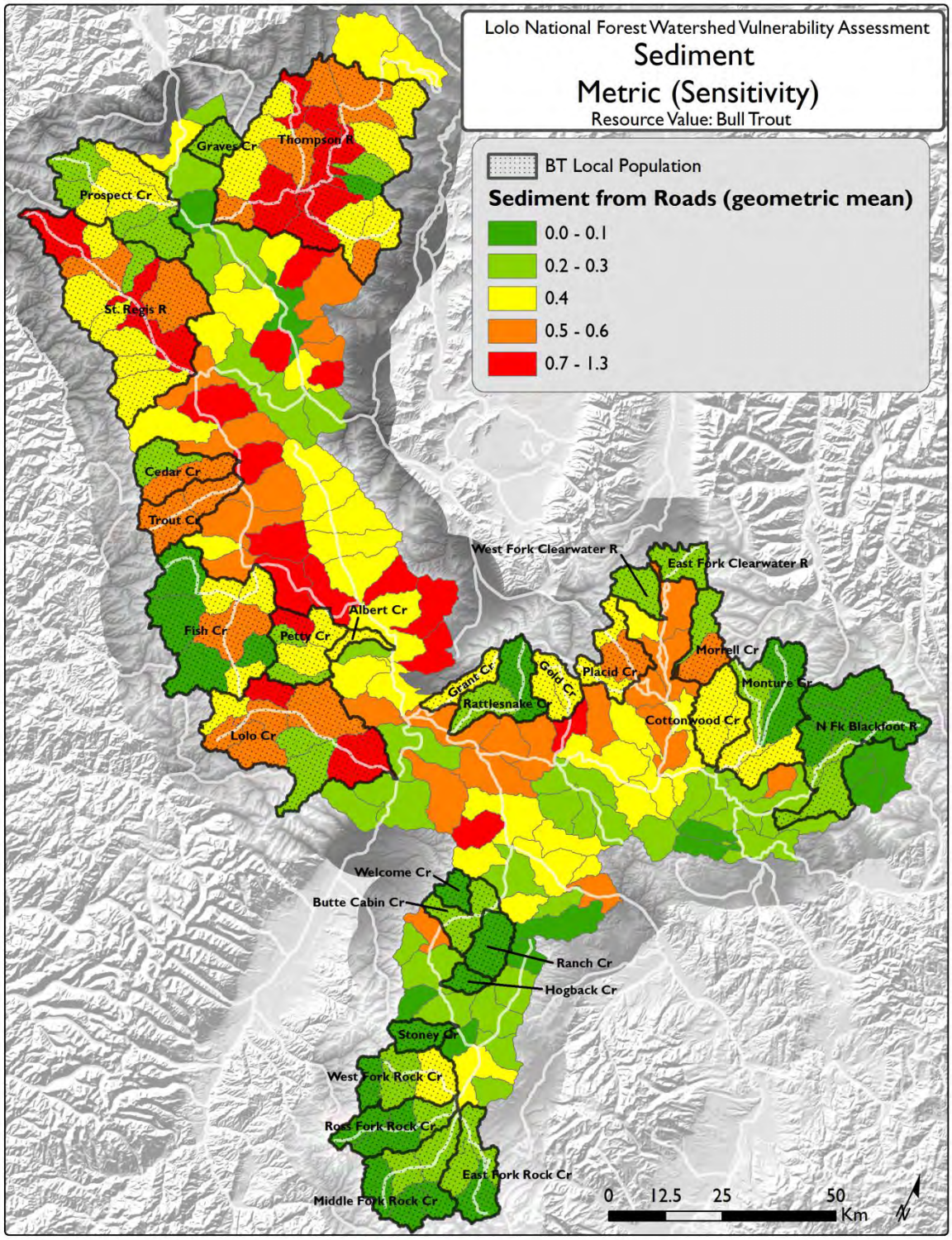

Figure 41. Sediment metric (sensitivity), calculated as the geometric mean of the two road sub-metrics (Figure 39 and 40).

Confidence in metric: moderate

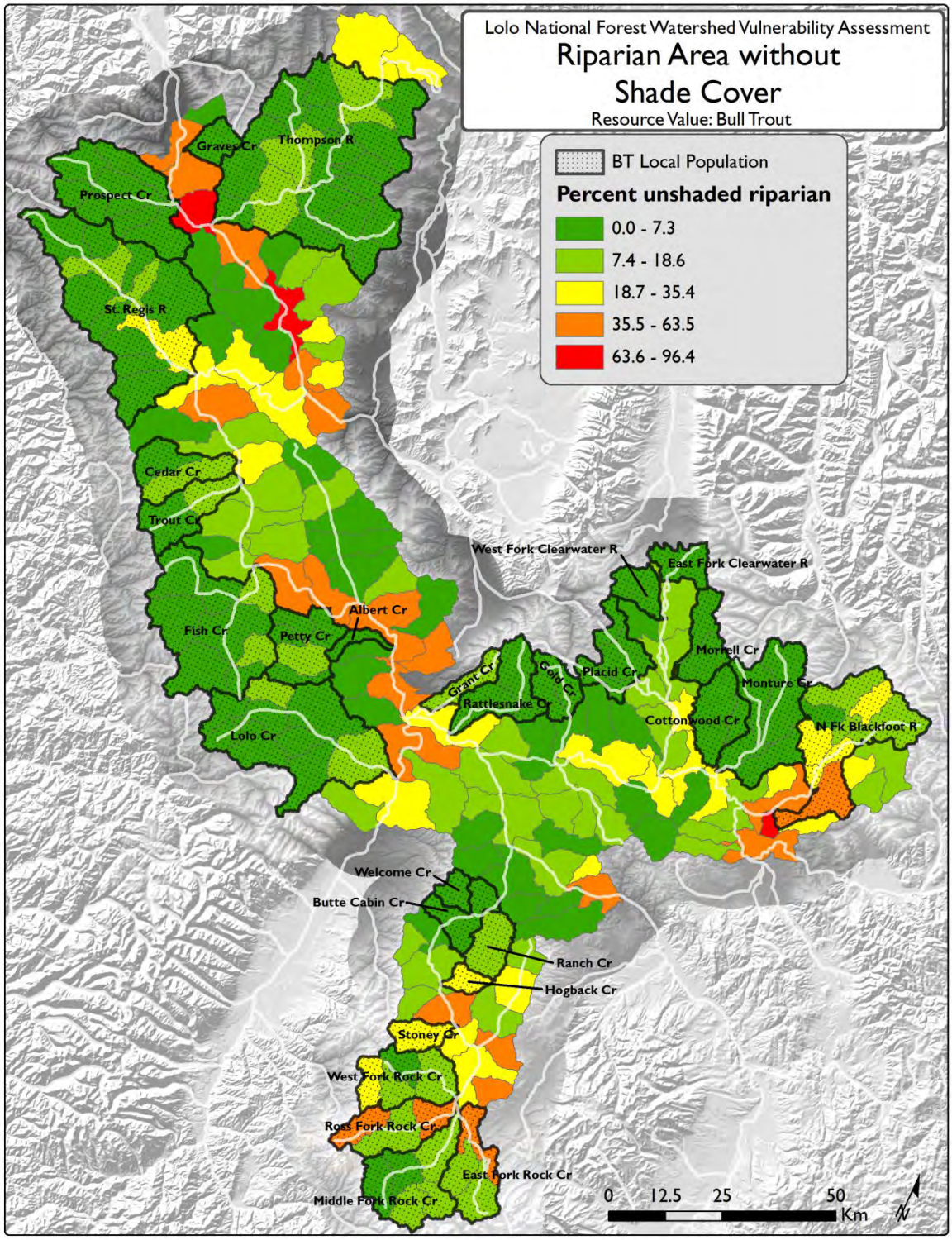

Figure 42. Percent of riparian area without shade cover. This sub-metric is used in calculating the physical complexity metric (Figure 46).

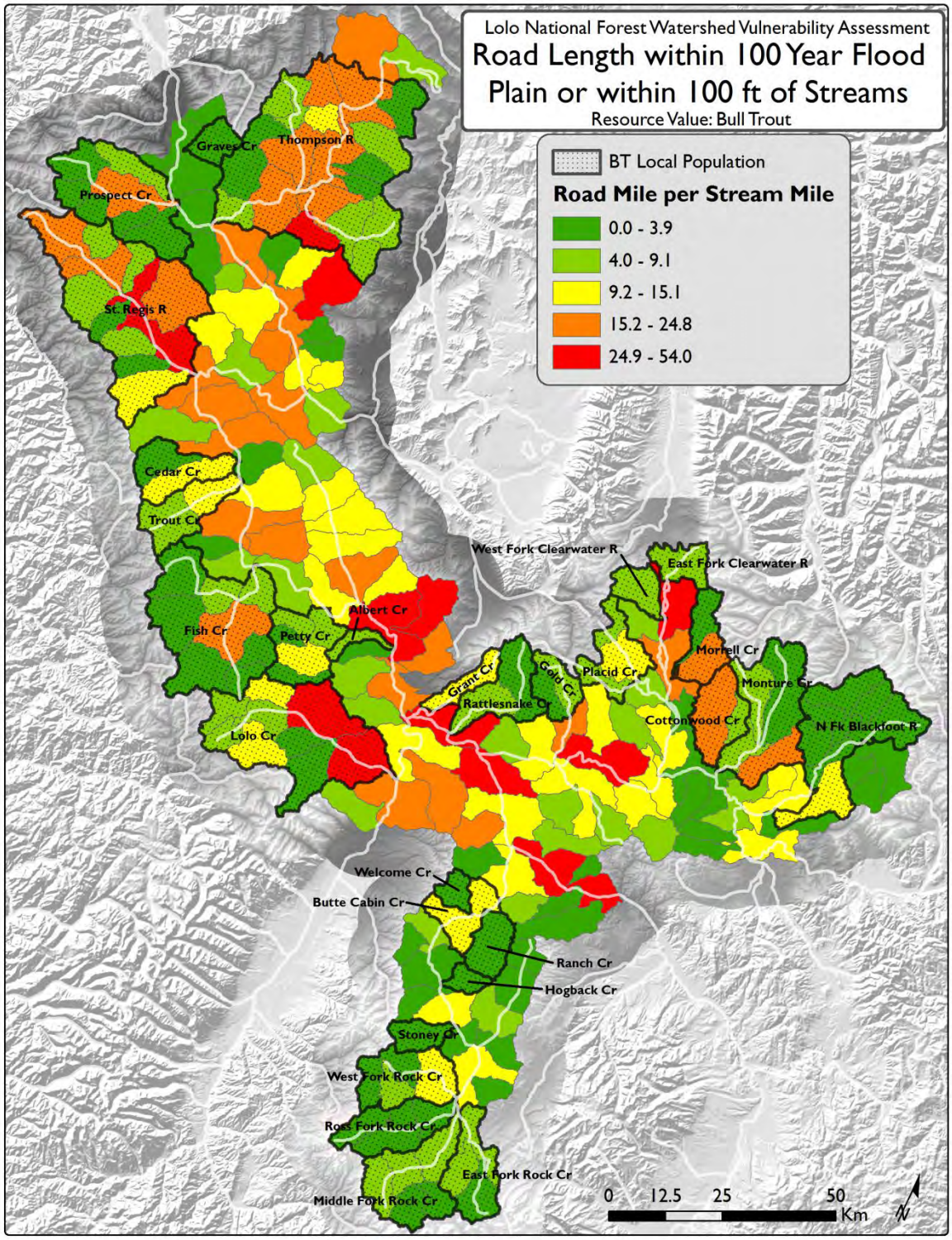

Figure 43. Road length within the 100 year flood plain or stand potential tree height (SPTH, assumed to be 100 feet) of streams as a proportion of stream length in each HUC This sub-metric is used in calculating the physical complexity metric (Figure 46).

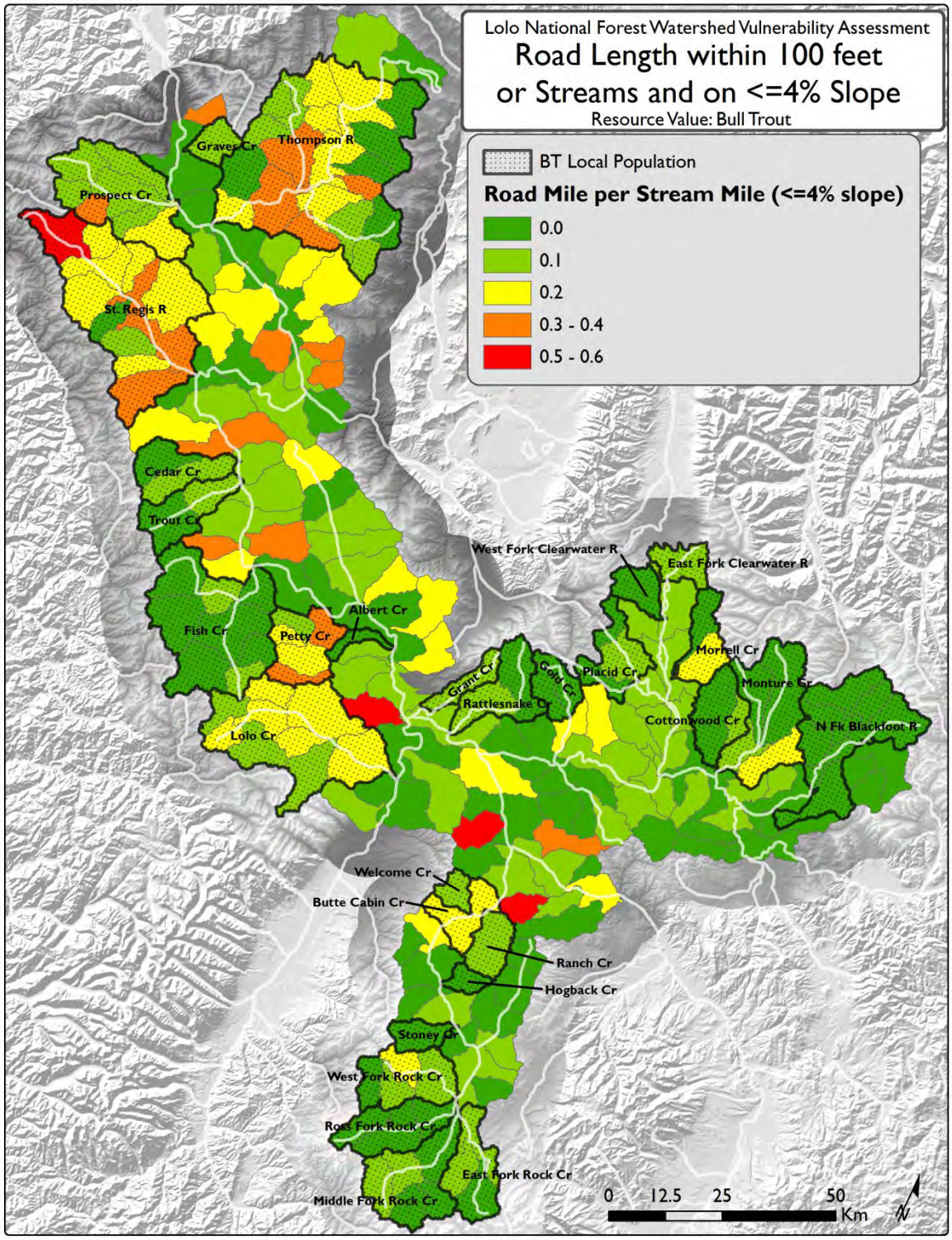

Figure 44. Road length within SPTH of streams and on low-gradient slopes (<=4%) as a proportion of low-gradient stream length. This sub-metric is used in calculating the physical complexity metric (Figure 46).

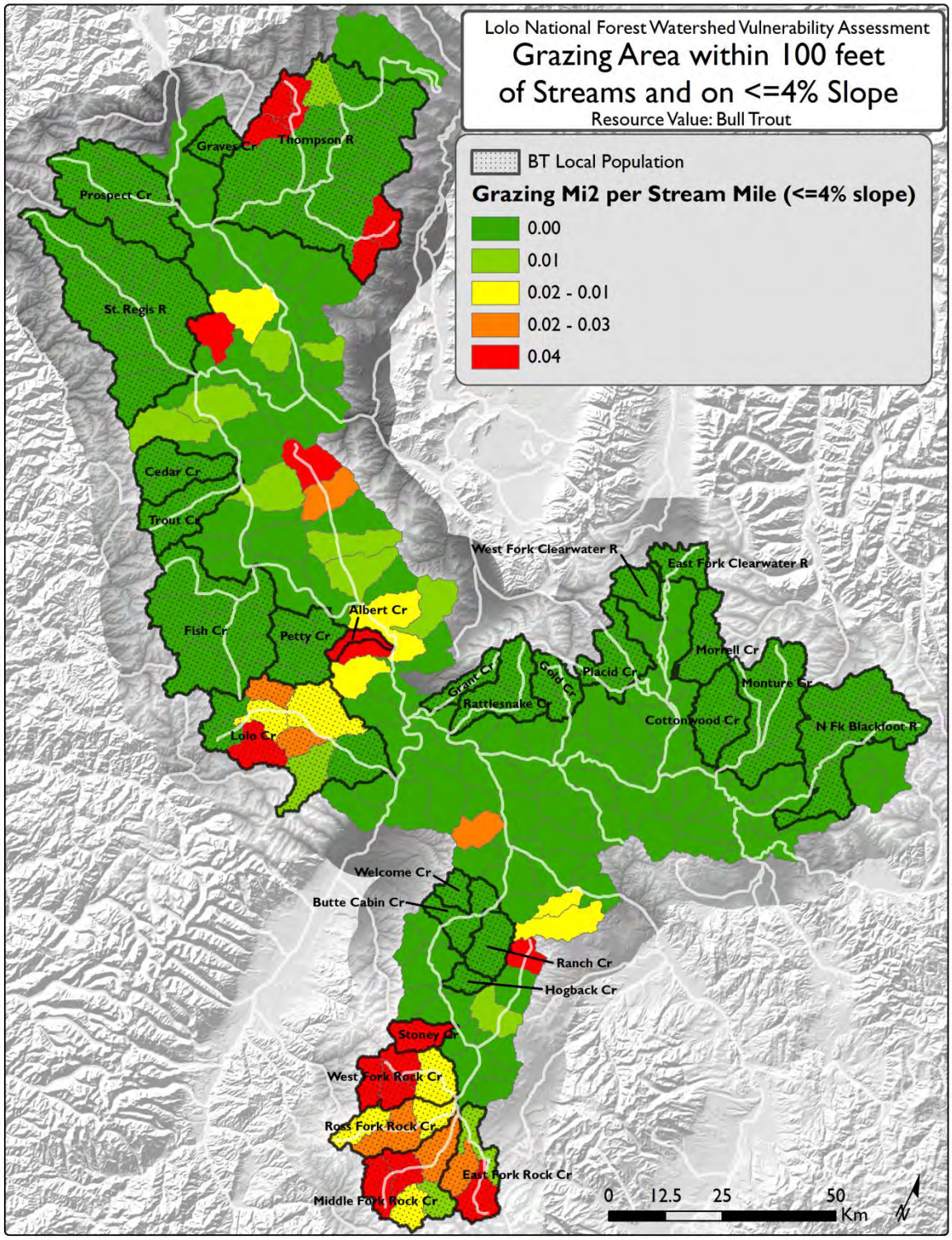

Figure 45. Grazing within SPTH of streams and on >=4% slope as a proportion of total area on >=4% slope and within 30m of streams in each HUC. This sub-metric is used in calculating the physical complexity metric (Figure 46).

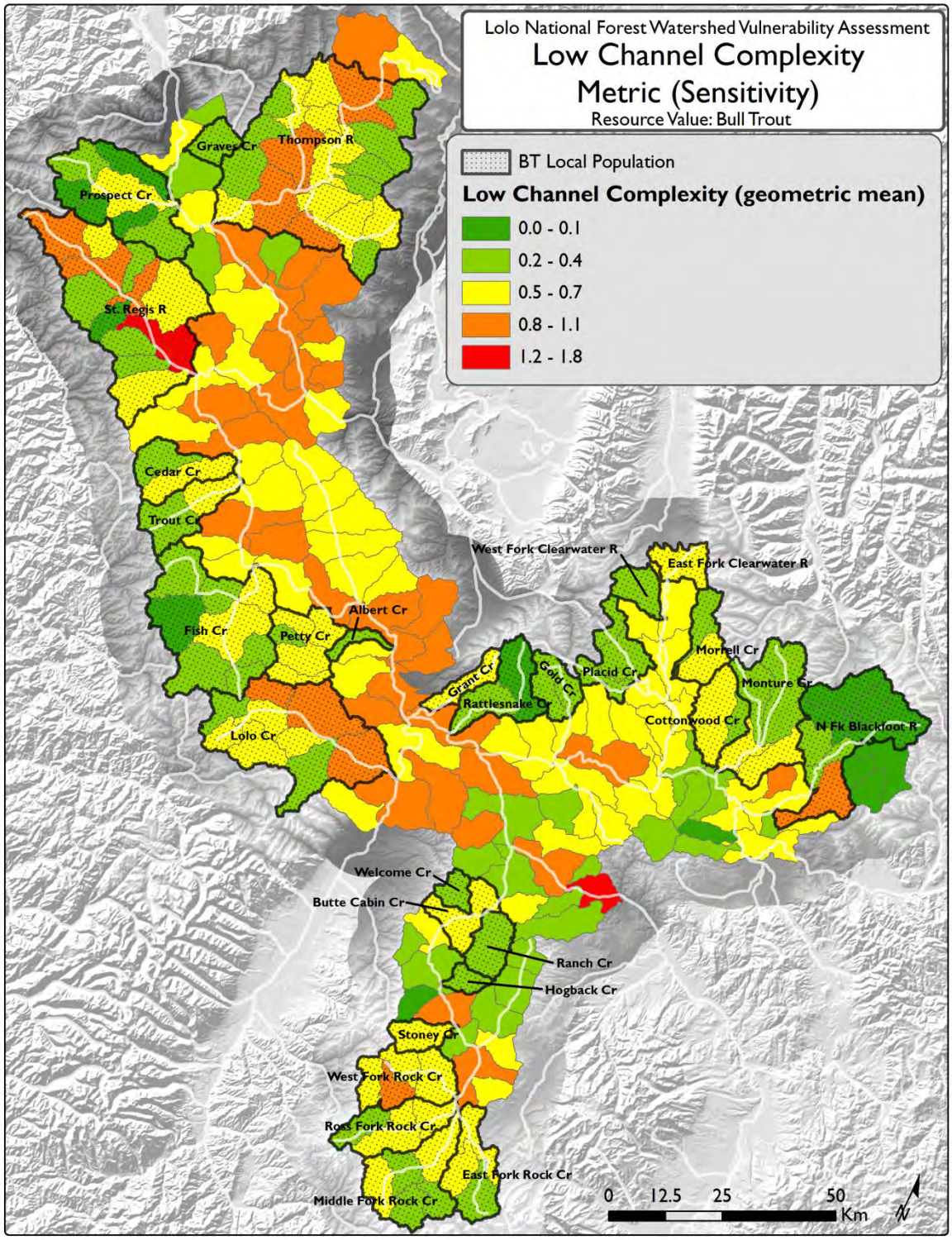

Figure 46. Low physical complexity metric (sensitivity), calculated as the geometric mean of the riparian, road length within SPTH or floodplains, road length within SPTH on low gradient areas, and grazing sub-metrics (Figures 42, 43, 44 and 45).

Confidence in metric: **low-moderate**

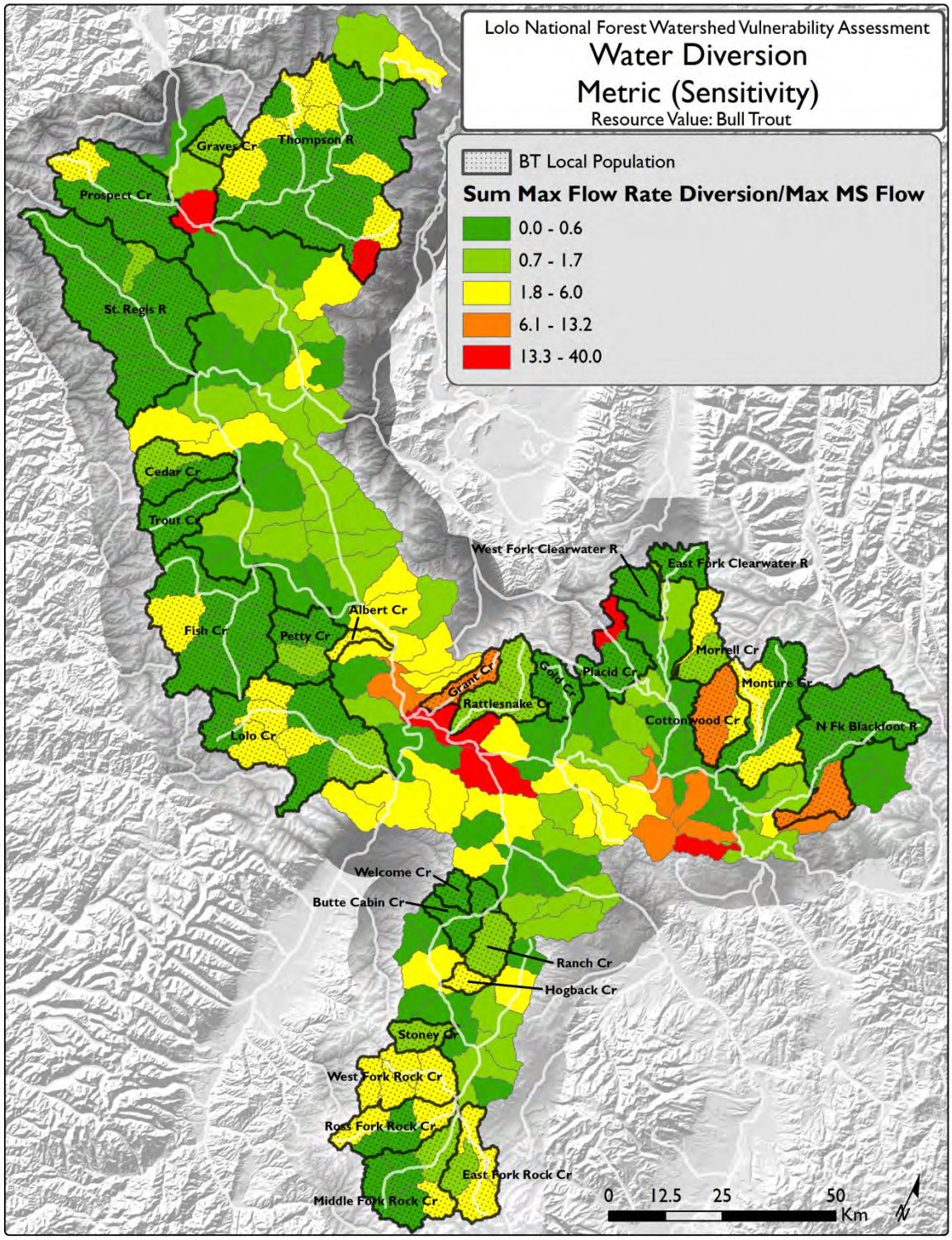

Figure 47. Water diversion metric (sensitivity). For each HUC, we calculated the ratio of (1) the sum of the maximum flow rate allowed for all water right points of diversion that fell in the HUC to (2) the maximum of the mean summer (MS) flow across all non-mainstem reaches within the HUC. Figure 24 maps the data inputs for this metric.

Confidence in metric: **low-moderate**

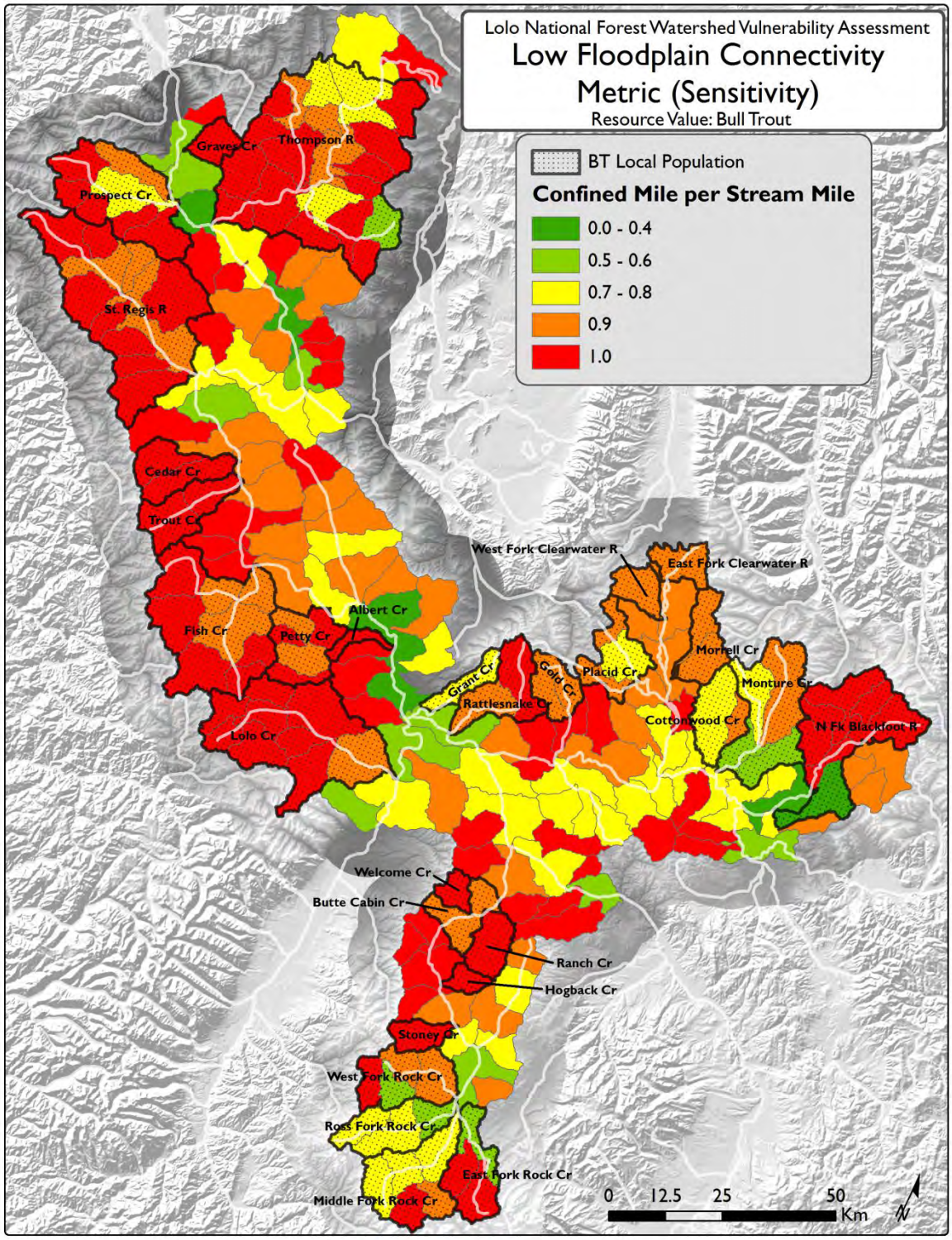

Figure 48. Low floodplain connectivity metric (sensitivity), calculated as the percent of stream length outside of the 100 year flood plain.

Confidence in metric: moderate

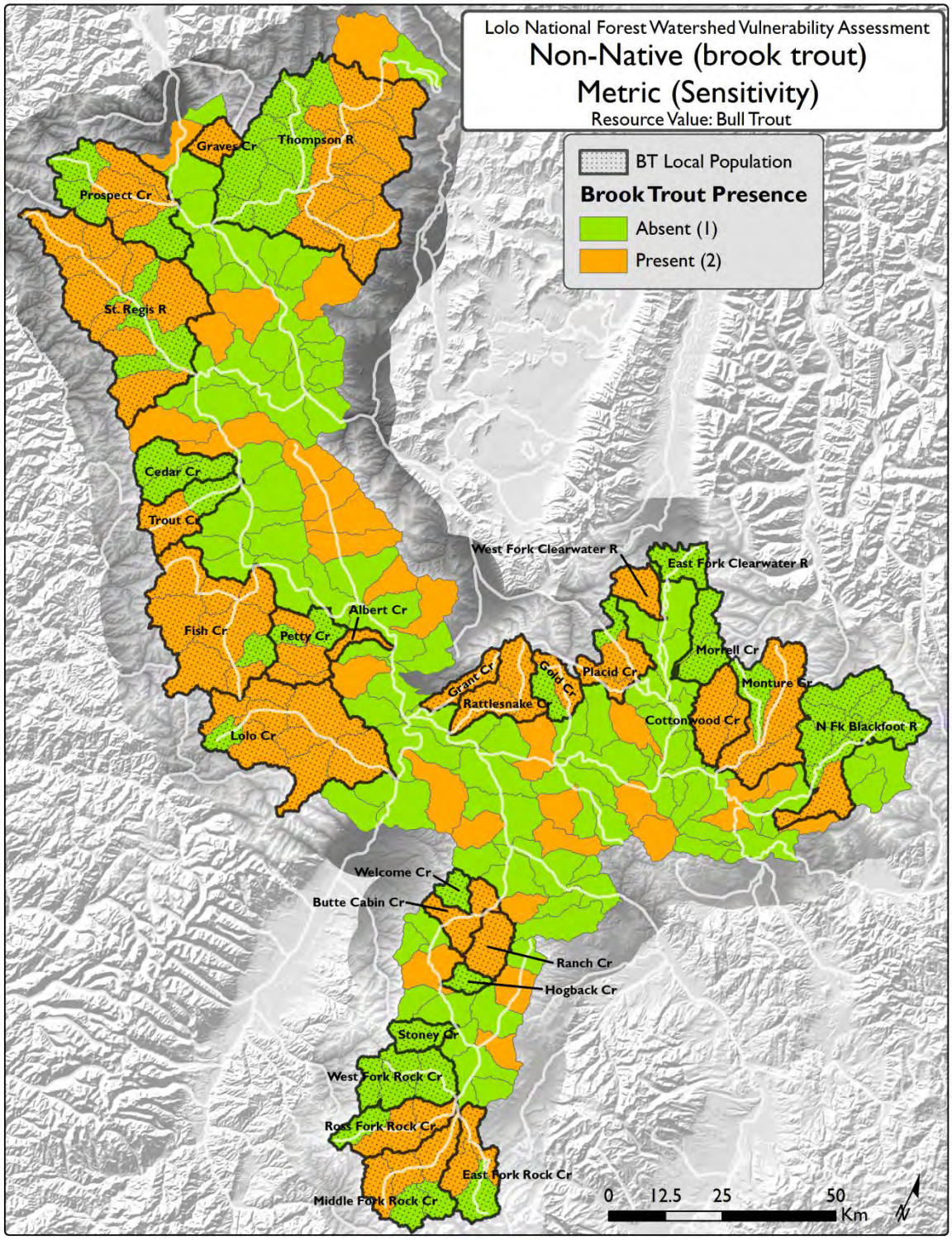

Figure 49. Brook trout metric (sensitivity), calculated as a binary measure of brook trout presence (value of 2) or absence (value of 1).

Confidence in metric: **low-moderate**

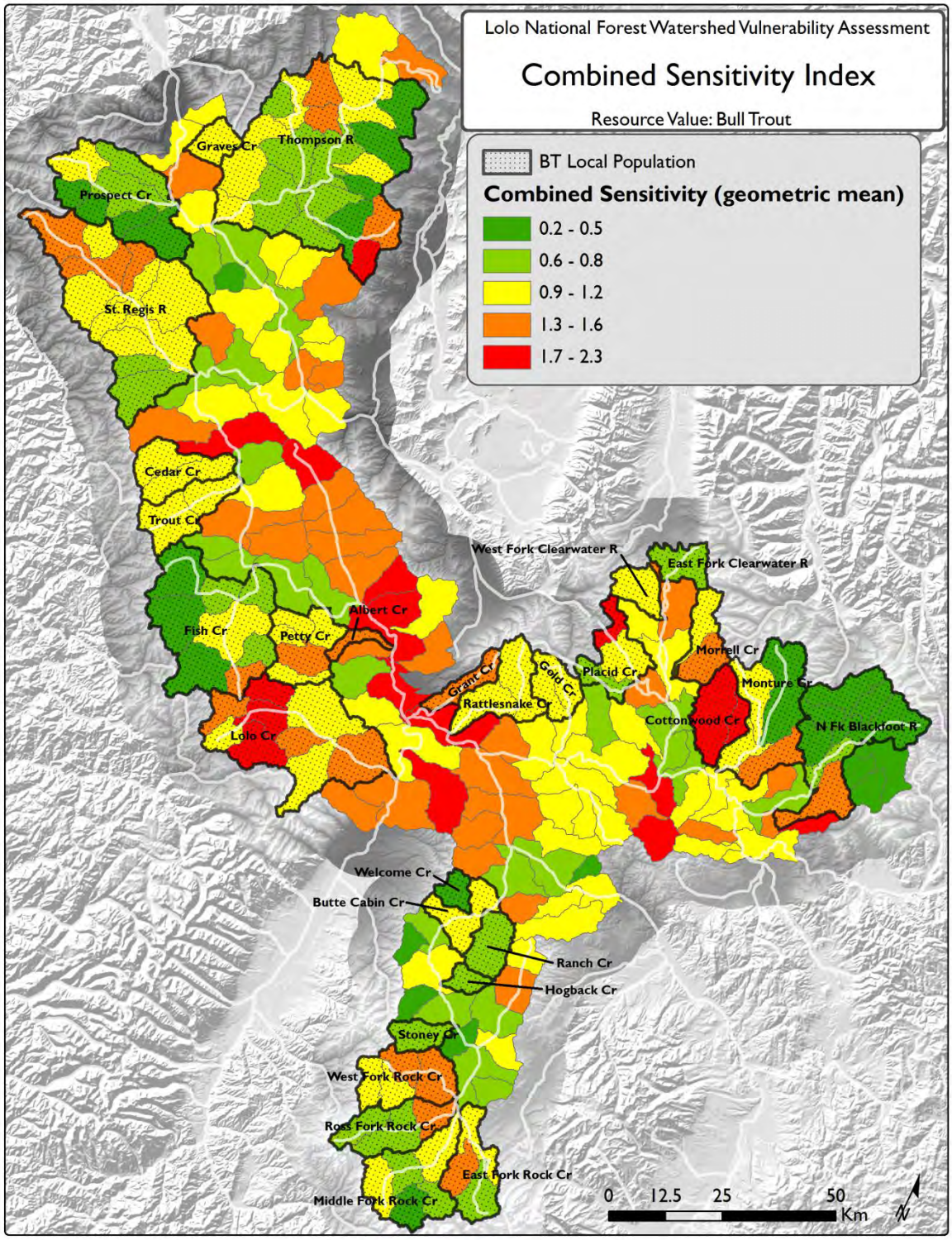

Figure 50. Combined sensitivity index for bull trout. We calculated the geometric mean of the low population viability (Figure 37), low stream connectivity (Figure 38), sediment (Figure 41), low physical complexity (Figure 46), water diversion (Figure 47), low floodplain connectivity (Figure 48), and brook trout (Figure 49) metrics.

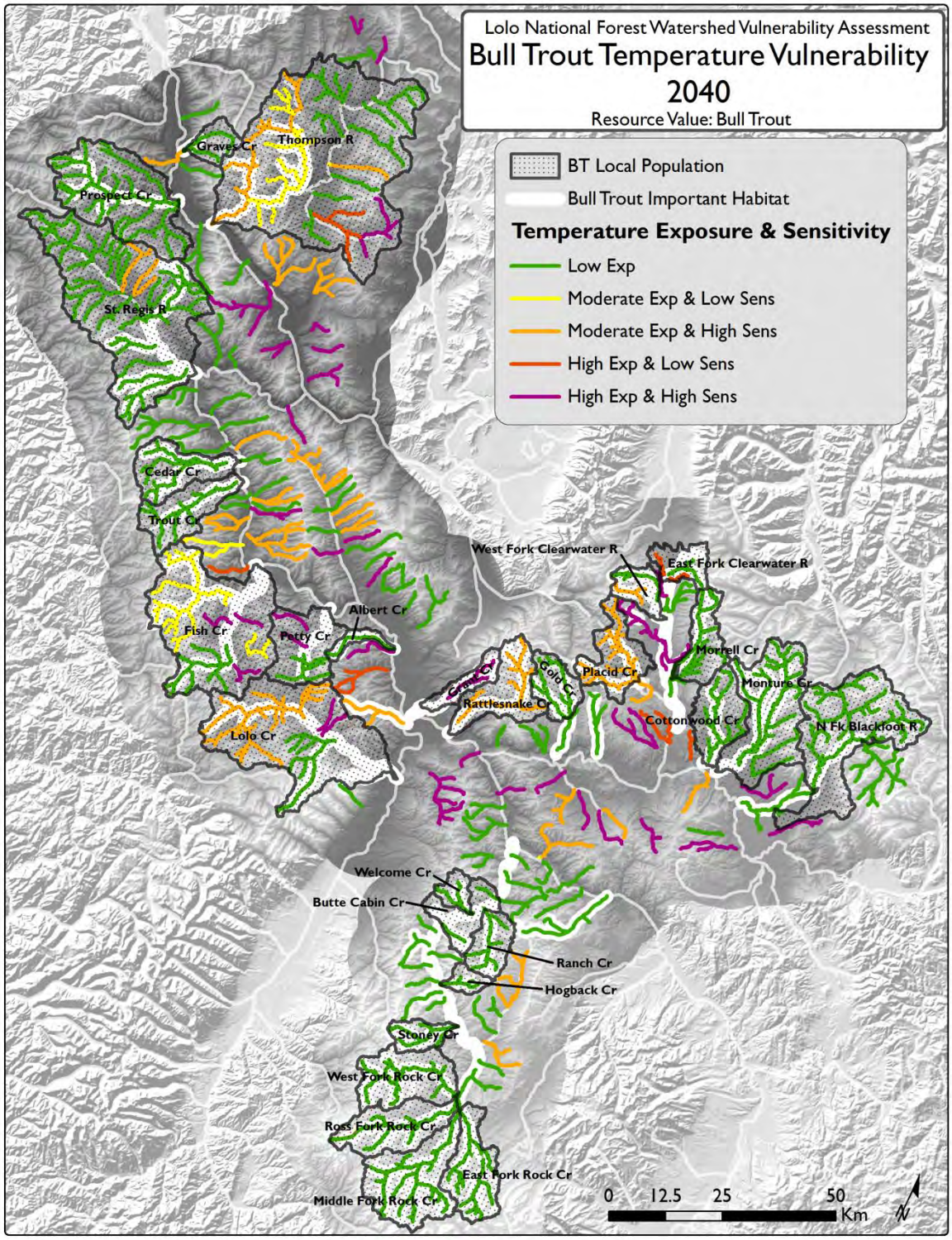

Figure 51. Estimated vulnerability of bull trout to projected temperature changes, by patch, by the 2040s, based on comparing the temperature exposure (Figure 29) and combined sensitivity (Figure 50) indices. Streams listed as having common or abundant bull trout by MFISH or as being critical habitat by FWS are shown in white ("Important Habitat") for reference (see methods for details).

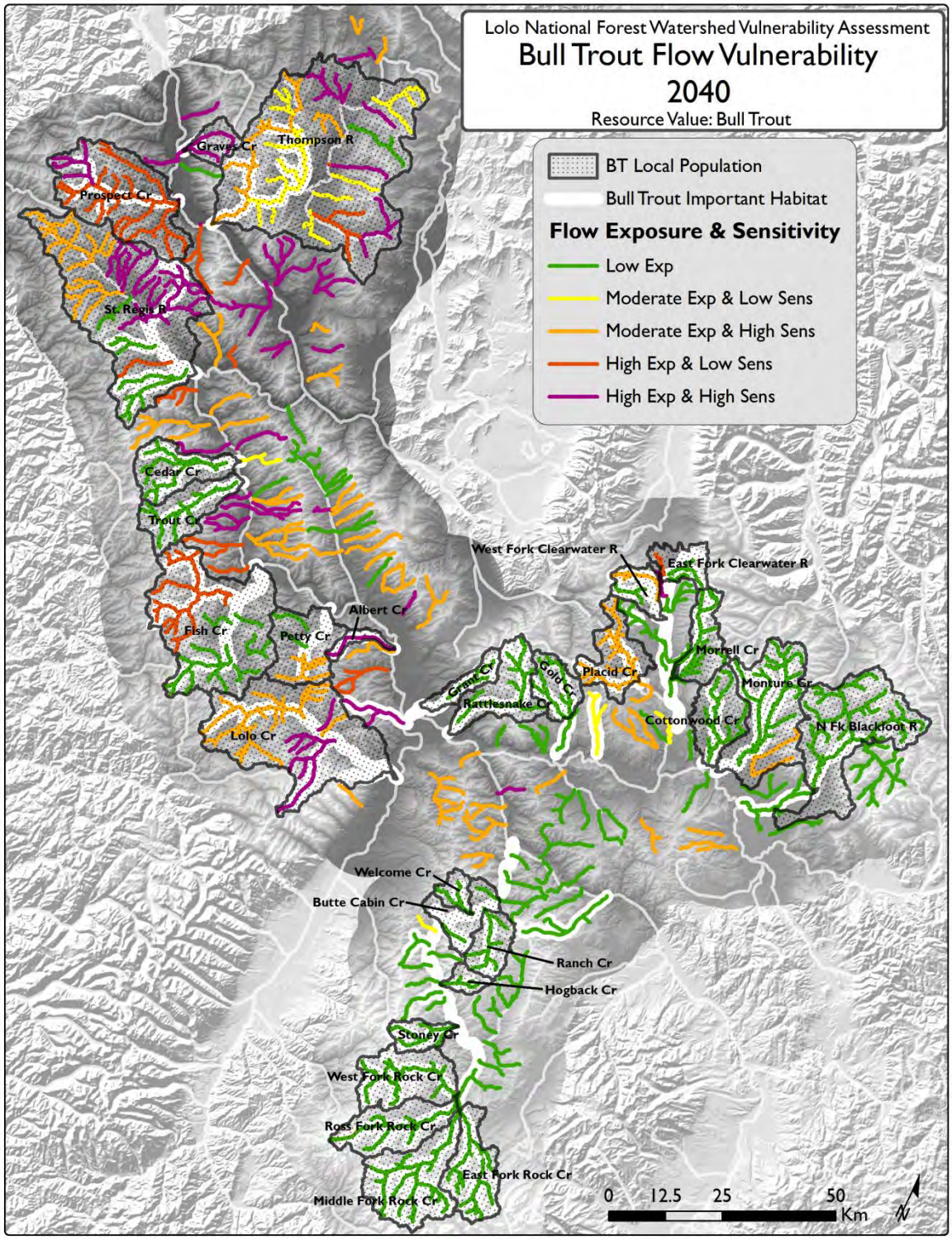

Figure 52. Estimated vulnerability of bull trout to projected flow changes, by patch, by the 2040s, based on comparing the flow exposure (Figure 35) and combined sensitivity (Figure 50) indices. Streams listed as having common or abundant bull trout by MFISH or as being critical habitat by FWS are shown in white ("Important Habitat") for reference (see methods for details).

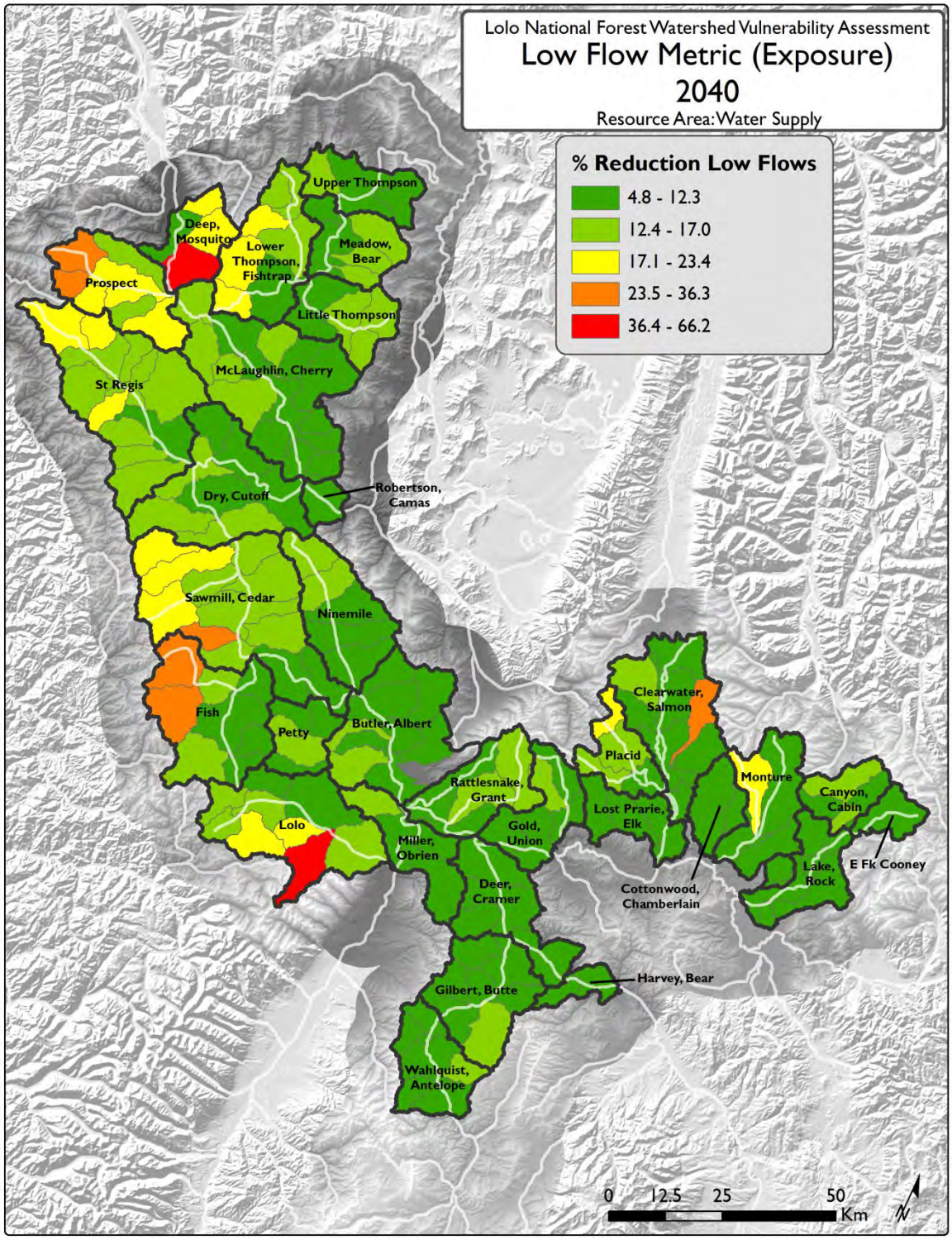

Figure 53. Low flow exposure metric for water supply by the 2040s. We calculated the percent decrease in mean summer flows between baseline modeled conditions and the 2040s.

Confidence in metric: **low-moderate**

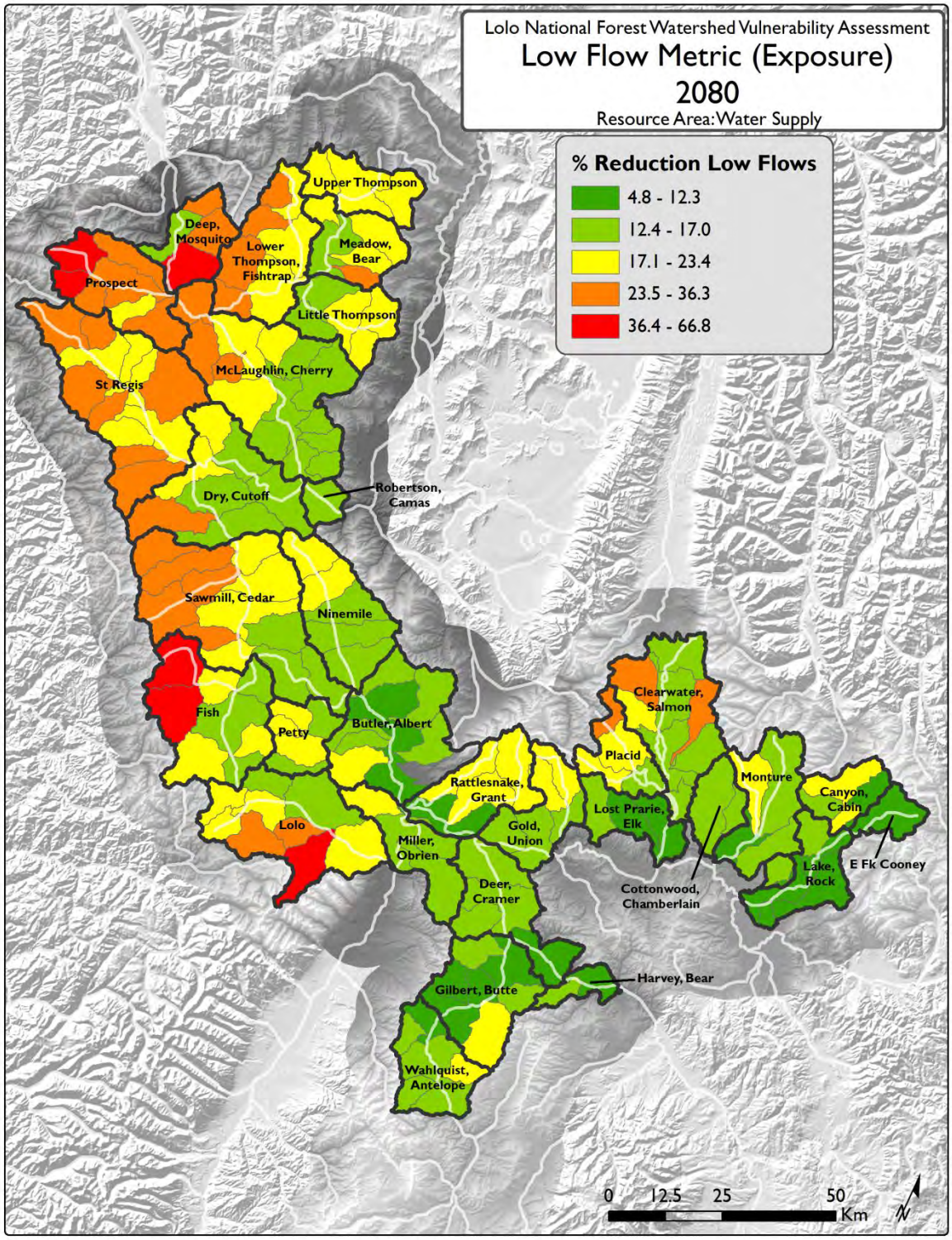

Figure 54. Low flow exposure metric for water supply by the 2080s.
Confidence in metric: **low**

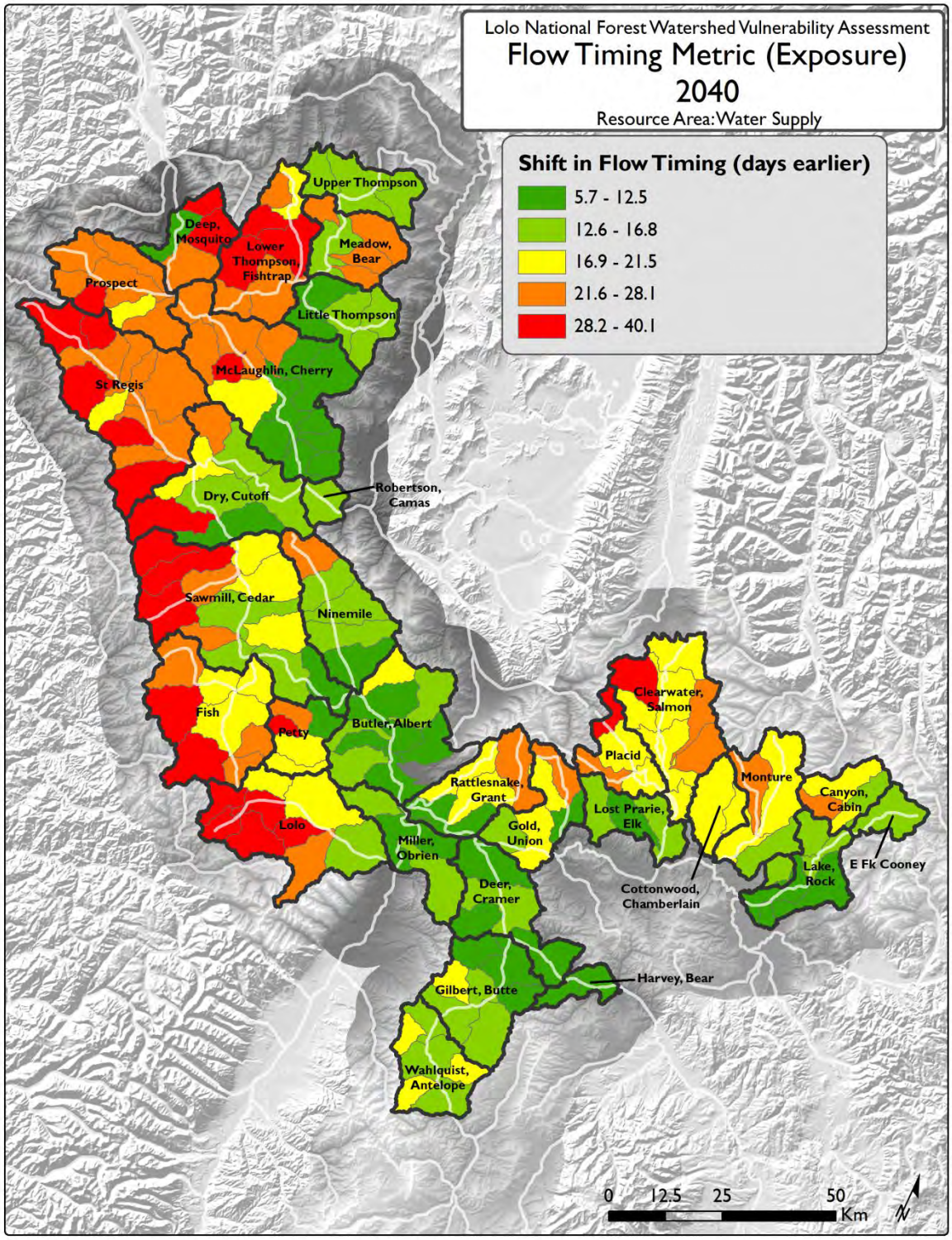

Figure 55. Flow timing exposure metric for water supply by the 2040s. We calculated the shift in the day of the water year when 50% of the annual flow has passed.

Confidence in metric: **low-moderate**

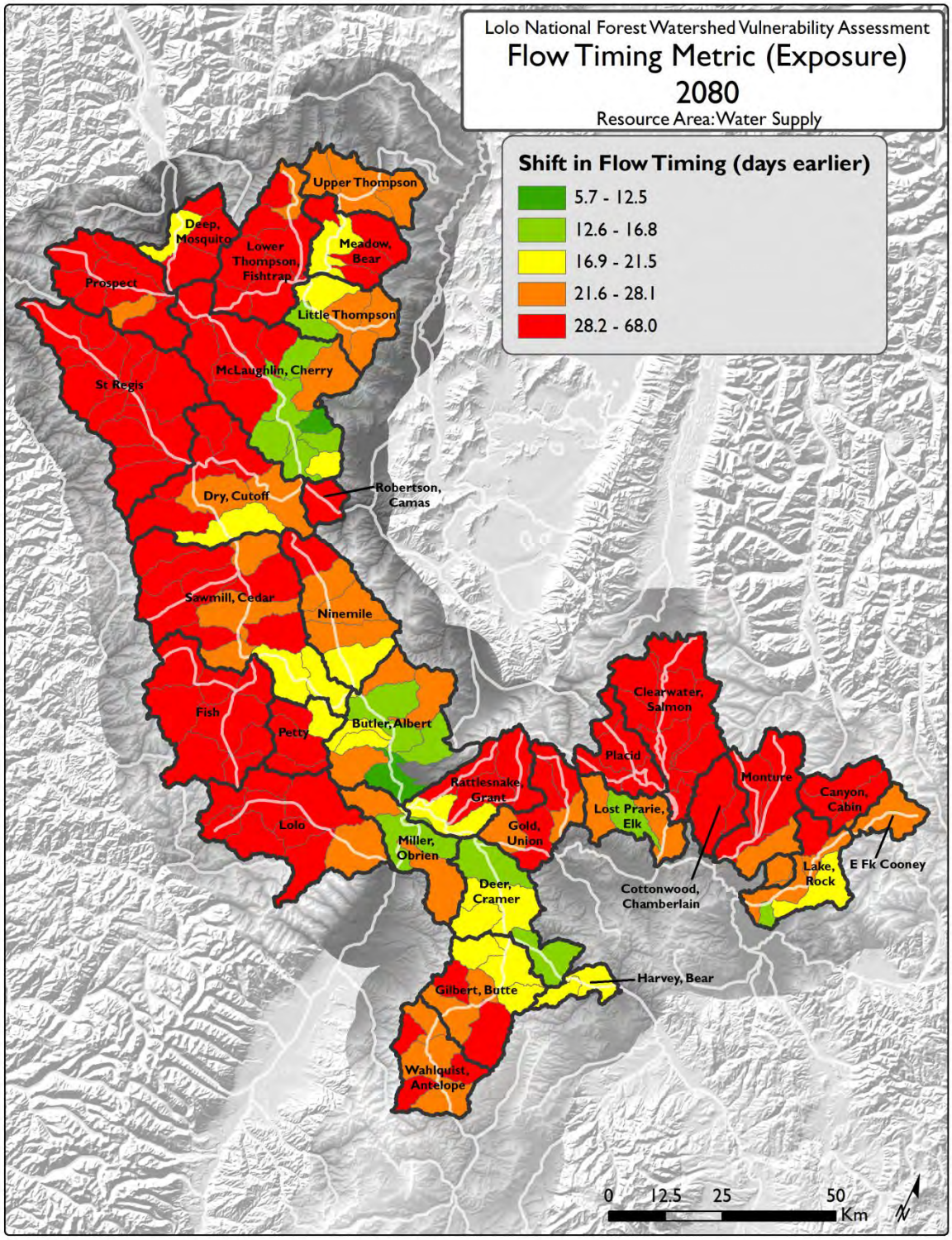

Figure 56. Flow timing exposure metric for water supply by the 2080s.
Confidence in metric: **low**

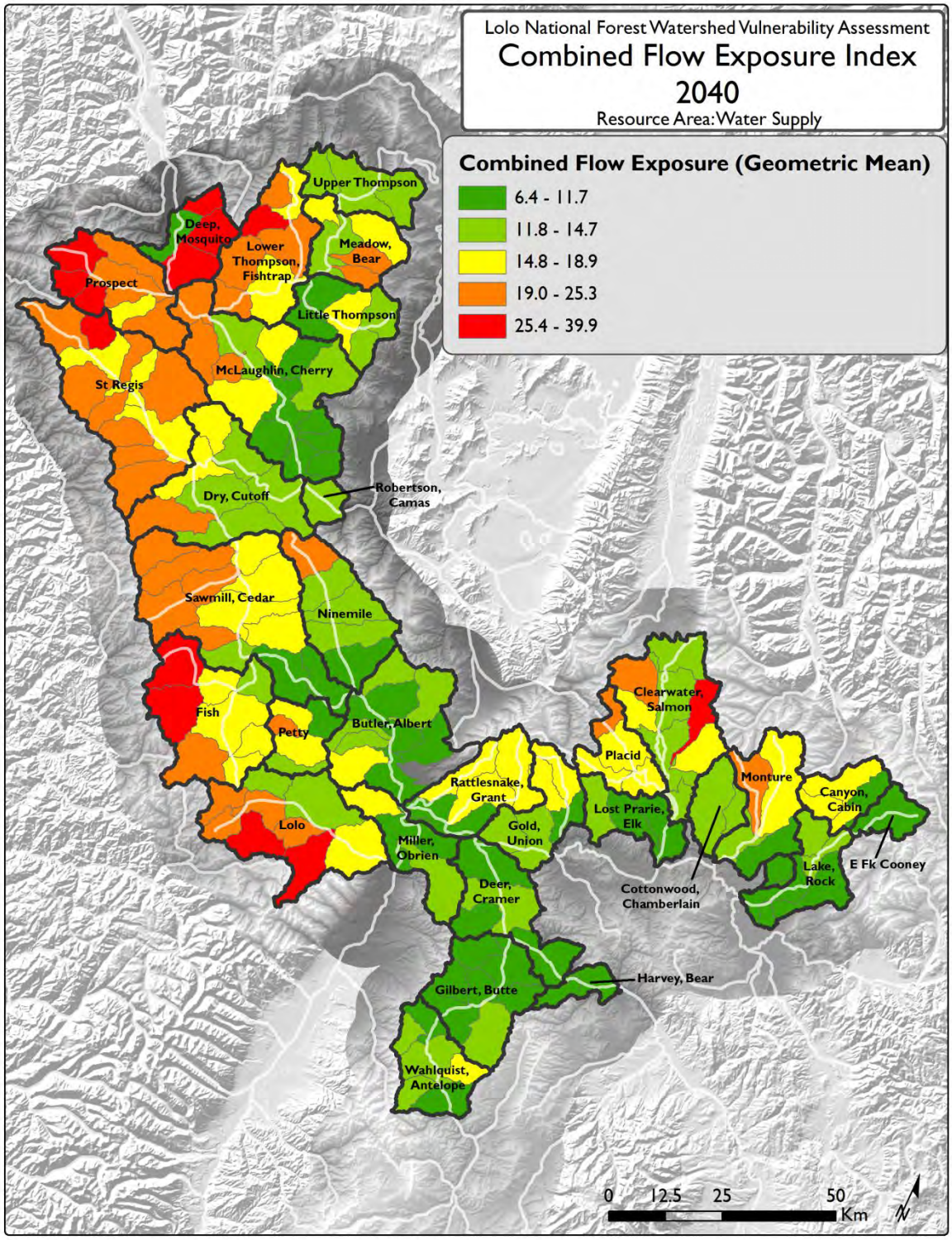

Figure 57. Combined flow exposure index for water supply by the 2040s. We calculated the geometric mean of the low flow (Figure 53) and flow timing (Figure 55) stressor metrics.

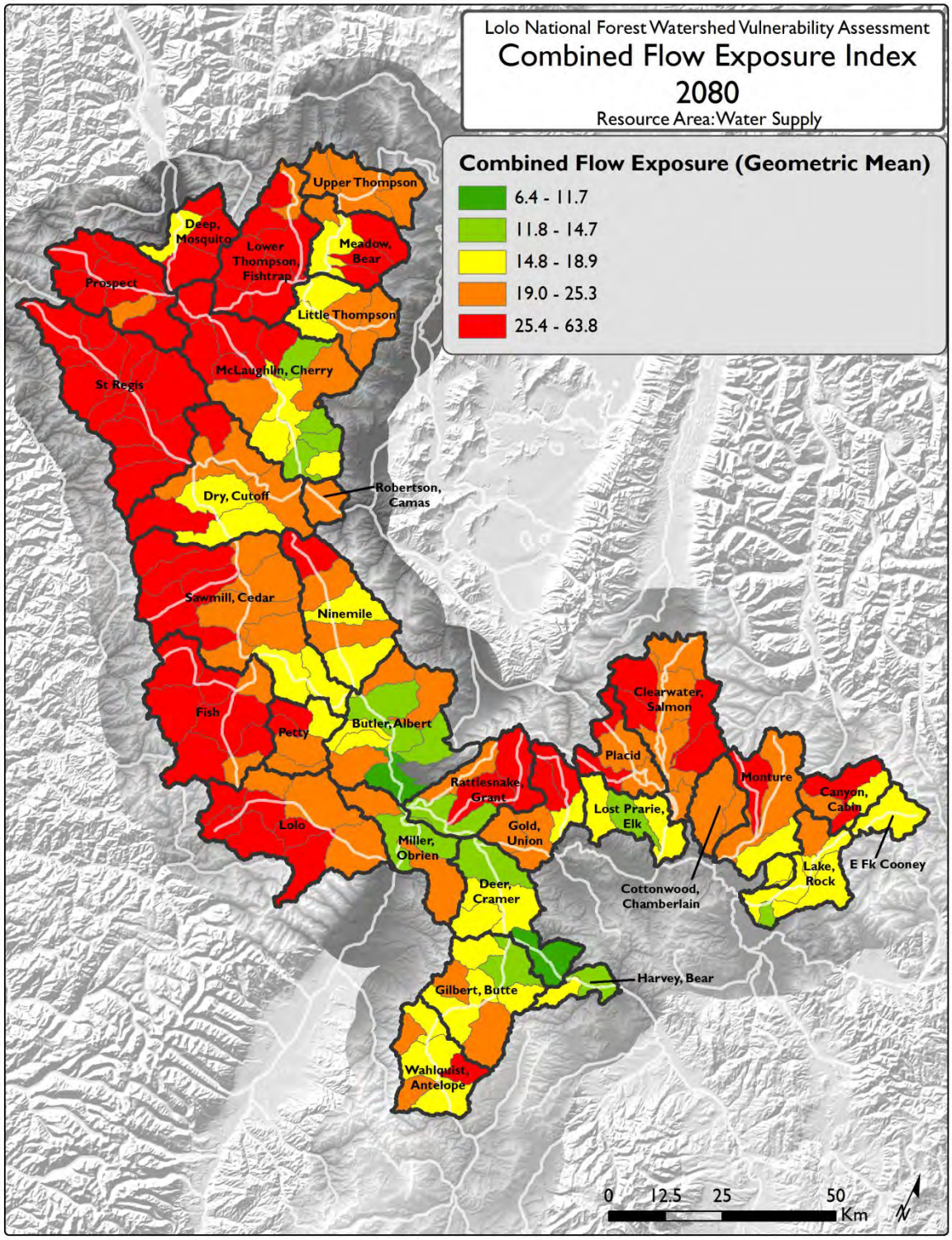

Figure 58. Combined flow exposure index for water supply by the 2080s.

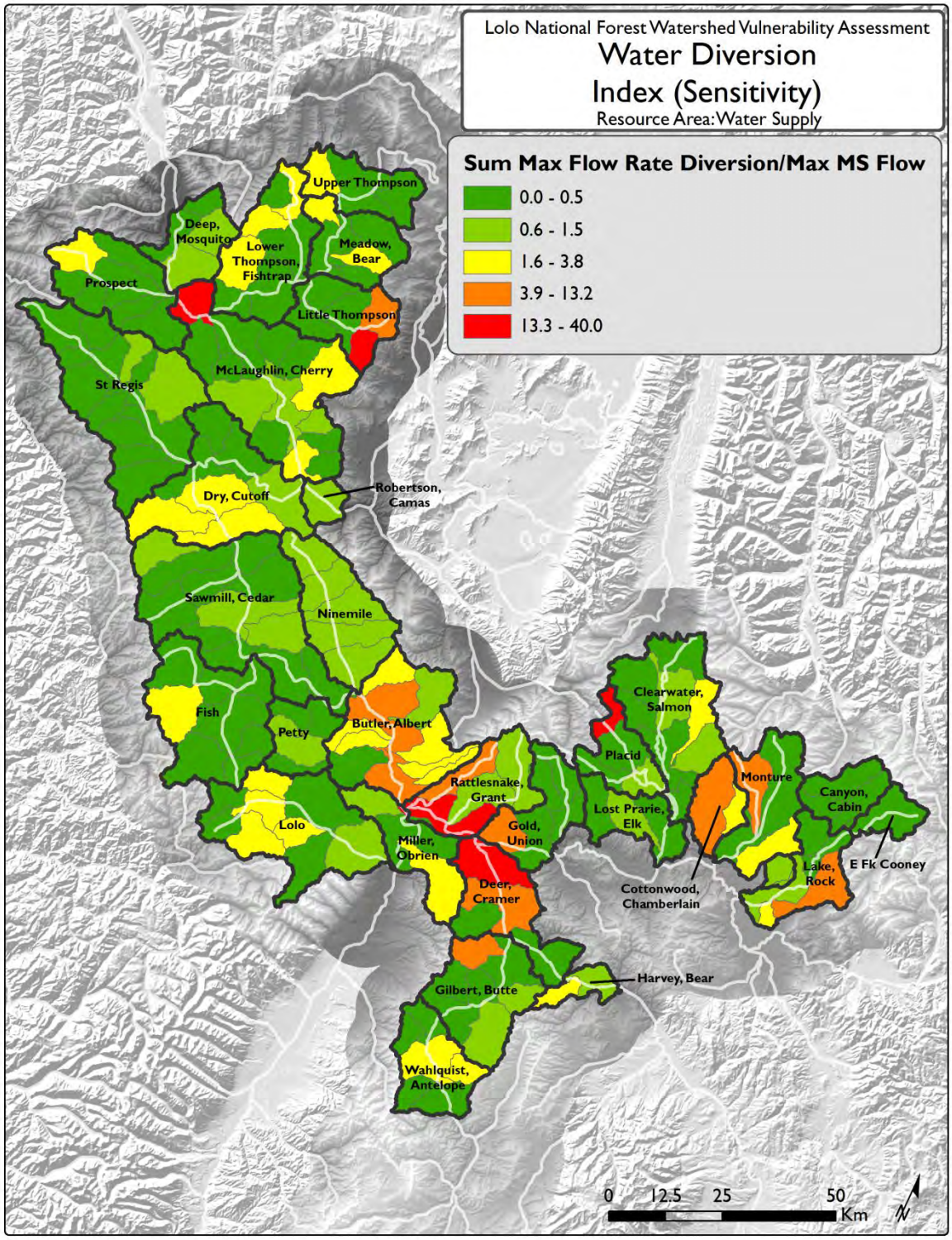

Figure 59. Water diversion index (sensitivity; here, only one metric used for this index). For each HUC-12, we calculated the ratio of (1) the sum of the maximum flow rate allowed for all water right points of diversion that fell in the HUC-12 to (2) the maximum of the mean summer (MS) flow across all non-mainstem reaches within the HUC-12. Figure 47 maps the data inputs for this index.

Confidence in metric: **low-moderate**

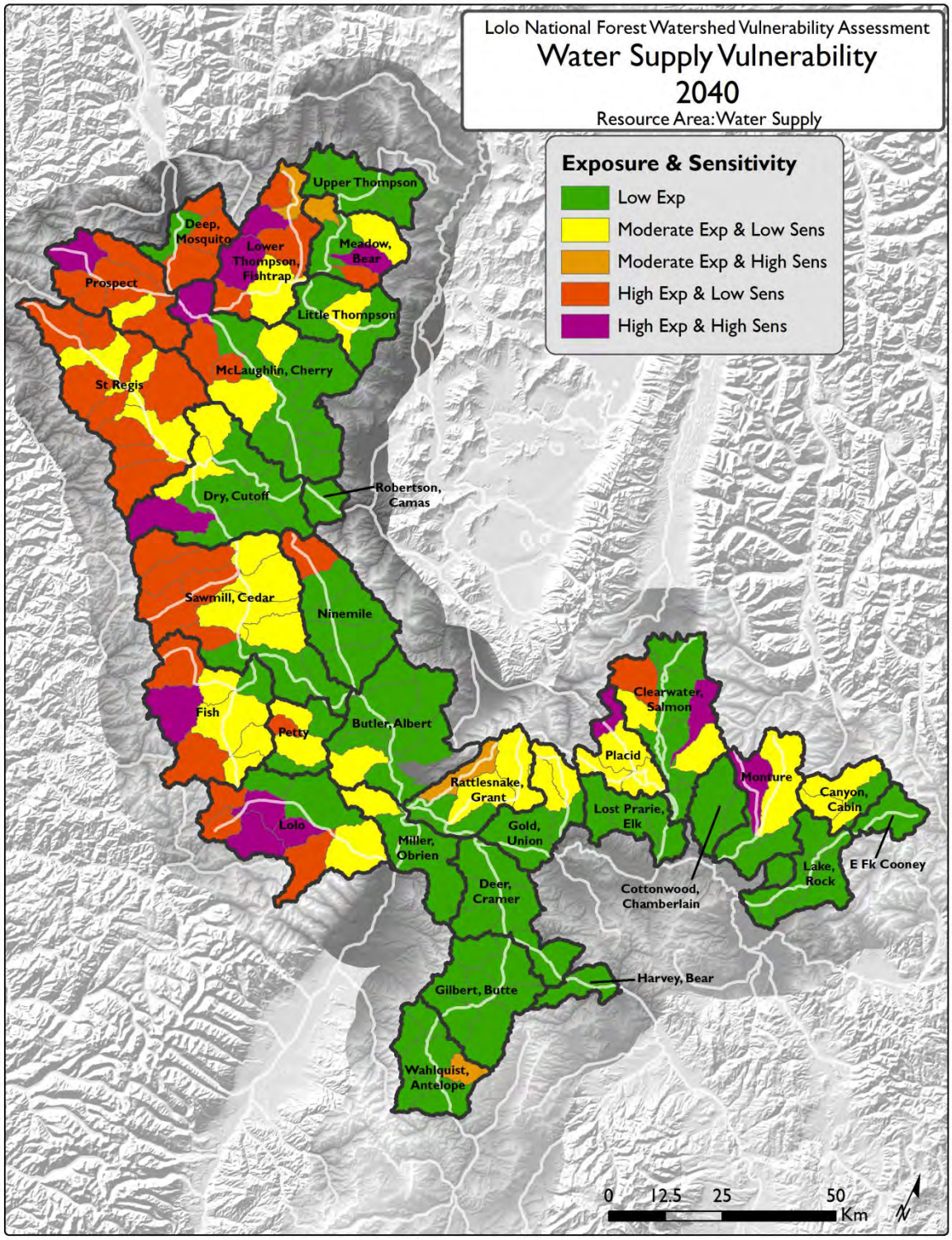

Figure 60. Estimated vulnerability of water supplies, by HUC-12, by the 2040s, based on comparing the flow exposure (Figure 57) and sensitivity (Figure 59) indices.

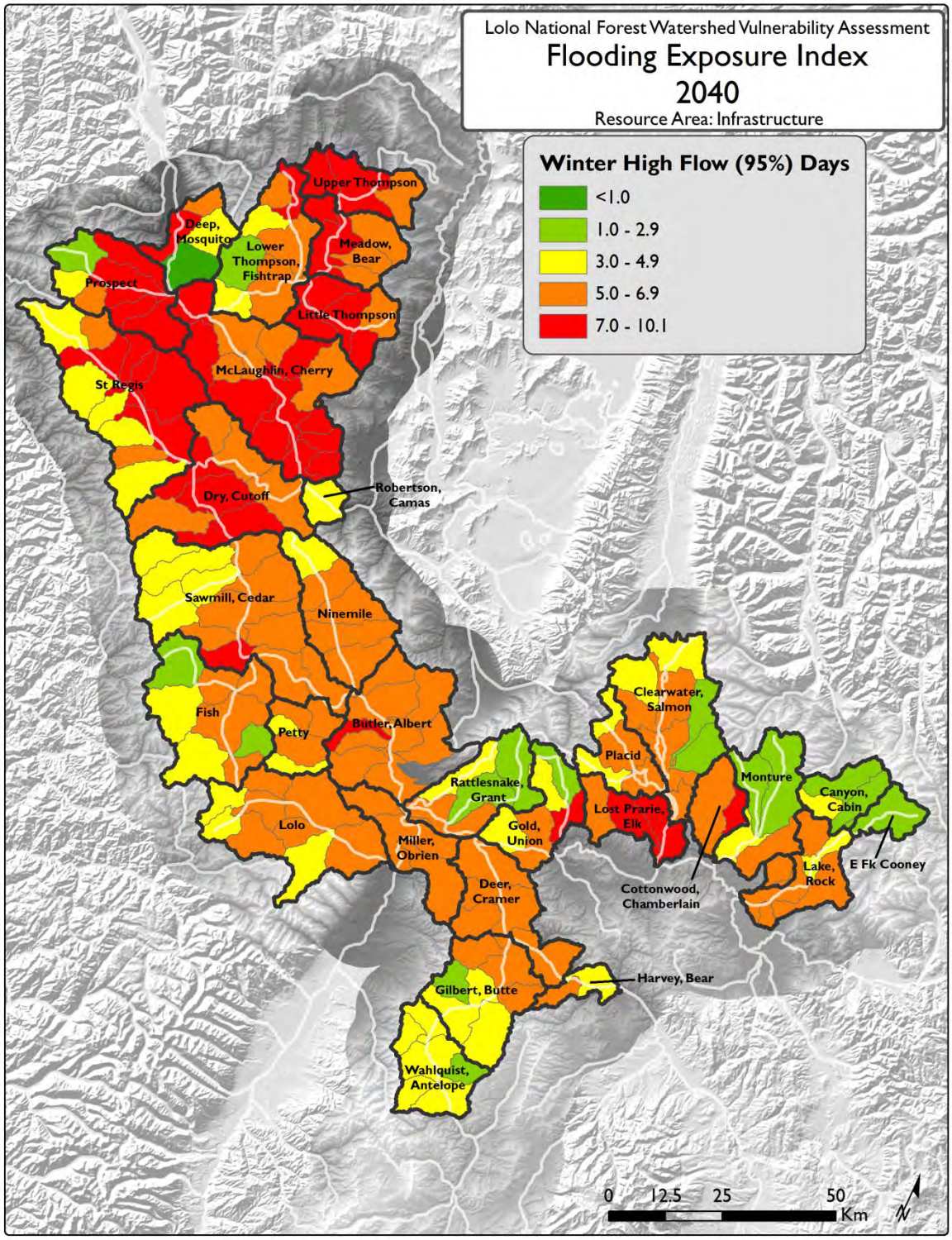

Figure 61. Flooding exposure index (here, only one metric used for this index) for infrastructure by the 2040s, using the number of projected future days with high (95%) winter flows.

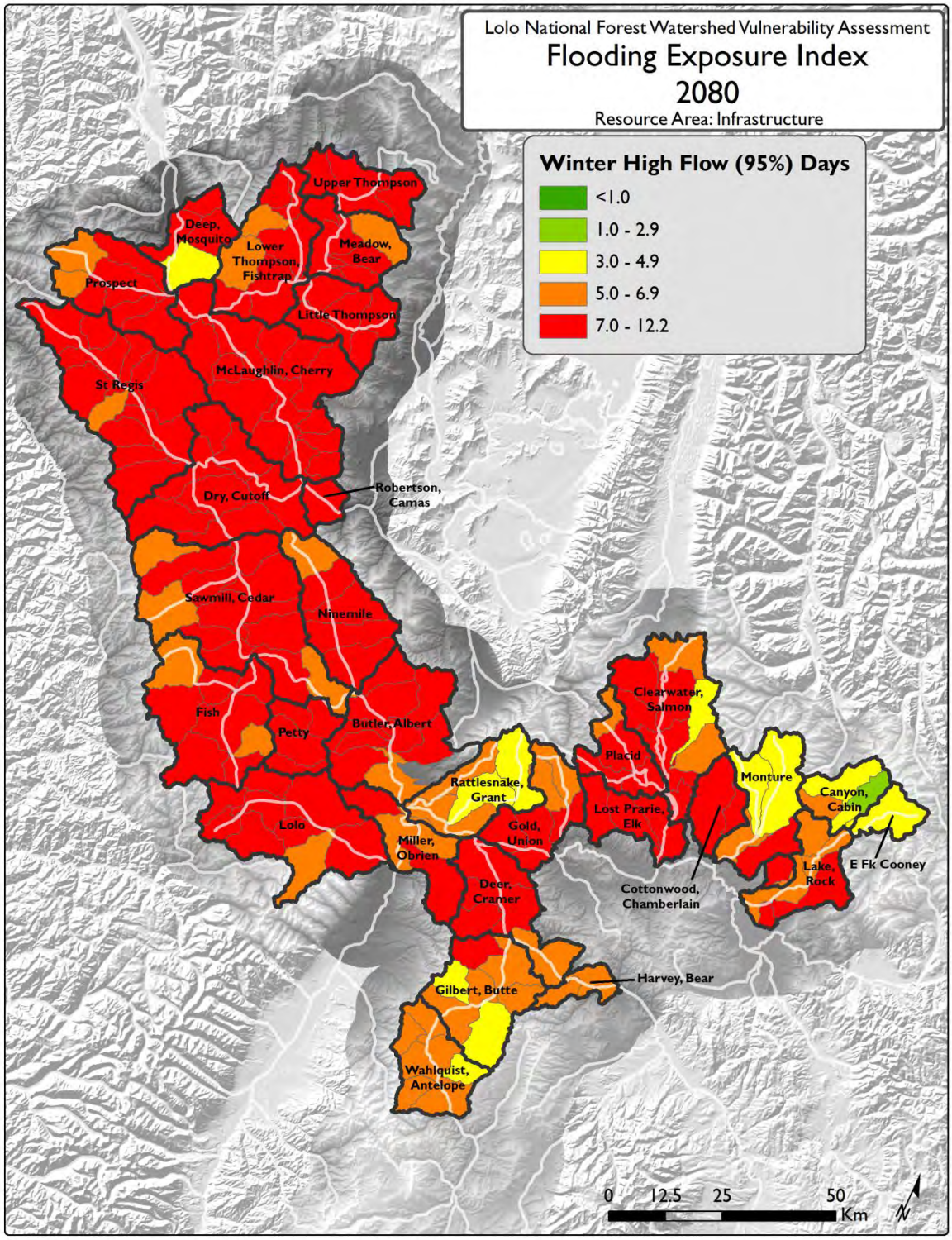

Figure 62. Flooding exposure index for infrastructure by the 2080s.
Confidence in metric: **low-moderate**

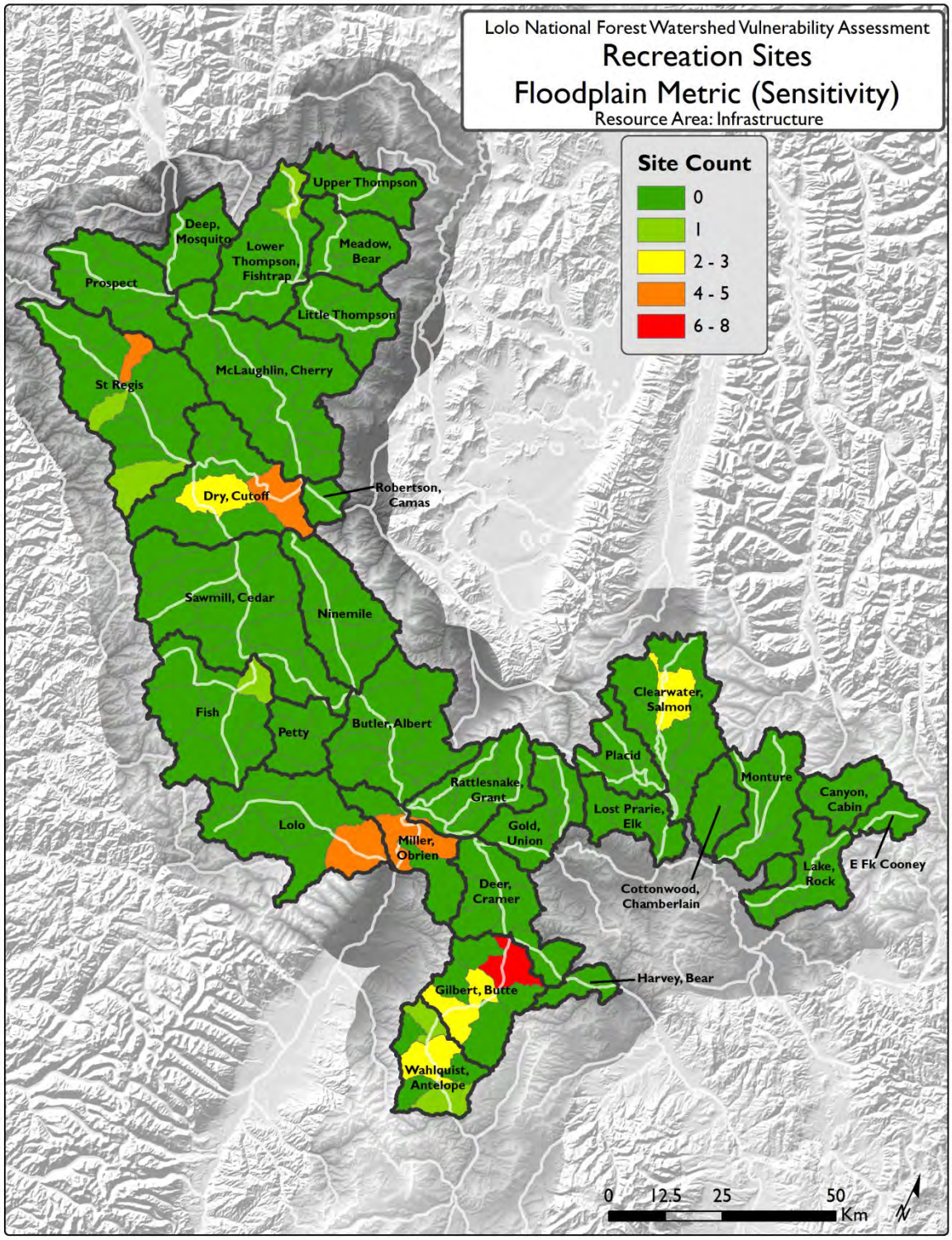

Figure 63. Floodplain metric for recreation sites (sensitivity), calculated as the number of sites located within the 100 year floodplain.

Confidence in metric: **moderate-high**

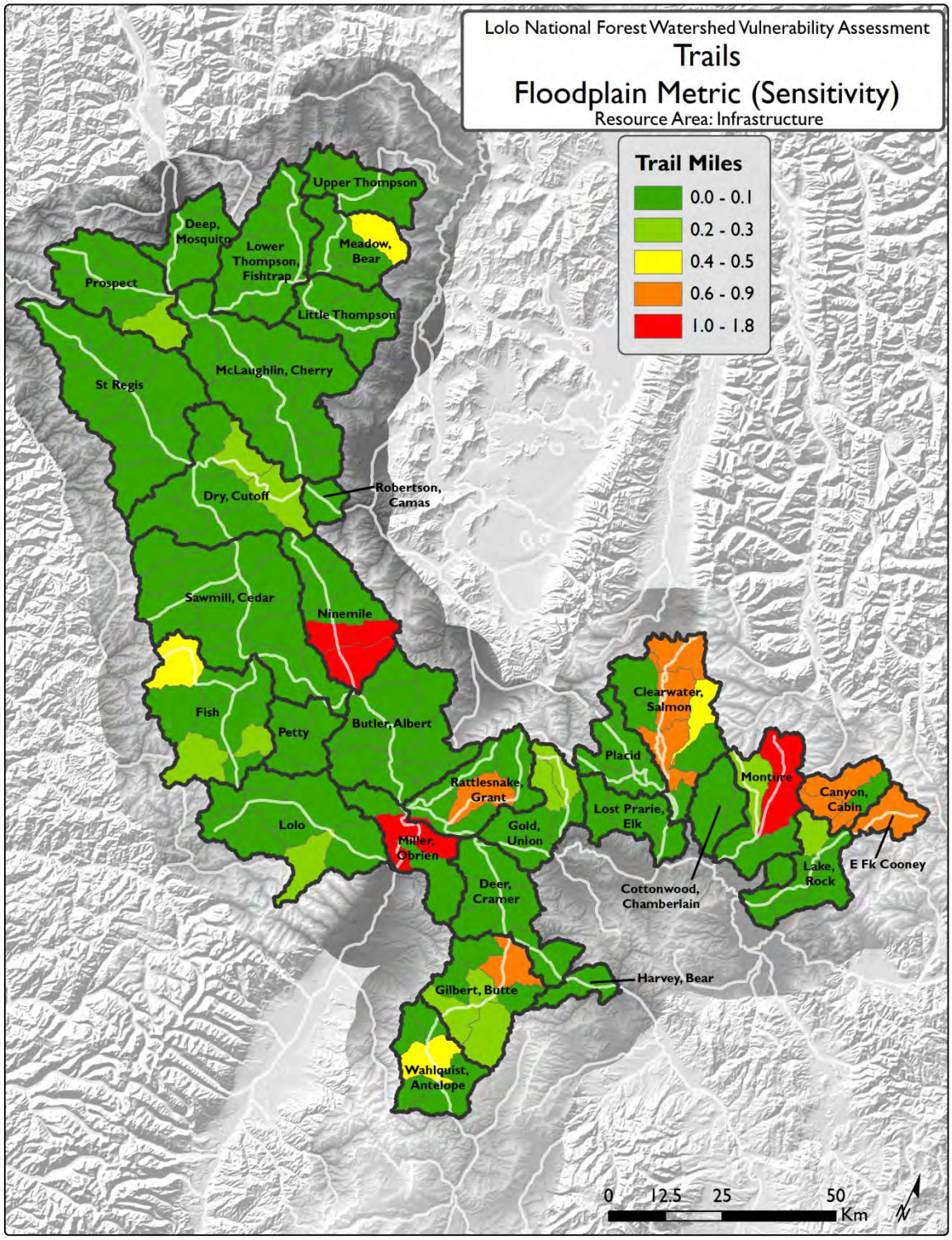

Figure 64. Floodplain metric for trails (sensitivity), calculated as the length of trails (mi) located within the 100 year floodplain.

Confidence in metric: **moderate-high**

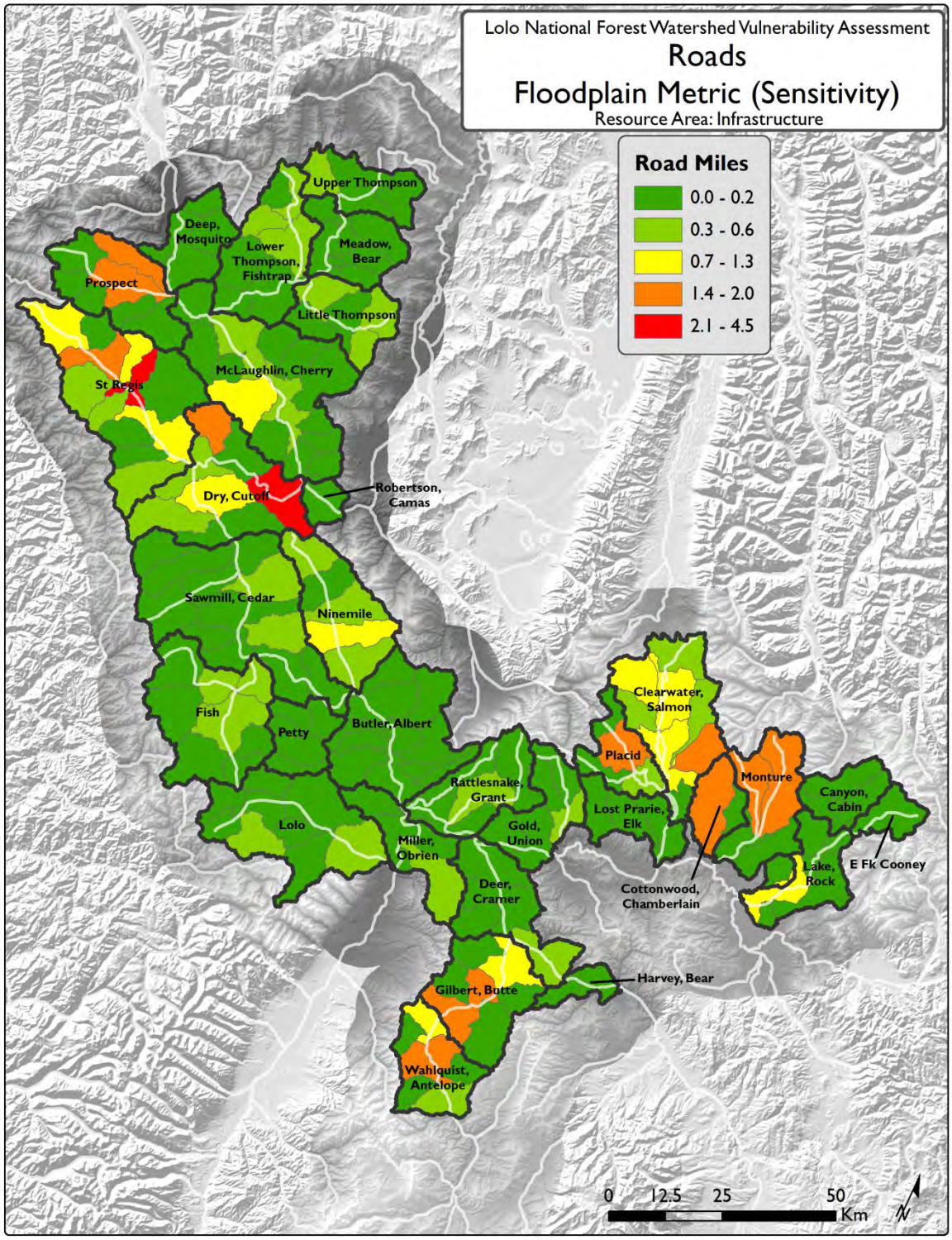

Figure 65. Floodplain metric for LNF-jurisdiction roads (sensitivity), calculated as the length of roads (mi) located within the 100 year floodplain.

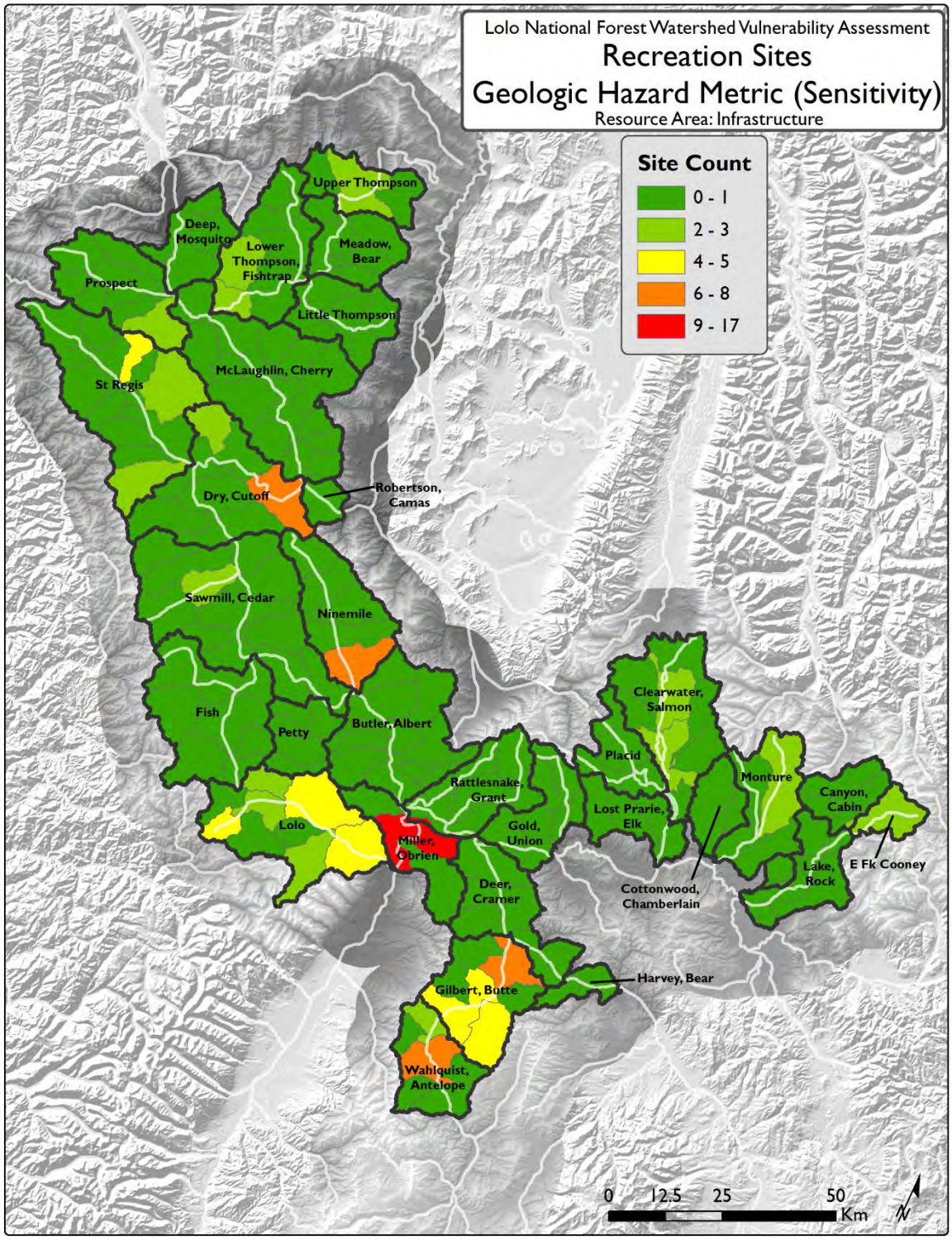

Figure 66. Geologic hazard metric for recreation sites (sensitivity), calculated as the number of sites located on an alluvial fan or within an area rated as having high geologic hazard.
Confidence in metric: moderate

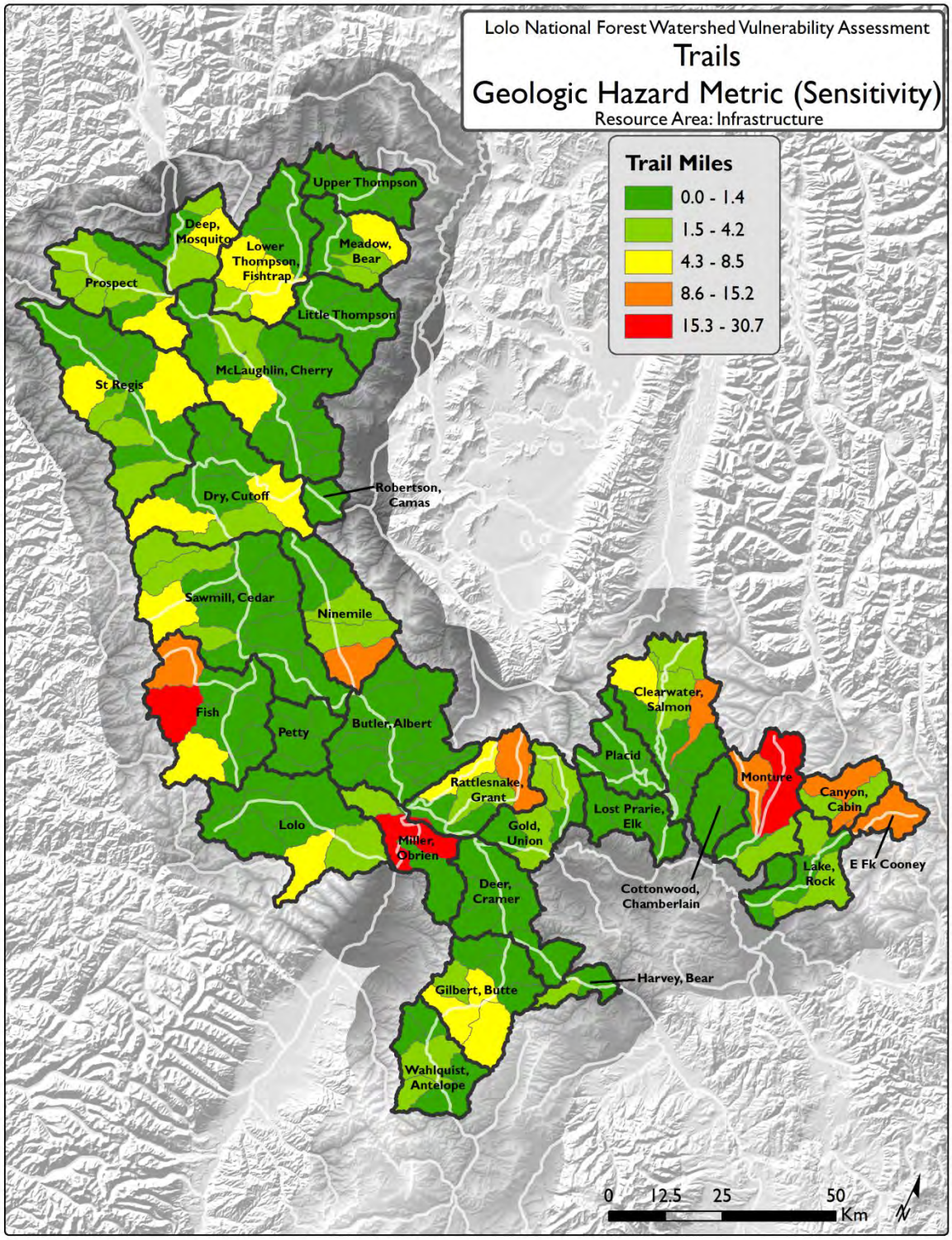

Figure 67. Geologic hazard metric for trails (sensitivity), calculated as the length of trails (mi) located on an alluvial fan or within an area rated as having high geologic hazard.

Confidence in metric: moderate

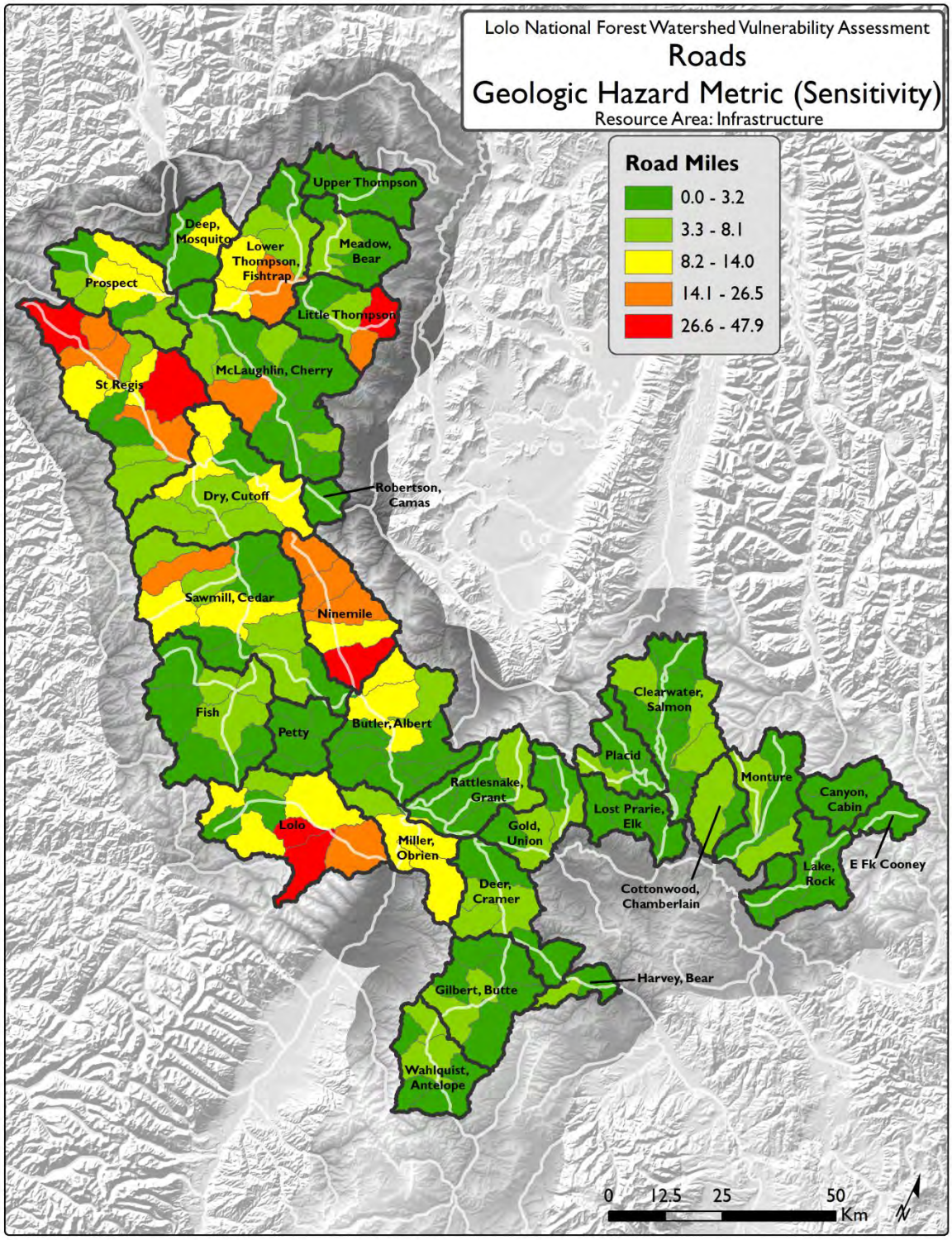

Figure 68. Geologic hazard metric for LNF-jurisdiction roads (sensitivity), calculated as the length of roads (mi) located on an alluvial fan or within an area rated as having high geologic hazard.
Confidence in metric: moderate

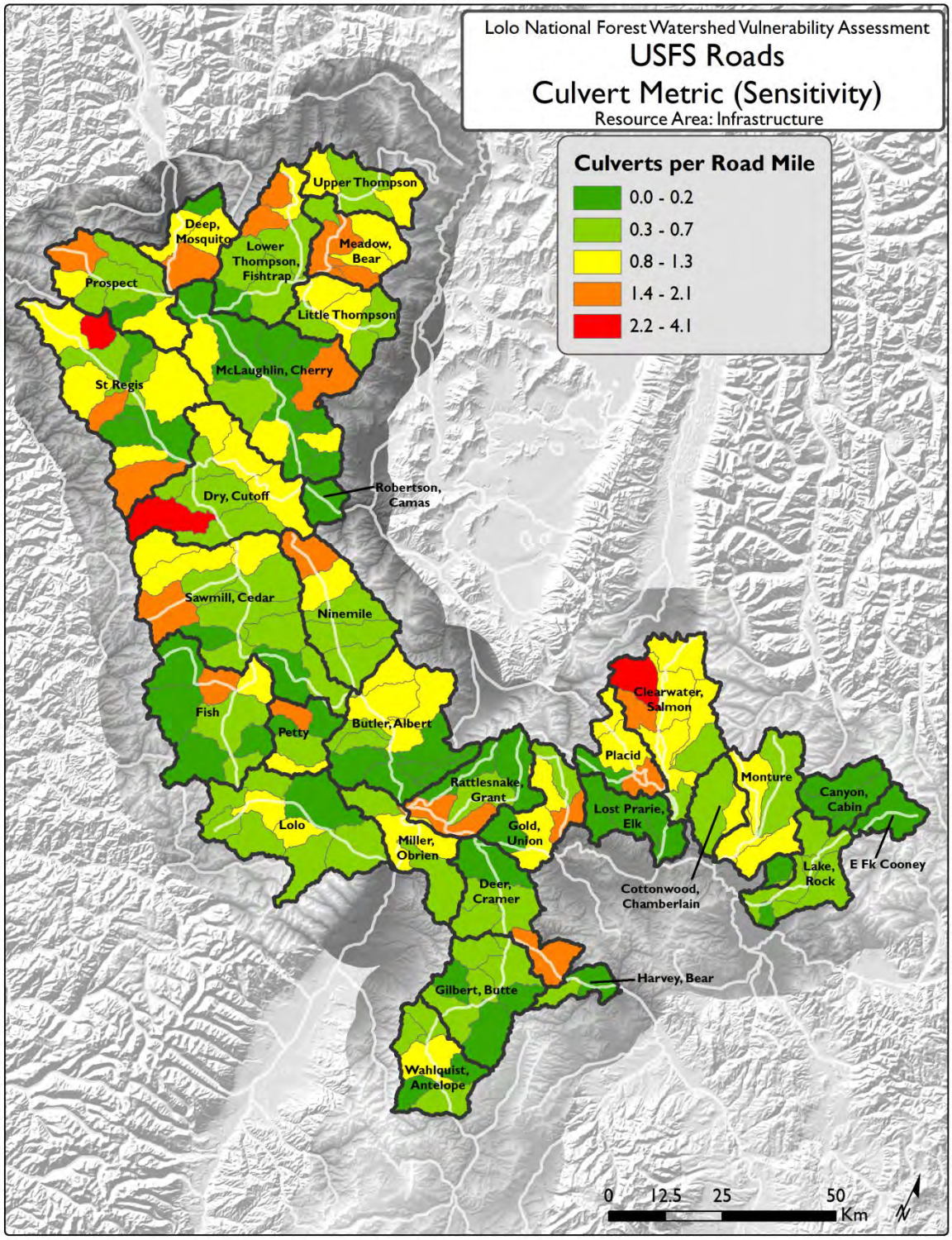

Figure 69. Culvert metric for LNF-jurisdiction roads (sensitivity), calculated as the count of LNF-maintained culverts per LNF-jurisdiction road length (mi).

Confidence in metric: **moderate-high**

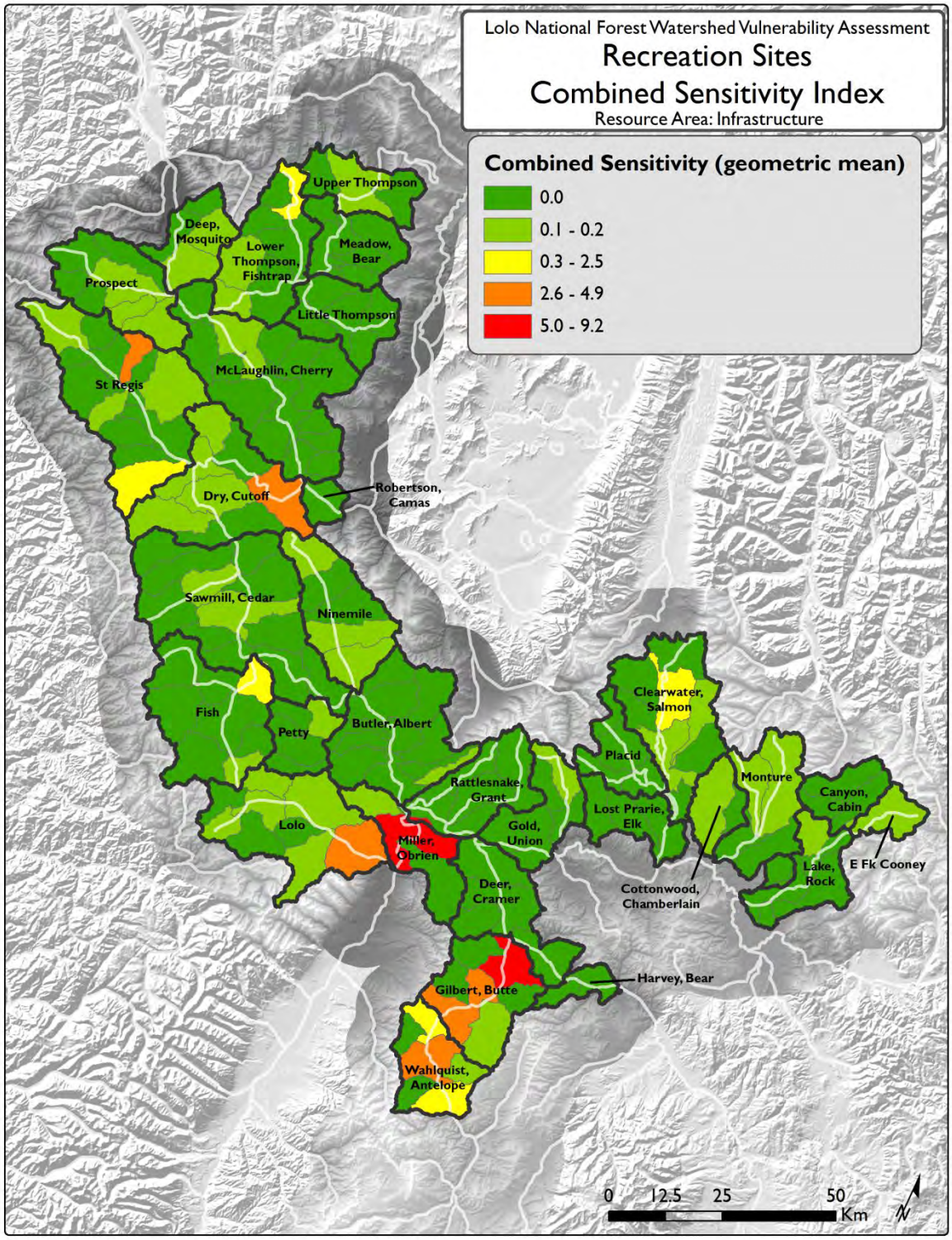

Figure 70. Combined sensitivity index for recreation sites. We calculated the geometric mean of the floodplain (Figure 63) and geologic hazard (Figure 66) metrics.

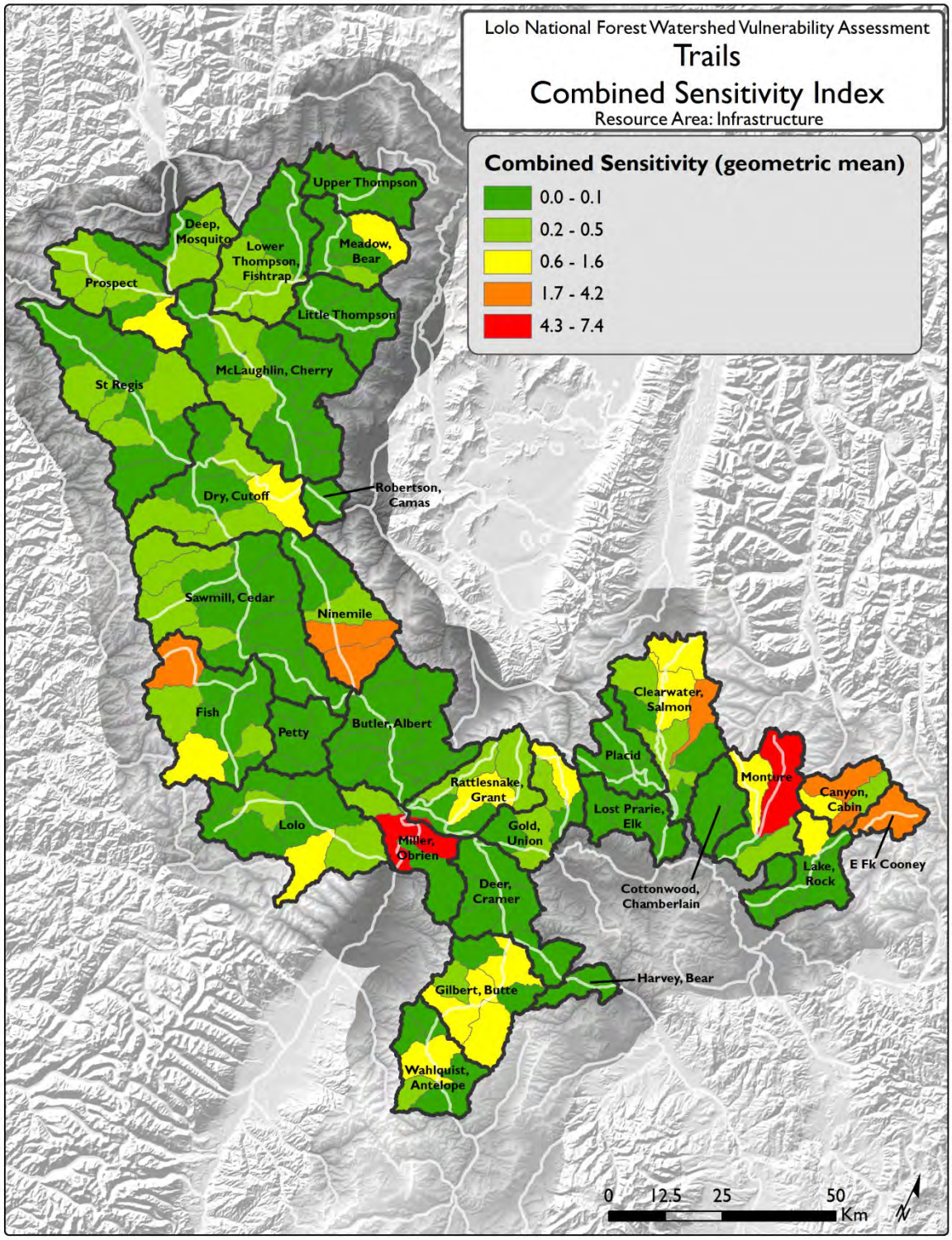

Figure 71. Combined sensitivity index for trails. We calculated the geometric mean of the floodplain (Figure 64) and geologic hazard (Figure 67) metrics.

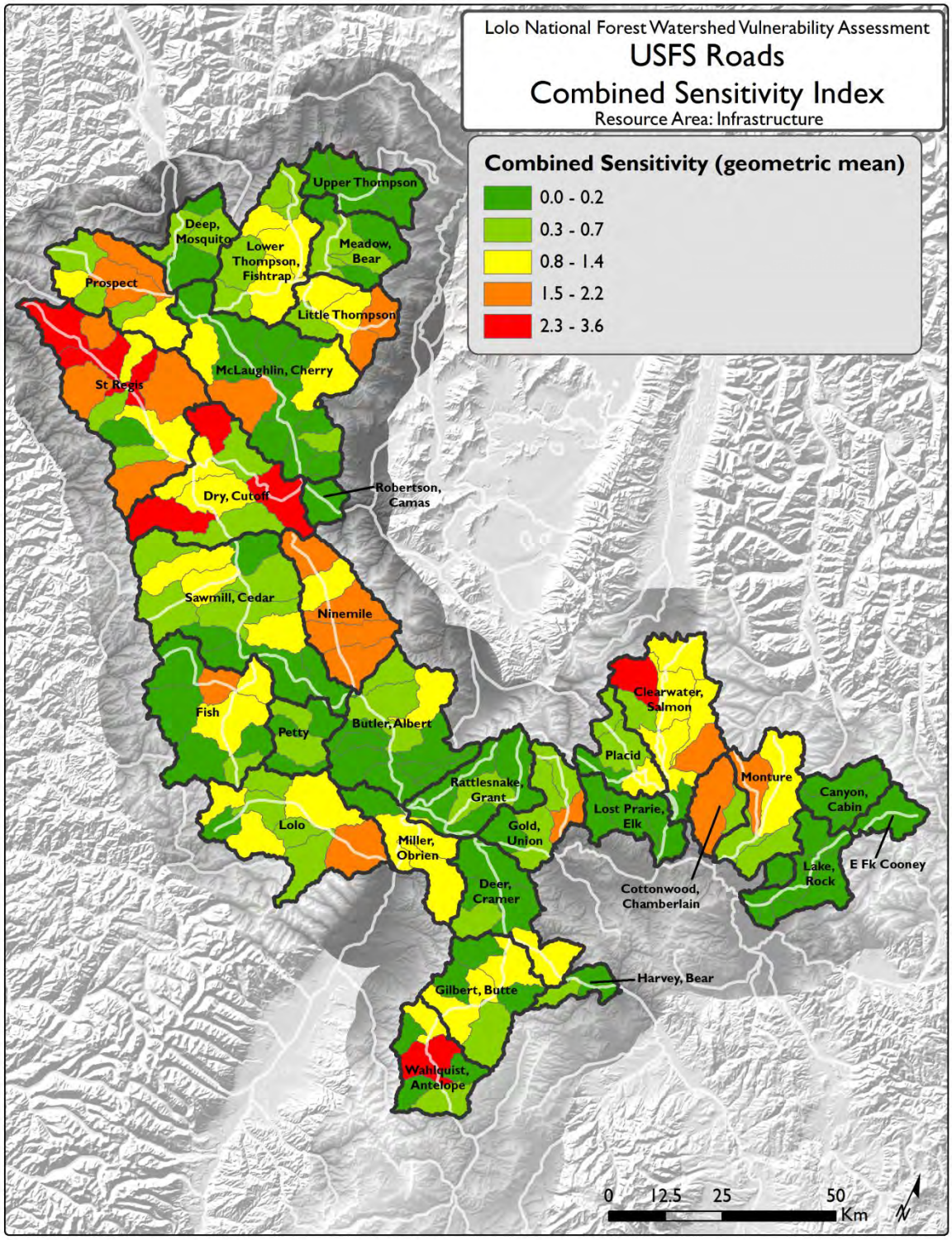

Figure 72. Combined sensitivity index for LNF-jurisdiction roads. We calculated the geometric mean of the floodplain (Figure 65) and geologic hazard (Figure 68), and culvert (Figure 69) metrics.

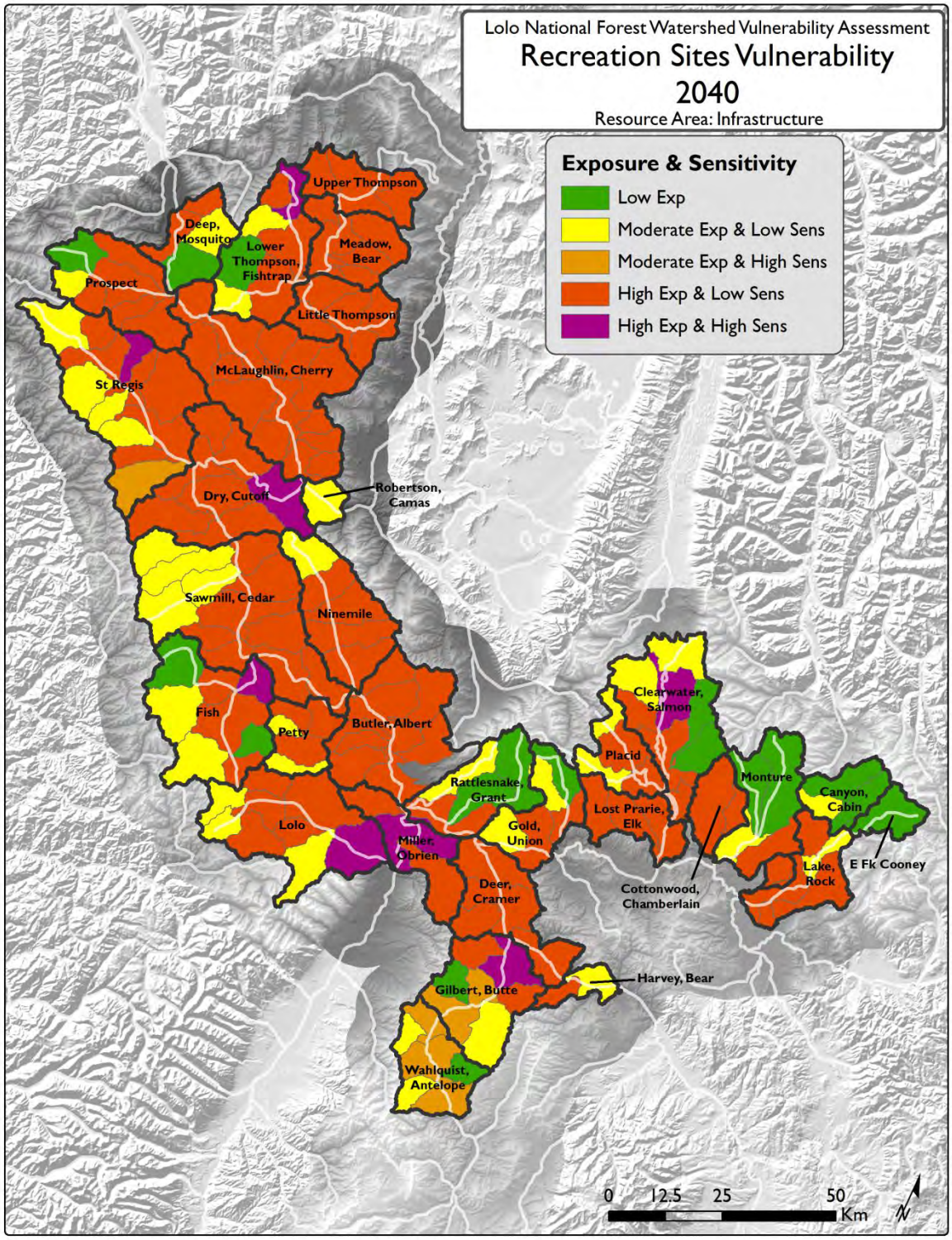

Figure 73. Estimated vulnerability of recreation sites, by HUC-12, by the 2040s, based on comparing the flooding exposure (Figure 61) and combined sensitivity (Figure 70) indices.

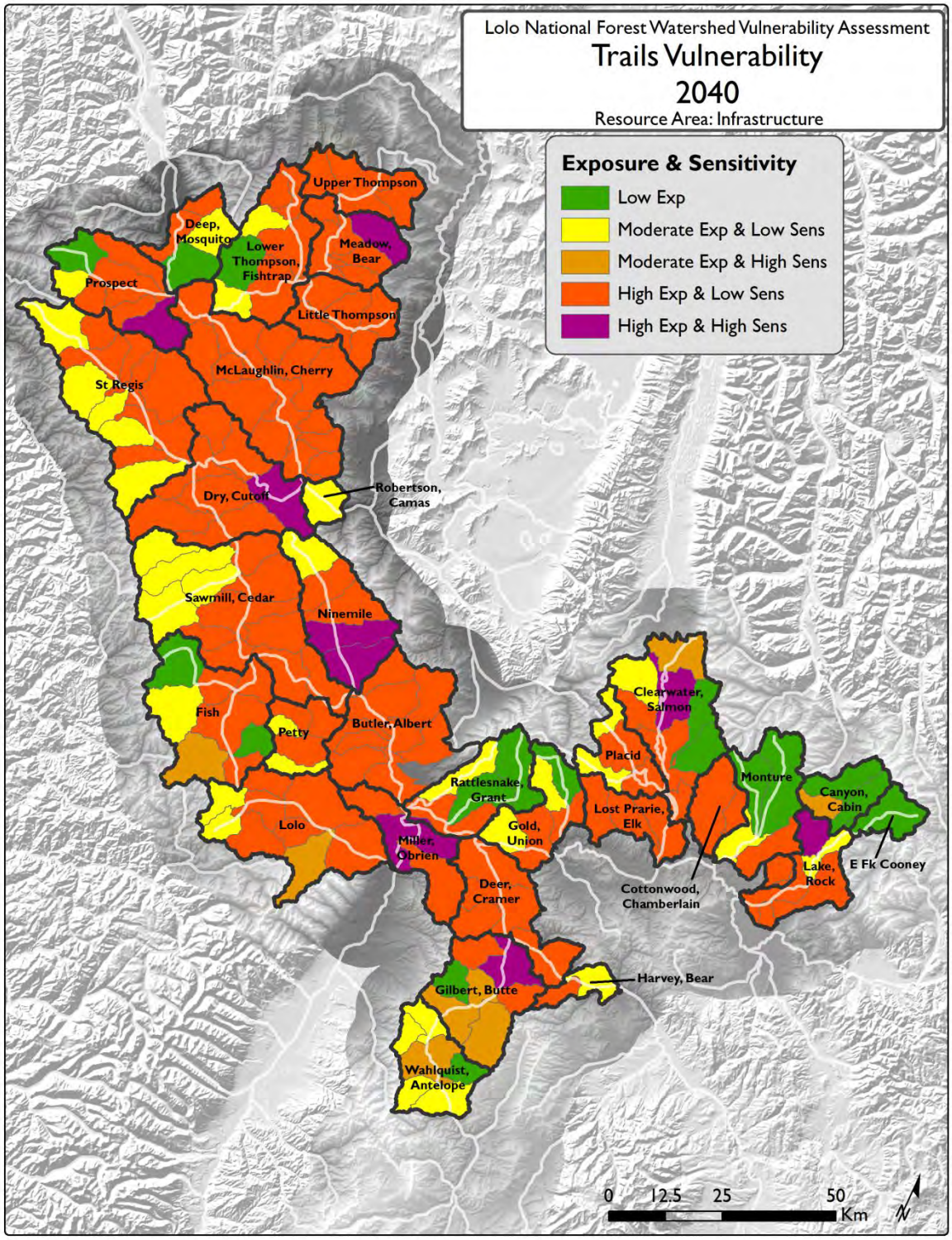

Figure 74. Estimated vulnerability of trails, by HUC-12, by the 2040s, based on comparing the flooding exposure (Figure 61) and combined sensitivity (Figure 71) indices.

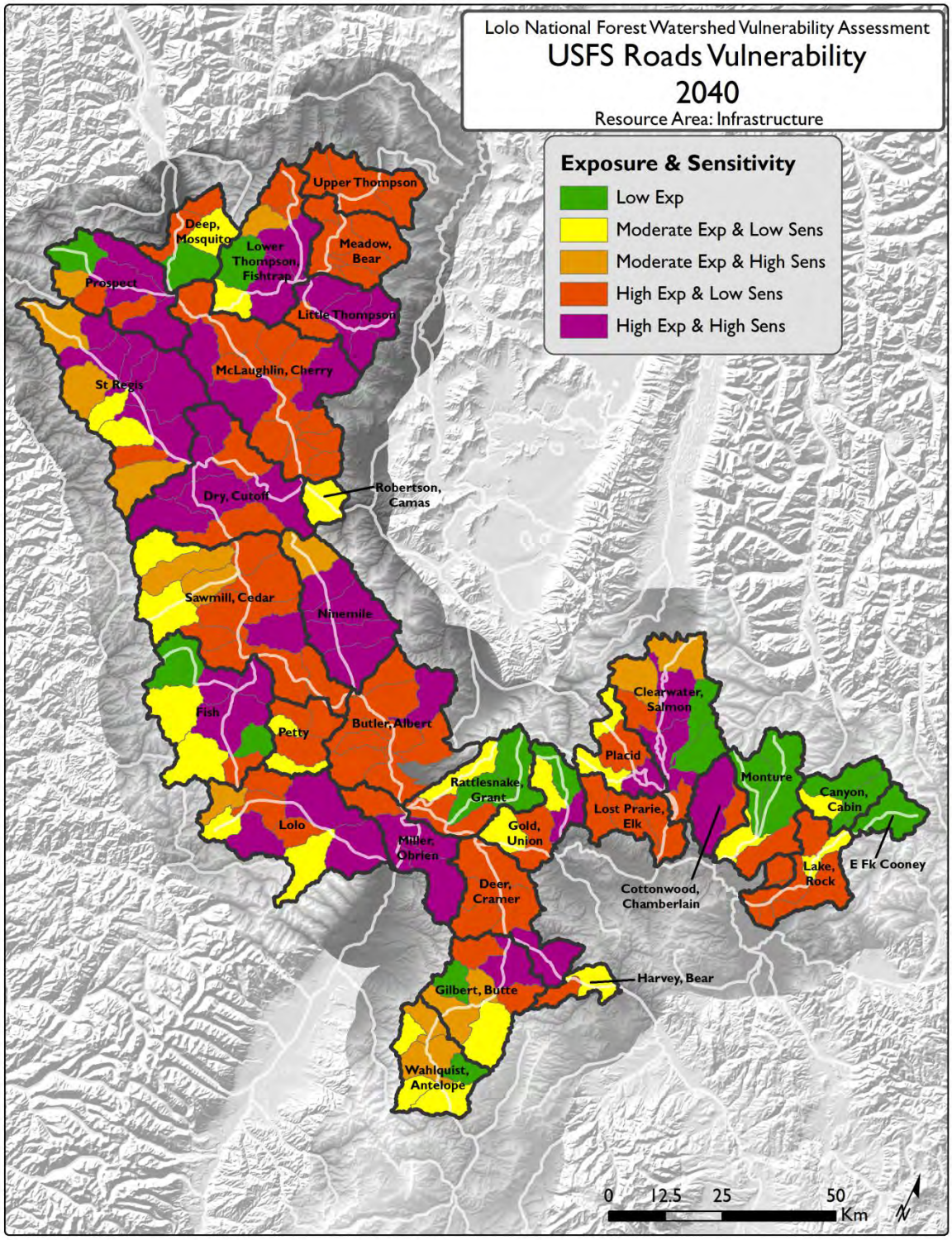

Figure 75. Estimated vulnerability of LNF-jurisdiction roads, by HUC-12, by the 2040s, based on comparing the flooding exposure (Figure 61) and combined sensitivity (Figure 72) indices.